MODEL-BASED QUALITY, EXERGY AND ECONOMIC ANALYSIS OF FLUIDIZED BED MEMBRANE REACTORS

By

Tabassam Nafees

School of Chemical and Material Engineering
National University of Science and Technology
August 2020

MODEL-BASED QUALITY, EXERGY AND ECONOMIC ANALYSIS OF FLUIDIZED BED MEMBRANE REACTORS

Name: Tabassam Nafees

Reg. No.: 2016-MS-CHE-04-00000171027

This Work Is Submitted As A Partial Fulfillment of The Requirement For The Degree Of

MS in Chemical Engineering

Supervisor Name: Dr. Iftikhar Ahmad

School of Chemical and Material Engineering (SCME)

National University of Sciences and Technology (NUST)

H-12, Islamabad, Pakistan

August 2020

Dedication

My Parents, Wife and My Kids

Acknowledgments

First and foremost, praise is to Almighty Allah Who bestowed upon me with His blessings and guided me in completing this task. This thesis work was an uphill task for me due to the immense workload at my office and to manage my family particularly the education matters of my kids. It would not have been possible without the support of family. The foremost help and support of several individuals/colleagues who were available all the time and helped me with their suggestions to compile this work. I would like to extend my sincere gratitude towards my supervisor **Dr. Iftikhar Ahmad** for his timely guidance, valuable and practicable approach throughout this work. It would be worth mentioning here that it is only his constant pursuance that leads to complete my work. There were so many hurdles and difficulties during my research work, but he remained not always available but chaser me to complete the work more efficiently I am also thankful to my (GEC) Guidance and Examination Committee Members **Dr. Sarah Farrukh**, and **Dr. Muhammad Ahsan** for their valuable guidance. Besides, the contributions of several past graduate students are acknowledged, they have been a great source of support and motivation, and their motivation and support throughout my MS and for this project have been most appreciated.

Abstract

Naphtha reforming units are of great interest for hydrogen and reformate production in petroleum refineries. Conventionally employed packed bed reactors for naphtha reforming have drawbacks such as a high pressure drop, diffusion limitations in catalyst, and radial and axial gradients of temperature and concentration. A fluidized bed reactor (FBR) attends to some of the draw backs of packed bed reactor. Coupled with the advantages of fluidization, the incorporation of membrane can improve the yield of products by selectively removing hydrogen from the reaction side. In this work, a sequential modular simulation (SMS) approach was used to simulate hydrodynamics of a fluidized-bed membrane reactor (FBMR) for catalytic reforming of naphtha in Aspen Plus environment. Aspen Plus is used for flowsheet development of the FBMR. The hydrodynamic parameters and membrane permeation phenomena were implemented using an interfacing of Excel with the Aspen Plus model of the FBMR. A fluidized-bed reactor without membrane, i.e., FBR, is also simulated and a comparison is drawn. FBMR outperformed the FBR in terms of increase in aromatics in reformate stream and effective separation of hydrogen during the reaction. The proposed method can be readily adopted by process engineers for design and optimization decisions.

Keywords: Naphtha catalytic reforming; Aspen Plus; Excel interfacing; Two-phase theory of fluidization; Hydrogen production; Fluidized-bed membrane reactor; Increase in aromatic production; Pd–Ag membrane.

Nomenclature

A_c	reactor cross-sectional area, m^2
CSTR	continuous stirred tank reactor
d_b	bubble diameter, m
E_i	energy of activation for the ith reaction, kJ/kmol
E_p	energy of activation of permeability, kJ/mol
FBP	final boiling point (°C)
$F^S{}_{H2}$	shell side H_2 gas flow rate of in, kmol/h
F^t	total molar flow rate, kmol/h
H_2/HC	hydrogen to hydrocarbon molar ratio
IBP	initial boiling point, °C
ICE	internal combustion engine
RON	research octane number
k_{ci}	coefficient for mass transfer of specie i, m/h
K_{ei}	equilibrium coefficient
k_{fi}	forward rate constant
L	length of reactor, m
MR	membrane reactor
PFR	Plug flow reactor
p_i	partial pressure of specie i, kPa
P_t	total pressure, kPa
$p^R{}_{H2}$	reaction side hydrogen partial pressure, Pa
$p^S{}_{H2}$	shell side hydrogen partial pressure, Pa
P	hydrogen permeability through Pd–Ag layer, $mol/m^2\ s\ Pa^{1/2}$
P_0	pre-exponential factor of hydrogen permeability, $mol/m^2\ s\ Pa^{1/2}$
R	ideal gas constant, kJ/kmol K

r_i	reaction rate for ith reaction, kmol/kg cat h)
T	temperature of gas phase, K
TBP	true boiling point, ^{o}C
t	time, h
u_b	velocity of rise of bubbles, m s^{-1}
C_{mp}	membrane permeation capacity (membrane surface area/thickness), km
E_p	activation energy for permeation, J mol^{-1}
k	pre-exponential factor, mol km^{-1} h^{-1} Pa$^{-0.5}$

Greek letters

α_H	hydrogen permeation rate constant, mol/m s Pa$^{0.5}$
d	thickness of palladium layer, mm
ρb	catalyst bed density, kg/m^3
ρg	density of gas phase, kg/m^3
v_{ij}	stoichiometric coefficient of specie i in reaction j
ΔH	heat of reaction, kJ/kmol
ε_b	void fraction of catalyst bed
ε_{mf}	void fraction of catalytic bed at minimum fluidization
ψ	catalyst particle shape factor
δ	bubble phase volume as a fraction of total bed volume (-)
η	membrane permeation effectiveness factor (-)

Subscripts

a	aromatic
h	hydrogen
n	naphthene
p	paraffin

Table of Contents

LIST OF TABLE

LIST OF FIGURES

Chapter-1

1.0 Introduction

Refinery process of converting low octane straight run naphtha to high octane naphtha Naturally, occurring crude oil cannot be used without processing it into the distillation units. The distillation unit split crude into different cuts with specific properties which are easier to use for a specific purpose. It was the invention of the internal combustion engine in 1862, that has increased the demand for gasoline instead of natural coal gas. Eventually, the petroleum industry was scale up to meet the demand of gasoline for automobile industry. The oil industry evolved from separation to molecular arrangement processes. Initially, the molecular arrangement was carried out mainly in thermal cracking units. This process had some very serious operational limits like low selectivity, poor yields etc. The sever conditions of temperature and pressure has also changed the metallurgical requirement of the units. The first catalytic reformer unit was established in 1939, that had boosted the octane number of average gasoline by 30 to 40 points. [1]

Reforming has two essential functions: improving octane number and producing hydrogen along with aromatics. The reformer operation is considered an indispensable source of hydrogen production. The reforming process under discussion based on catalyst bed formation can be categorized into (1) moving bed process and (2) fluidized bed process. The advancement in the technology has changed the design of the reforming unit, which helps in operational issues. However, the basic principle is the same for both systems. Thermafor catalytic process (TCC) is known as a moving bed system while fluid catalytic cracker (FCC) is termed as a fluidized catalyst bed process. The TCC process was obsoleted since very few units are presently in operation in the world. Having the technical edge, FCC units have taken the lead in the process of naphtha reforming units in refineries operation. [2]

Table 1.1 Thermal versus Catalytic Cracking Yields [2]

Comparison of both system yields for similar Crude Feed				
	Thermal Cracking		Catalytic Cracking	
	wt%	vol %	Wt %	Vol%
Fresh Feed	100.0	100.0	100.0	100.0
Gas	6.6		4.5	
Propane	2.2	3.7	1.3	2.2
Propylene	1.0	1.8	2.0	3.4
Isobutane	0.8	1.3	2.6	4.0
n-Butane	1.9	2.9	0.9	1.4
Butylene	1.8	2.6	2.6	3.8
C5+Gasoline	26.9	32.1	40.2	46.7
Light Cycle Oil	1.9	1.9	33.2	32.0
Decant Oil	0.0		7.7	8.7
Residual Oil	57.0	50.2	0	0
Coke	0.0	0	5.0	
Total	100.0	96.5	100.0	102.2

Initially, the thermal cracking process was used as a prime source of naphtha reforming. But now fluidized catalytic process has taken the lead by improving the production rates of gasoline with high octane number and less production of heavy fuel oils and light gases

[2]. The fluidized catalytic process, produces light gases, have more olefins in comparison to thermal cracking process as shown in Table .1

Gasoline (Motor Fuel) is one of the most common fossil fuels used in transportation that has global warming issue but still in use by addressing stringent environmental and safety concerns of regulating bodies.

As the catalytic cracking reforming process is continually improving with the combined efforts in the field of catalyst and engineering development both collectively made it possible to meet the present and future anticipated needs of the industry. A very important step in catalyst development was made in 1960 [3] which was the commercialization of the bimetallic of Platinum/Rhenium catalyst and shows a proven better activity, stability, and selectivity than all platinum catalysts. Worldwide, there are more than 600 UOP reforming units are in operation. These units provide, practically high selectivity for high charge rate and high-octane levels than any other units [3]. The catalysts used in the reforming process are very sensitive to temperature and feed compositions. The sensitivity of these catalysts requires more precautions for clean, continuous, upset free operation from the feedstock contaminants.

In 1971, a new Continuous Catalytic Regeneration (CCR) has revolutionized the platforming unit by introducing the operation on very sever conditions, by addressing the problems of catalyst deactivation and running the system with simultaneous regeneration of the catalyst and consequently save the overall downtime of the naphtha reforming unit. The performance of a high-efficiency combustion engine needs efficient fuel quality to mitigate the premature burning that causes the knocking problem during the running cycle. Efforts have been made to produce high-quality fuel of high RON to fulfill the operating limits of the high compression engines more efficiently.

All operational and technical procedure to boost the gasoline octane number is carried out in the catalytic naphtha reforming units in a series of three or four radial or axial flow reactors. The later gives less pressure drop with high surface area as compared to radial flow with low-pressure drop configuration can be subject to an uneven vapor along the axial length. There are three modes of operation, semi-regeneration, cyclic, and continuous catalytic regenerative. Naphtha reforming produces aromatics from catalytic reforming regeneration unit consist mainly, paraffin, and naphthenic can be used either as high rating motor fuel or a good source of aromatics for specific petrochemicals applications. The basic chemistry of the aromatics remains unchanged. The aromatics processing system is very complex and involves those reaction sets of reaction for C_6 and C_7 hydrocarbons processing that is difficult to promote and slower.

Most of the refineries set up use Packed Bed Reactors (PBRs) for naphtha reforming. The catalysts are dumped in these arrangements. Since catalyst particles have certain limits and cannot be reduced further down to this limit and smaller diameter cannot be used due to excessive pressure drop [4]. On the contrary Large particles have other disadvantages like resistance with very low particles effective factor to heat and mass transfer large particle size comes with disadvantages such as resistance to heat and mass transfer. Also, large particles have a low particle effectiveness factor. Thus, to control these problems, catalyst particle size needs intensive work to make the very appropriate particle size.

Chemical reactants are converted into products under Le Chatelier's Principle by separating a part of the reactants material to form the product gases [5,6]. There are several techniques of linking separation and reaction processes in a single vessel that has already been discussed in most of the reviewed papers published in the past (Krishina, 2002). A method was proposed to incorporate membrane in the chemical reactors. In this method, reactors were divided into different sections as per membrane's property of permeation and selectivity towards a particular component. It resulted in achieving better separation between reactants and products. Since then, it is being used in the application of reactor operation system.

This system has shown good results in the chemical engineering system for continuous operation to trap homogeneous catalysts. (Sirkar et al., 1999; Greiner et al., 2003). Similarly, there are so many devoted activities are focused on from the reaction zone which is produced in reversible reaction system to avoid reversibility process (van de Graaf et al., 1999; Assabumrungrat et al., 2001; Itoh et al., 2003; Wang et al., 2003).

All available material and references are sufficient enough to use them for further study and practical work at the pilot plant and industrial levels. The aim of this study was to focus on the Fixed Bed Membrane Reactor for the separation of H_2 and aromatics formed in naphtha reforming reactors by simulating the Pd-Ag alloy membrane through excel interfacing. The Pd-Ag membrane show excellent permeation results for Hydrogen.

A simple reactor can be converted to a membrane reactor by replacing its outer wall with a perm-selective membrane material. [5,6]. Various researchers have used membrane reactors for enhancement of product by shifting of thermodynamic equilibrium. Developing membrane reactor technology carries significance as a promising method for increasing hydrogen production by improving separation and recovery which will economize overall hydrogen production. In different studies, palladium, and its alloys such as palladium-copper, palladium-silver, and pure palladium-based membranes were fitted inside conventional reactors [7, 8, 9, 10, 11]. For the synthesis of methanol, Rahimpour proposed a membrane reactor with a pure Pd membrane [12]. Pasha developed Excel interfacing with Aspen Plus to simulate an FBMR for steam reforming [33]. Tosti et al. carried out experiments to extract ultra-pure hydrogen by investigating the insertion of palladium-based membranes in different configurations inside conventional reactors [13]. One paper by Roy focuses on the simulation of membrane-based fluidized bed reformers and its economic aspects [14]. Khosravanipour presented a concept of membrane assisted naphtha reformer and studied the effects of in situ hydrogen separation within a packed-bed reactor [15]. In another paper, Rahimpour compared the results from a packed bed naphtha reformer with a fluidized bed membrane reformer [16].

H_2 is generated as the naphtha reforming reaction proceeds in the reactor. Hydrogen separation from the product side could lead to the formation of dehydrogenation products which are associated with an increase in reformate RON. In another study, Rahimpour et al. simulated a thermally coupled reactor inside which two separate reactions, one endothermic and the other exothermic are occurring [17]. It was demonstrated that by this method the heat released by nitrobenzene to aniline conversion can be utilized by the heat requiring naphtha reforming reactions. All of the studies presented use MATLAB, FORTRAN, or other software-based modeling approaches that are not commonly available to chemical engineers employed in the process design industry. Modeling of a membrane reactor is a challenging task because of the simultaneous occurrence of diffusion coupled with mass transfer and chemical reaction inside the reactor [18].

Aspen Plus is a widely employed process simulator for industrial process simulations in addition to other simulation programs. In this study, an FBMR for naphtha reforming is developed on the Aspen Plus platform with Excel interfacing. In an FBMR both physical and chemical phenomena coexist and need to be taken into consideration.

An adequate model for an FBMR should be able to represent the physical and chemical phenomena simultaneously. The physical phenomena are implemented by utilizing the hydrodynamics theory as an integrated sub-model and chemical reactions are conveniently implemented by the built-in power-law input panel of Aspen Plus. Ideal reactor models are available as modules in Aspen Plus and are combined sequentially in a certain way to simulate the behavior inside the fluidized bed membrane reactors [19]. Excel is used for calculation and transfer of the hydrodynamic parameters to the Aspen Plus for calculation of volumes and voidage of the continuous stirred tank reactor (CSTR) and the plug flow reactor (PFR) blocks inside to flowsheet. Membrane permeation model is based on Sievert's law.

Cost estimation and economic evaluation of both FBMR and FBR configuration was carried out and discussed in chapter 5. There are so many techniques and methods are used to estimate the costs of chemical process industries. This study objective is to develop the simulation models to show the aromatics production difference between a simple Fluidized bed reactor with a membrane-based reactor (FBMR). Most of the cost estimation data available are based on capital investment of the overall refinery. The profitably is calculated on the products a refinery produced. To calculate the capital cost of a reformer system the aspen economizer analyzer tools were applied by mimicking the cost of different equipment of a particular naphtha reforming unit. The payback periods were evaluated based on capital cost, operating cost of the simulated naphtha reforming units for FBR, & FBMR. The cash flow and project benefits were based in connection with reformer products i.e. Natural Gas, Gasoline, Aromatics, and Hydrogen.

Likewise, energy and entropy, exergy concept is also a branch of thermodynamics and is equally applied in the fields of engineering. Thus, the thermodynamics concept of exergy was studied and adopted to calculate exergy of the system by the interfacing of MATLAB and Excel. With the help of the second law of thermodynamics application, maximum work a system provides can be calculated. System Exergy is a very important parameter which is stem by the second law of thermodynamics can help evaluate a system and other processes energies involved in another process by definition exergy did not mean simply a thermodynamic property but it is considered as a property for the system as well for the environment in which a system work. The terms like available energy, exergy, utilized energy most commonly used in the literature may also be used as equivalent to exergy.

All through the previous several decades, exergy related studies have received much attention from a different area that includes mechanical, chemical, environmental engineering, and many more. Thus, the canvas of the exergy community has expanded to some extent. It implies thermodynamics properties and on other forms of energies and quantities i.e. on work and heat. The shaft work exergy which transferred due to shaft work is termed as shaft work exergy, but if the exergy transmitted due to heat it relies on the environment temperature as well as on the temperature at which it happened. The thermodynamics is the science of energy and exergy including entropy even though Zeroth and third laws of thermodynamics are very existing, the first law of thermodynamics refers to the conservation of energy and does not identify the losses of energy, quality and possible improvement in the use of the resources. However, the second law of thermodynamics includes exergy and entropy concepts and also considers the irreversibility and the consequent non-conservation of exergy and entropy.

Exergy analysis was conducted by mimicking the aspen plus data into MATLAB and then transferring the exergy output of physical exergy, chemical exergy, mixing exergy, and total exergy of both FBR and FBMR configurations.

1.1 Thesis Outline

The thesis work based on the simulation model of the Packed Bed Reactor Model by phasing for three reactors reforming the system by phasing each reactor into five sections. The Packed Bed Reactor was changed by the introducing Membrane into the reactors through Excel Interfacing.

- A brief outline of current work is explained in Chapter-1
- The Catalytic Reforming Process is described in chapter -2. An industrial system of three reactors for a semi regenerative reactors is taken from the literature.
- Literature survey is documented in Chapter -3
- Model development in Chapter -4
- Chapter 4 explains the detail of Model Building and flow sheeting in Aspen Plus along with Excel Interfacing.
- Results, Economic and Exergy analysis, and discussion are presented in chapter 5

Chapter-2

2.0 Process Principles and Theoretical Description

The focus of this thesis is the Catalytic Reforming System of converting C_7 to C_{10} compounds having less octane number to aromatics and iso-paraffins, that have high octane rating. This process is greatly endothermic which needs excess energy to proceed. In general, the naphtha reforming system operates on two types: a high severity set up to produce aromatic mainly (80-90 vol %) and a moderate severity system to produce gasoline (70 vol % aromatic content) having high octane value. The simulation work of the thesis is comprised of moderate severity conditions for temperature and pressure along with Platinum/Rubidium based catalyst that gives aromatics production between 45 to 50 % aromatics. Before introducing straight run naphtha in the reformer, it is treated into the desulfurization unit to the inorganics compounds like Sulphur, Nitrogen, and Oxygen which causes deactivation of the reforming catalyst. The heavy naphtha comprised of C_7-C_{10} hydrocarbons is a feedstock for a catalytic reforming unit as explained earlier that naphtha that has been desulfurized or hydrotreated. When benzene is desired then sometimes full range stocks are also used. Figure 2.1 shows a processing scheme followed in a refinery for the production of gasoline with an integrated catalytic reforming unit. The naphtha reforming feed after being treated in the desulphurization unit enters into the first reactor along with recycling hydrogen gas to maintain the hydrogen to hydrocarbon ration from 4 to 7 to suppress the coking process of the catalysts. The naphtha reforming units usually comprise three to four reactor system with an intermittent fired heating system. The feed of each reactor was heated before introducing in the next reactor, these intermittent fired heated facilitate the endothermic reaction to promote in a controlled environment for better and efficient products yields. The reformate stream from the last reactors exchanges the heat with incoming naphtha feed by giving its heat to the feed then further cooling with installed condenser splash into a separator for separating hydrogen. The bottom of the separator becomes the feed of the stabilization unit while reformate is removed as a liquid stream. The stabilized unit operates on the principle of atmospheric distillation and it removes the light gases from the reformate (gasoline) product. Reactors are loaded with Pt-Re catalysts on an alumina support. The catalyst is bi-functional, the alumina provides acid function and Pt-Re provides the metal function for dehydrogenation of naphthenes.

The focus of the current study is to simulate three reactor systems for a membrane-based packed bed reactor as well as for fixed bed reactors to compare the productions of each configuration and to do an economic evaluation and afterword the exergy analysis of the Fixed Bed Membrane Reactor System.[40]

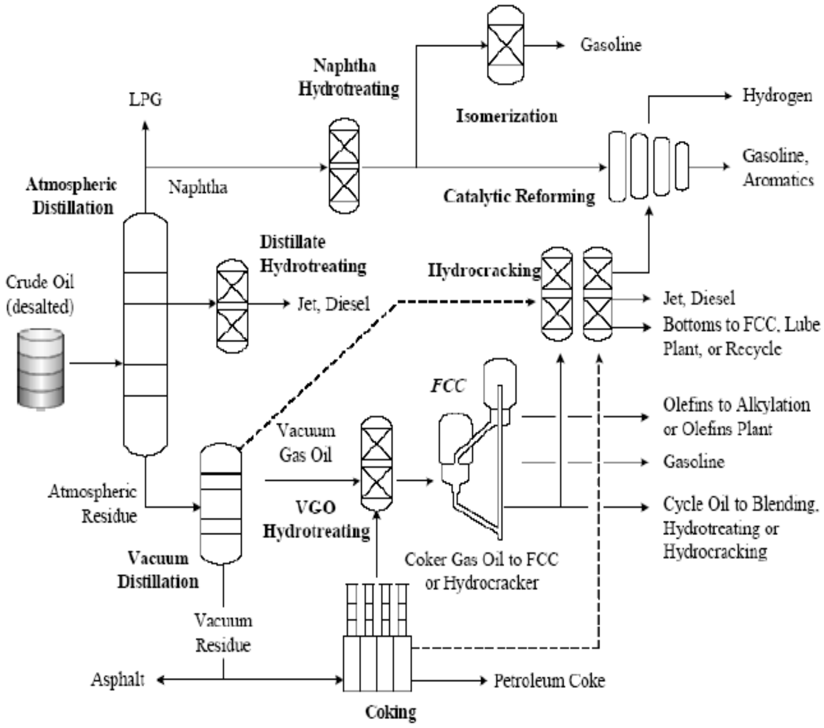

Figure 1.1: A fully integrated Petroleum Refining Unit PFD.

2.1 Hydrocarbon Chemistry, Composition of Reformer Feed and Products:

Naphtha Feed to a reforming system consists of C_6 to C_{11}, paraffin, naphthenes, and aromatics The reforming system, process naphthenes, and paraffin into aromatics, and make for the usable either as motor fuel (high octane rating) or as good source of high-value petrochemical industries feedstock aromatics. These aromatics are termed as specifics stock for other industries.

2.2 Reforming Reaction

2.2.1 Naphthenes Dehydrogenation Reaction

The mechanism of conversion of an aromatic from a naphthene (either a cyclo-hexane or a cyclo-pentane) is the dehydrogenation of cyclohexane, this of the reaction of an aromatics from its corresponding cyclo group is quantities and is very rapid. The dehydrogenation reaction is very easy to promote with naphthenic feed contents and produce hydrogen as by-products, The dehydrogenation of Naphthenes is very easy to proceed and being endothermic, it is promoted with a metal catalyst function that requires low pressure and elevated temperature conditions. So it is termed as high severity condition reactions.

Cyclohexane $\longrightarrow$ Benzene + 3 H2 Reaction - 1 Naphthenes

2.2.2 Naphthenes and Paraffin Isomerization Reaction

The isomerization of cyclo-pentane to a cyclo-hexane, as shown in reaction-2, must have to proceed as the first step for the production of an aromatics. The ring-opening and the rearrangements of the rings in paraffin are quite high that shows the formation of alkylcyclopentaes to cyclo-pentane is not a quantitative one, further this reaction mainly depend on operating conditions of the reactors. Paraffin isomerization, shown in reaction-3, occurs readily in commercial reforming operations but at typical operating temperatures the thermodynamic equilibrium is not strongly in favor of the more desirable (higher octane) branched isomers. In motor fuel applications, this reaction does contribute to the octane improvement of naphtha. Isomerization reactions result, from carbonium ion intermediate reactions. These reactions are promoted by an acidic catalyst function and are only slightly dependent on the operating pressure.

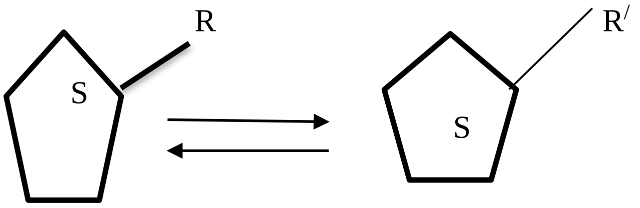

Reaction - 2 Naphthenes

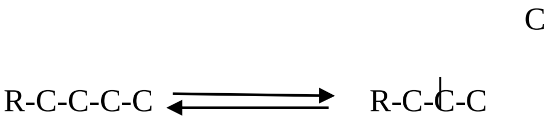

$$R\text{-}C\text{-}C\text{-}C\text{-}C \rightleftharpoons R\text{-}C\text{-}\overset{C}{\overset{|}{C}}\text{-}C$$

Reaction- 3 Paraffins

2.2.3. Paraffin Dehydrocyclization Reaction

It is the most difficult reaction to proceed with having very complex molecular arrangements from paraffin to Naphthenes. The equilibrium consideration limits this reaction in the case of light paraffin in the naphtha feed. If the molecular weight of the paraffin increases the paraffin cyclization steps easily promoted due to the increased probability of the Naphthenes formation. Might be this effect also suits for the heavier paraffin to hydrocrack? Further Dehydrocyclization is carried out at low pressure and high-temperature conditions. This reaction requires catalysts metal as well as acidic function for promotion.

2.2.4 Hydrocracking

This reaction requires high pressure and high-temperature conditions contrary to the first two reactions described above. Probably, it is because of the strained ring isomerization and ring formation of the feed alkylcyclopentanes and paraffin must experience, which requires an acid function of the catalysts to promote for acid-promoted hydrocracking which is very strong. This reaction consumes hydrogen and resultantly less yield of hydrogen. But the conversion of paraffin to concentrate aromatics gives high boiling range gasoline.

2.2.5 DE methylation

This also very high pressure and temperature conditions reaction and is generally termed as a very high severity reforming reaction. It is often occurring during the star-up of a unit followed by catalysts replacement or regeneration. This is a metal-catalyzed reaction carried out at a high temperature and pressure conditions, which can be inhibited by reduction of the metal catalyst function by introducing sulfur or another metal similar to some bimetallic catalysts system.

2.2.6 DE alkylation of Aromatics

This reaction is almost similar to the reaction of aromatic demethylation, having a difference in the size of the fragment removes from the main ring. If the alkyl side chain is sufficiently large, this cab seen and analyzed as acid carbonium ion cracking side reaction of the sude chain. This also carried out at high pressure and temperature conditions. The reaction rates change considerably due to the presence of an excess amount of paraffin and naphthenes in the reformer feed, further, these reactions are undergoing a very complicated reaction mechanism of occurring in parallel and series.

2.3. Relative Reaction Rate

In experimental pure component work, individual hydrocarbons were reformed in a pilot plant unit. Compounds studies were normal hexane, methylcyclopentane and cyclohexane in the C_6 hydrocarbon group, and normal heptane group, methyl cyclohexane pressure was varied between 5 and 21 kg/cm2 (70 and 300 PSIG), and reaction temperature was varied between 450 and 500^{o}C (840 and 1021^{0}F)". Hydrogen to hydrocarbon mole ratios were nominally 5 to 7, using recycle Hydrogen.

Table 1: Relative reactions rated of a commercial reforming process

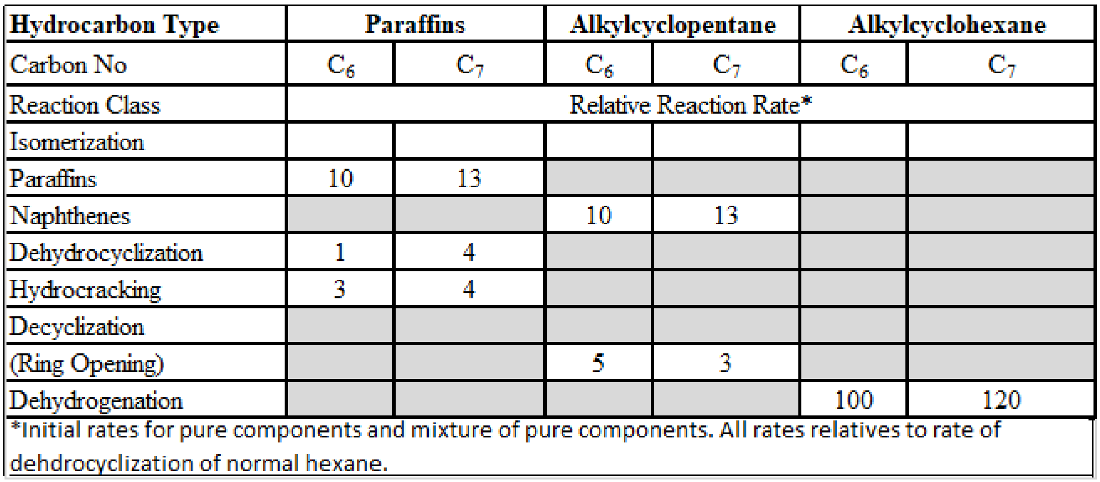

Hydrocarbon Type	Paraffins		Alkylcyclopentane		Alkylcyclohexane	
Carbon No	C_6	C_7	C_6	C_7	C_6	C_7
Reaction Class	Relative Reaction Rate*					
Isomerization						
Paraffins	10	13				
Naphthenes			10	13		
Dehydrocyclization	1	4				
Hydrocracking	3	4				
Decyclization						
(Ring Opening)			5	3		
Dehydrogenation					100	120

*Initial rates for pure components and mixture of pure components. All rates relatives to rate of dehdrocyclization of normal hexane.

2.4 Heats of Reaction

Heats of reaction for the reactions of paraffin to naphthene, naphthene to aromatic, and paraffin hydrocracking are shown in Table 2.2.

Table 2: Heat of Reactions

Reaction	ΔH (Kcal/mole H_2	
Paraffins → Naphthenes	+10.5	Endothermic
Naphthenes → Aromatics	+16.9	Endothermic
Hydrocracking	-13.5	Exothermic

2.5 Dual Function Reforming Catalyst Chemistry

The reaction mechanisms are shown in Figure 2.5 reveals that there are two types of catalysts reaction in which some are termed as acidic and others are known as metallic catalysts. It defined that the reforming process belongs to the dual-function catalysts system. Such a catalyst system shows a phenomenon of separate and distinct sites of the reacting molecule transferring from one site to another. Current thinking leads toward a modified picture in which a single site or single complex is responsible for the entire reaction sequence. It should be pointed out that presently it is only a concept and is not supported by unequivocal evidence. Besides, one must question the mass transfer limitations that would be involved in migration between separate sites.

The selection of a catalyst and a set of operating conditions will depend on the relative reaction rates and emphasis that is to be put on activity or yield or stability or some particular combination of all factors. This makes the picture complex, but it also provides a great deal of flexibility which permits the selection of specific catalyst formations for specific applications.

2.6 Major Reforming Variables

The purpose of this section is to discuss the major Reforming operating variables, their relation to unit performance, and the estimation of shifts in performance due to operational changes. The operating variables which are the most pertinent are shown in Table 3. For practical purposes, these variables are sufficient to define a Reforming Operation.

Table 3: Independent and dependent variable

INDEPENDENT VARIABLE	DEPENDENT VARIABLES
Types of Catalysts	Catalyst activity
Temperature of Reactor	Rx. Effluent
Space Velocity	Product quality
Pressure of Reactor	Catalyst stability

2.6.1 Types of Catalysts

Catalyst selection has most likely been in the sole priority and a subject to of the client for its particular requirements and it requires a very detailed FEED and advanced level consultancy involvement to decide the types of catalysts for its system. The reforming catalyst system is through valuable and viable consultant recommendations to meet the basic requirements that are chosen to meet reforming yield, catalyst activity, stability parameters. For instance, catalyst type will affect by the required temperature to meet a particular product quality.

2.6.2 Temperature of Reactor

The reactor temperature of a reforming system plays a very key role. Reforming catalyst adversely affected by the elevated temperature conditions and it leads to loss of production in general and of course the catalyst stability too. At very high temperatures due to thermal degradation the reformate yield and catalyst stability badly affected at the temperature of 543 ^{0}C (10I0 ^{O}F).

The reactor temperature cab is defined as (1) Weighted Average Inlet Temperature (WAIT) and (2) Weighted Average Bed Temperature (WABT). These can be calculated as follows:

WAIT = The summation of the Wt. fraction catalyst in bed multiplied by Bed inlet temperature.

WABT= The summation of the Wt. fraction catalyst in bed multiplied by Average of the bed inlet and outlet temperatures.

2.6.3 Space Velocity

Space velocity is a measure of the naphtha which is processed over a given amount of catalyst over a set length of time. When the hourly volume charge rate of naphtha and the volume of catalyst are used, the term is liquid hourly space velocity / LHSV'. When weights are used, the term is weight hourly space velocity Either is applicable in following a reformer unit operation when a set catalyst density and volume is involved. Space velocity has a major effect on product quality (for example octane number). The higher the space velocity the lower the product RONC or the less the amount of reaction allowed at a fixed WAIT. Increased reactor temperature will offset this effect-Within Normal Platforming design parameters, space velocity has little effect on product yields and catalyst stability (on a barrel per pound basis). At very low velocities, thermal reactions can occur to a sufficient degree to decrease reformate yields. there is no known upper limit on space velocity, reactor temperatures have to be increased to maintain the product quality and above a certain point, this can again cause unfavorable thermal reactions which will lower selectivity.

2.6.4 Pressure of Reactor

As the reactor temperature is a very vital operating variable in the naphtha reforming process, similarly the reactor pressure is equally important for the smooth and safe operation of the reactors system to provide the good yields, and it also affects reactor temperature requirement and the stability of the catalysts. Reactor pressure has no theoretical limitations, although practical design limitations have effect reactor pressure as high as 49 kg/cm2 (700 PSIG) and as low as 5.6 kg/cm2 (80 PSIG) have been run commercially with units under construction for pressures as low as 3.5 kg/cm2 (50 PSIG). By lowering the reactor pressure will increase the production of hydrogen and reformates.

2.6.4 Hydrogen/Hydrocarbon

Hydrogen/hydrocarbon (H_2/HC) ratio is defined as the moles of recycle hydrogen /per mole of naphtha charged to the unit. Recycle hydrogen is necessary for the reforming unit operation for purposes of catalyst stability. It has the effect of sweeping the reaction product and condensable materials from the catalyst and supplying the catalyst with readily available hydrogen.

An increase in the H_2/HC ratio will move the naphtha through the reactor at a faster rate and supply a greater heat sink for the endothermic heat of reaction. The result is increased stability with little effect on product quality or yields.

2.7 Thermodynamics of Reforming Reactions

The reforming reaction is like dehydrogenation is highly endothermic and has a pivotal role in the reforming system for the production of gasoline and hydrogen as a by-product. There are commonly three reactor system is being operated in most of the world refinery with preheating fired heater system for each reactor. This reaction is reversible and equilibrium is established with temperature and pressure. The equilibrium constant is calculated for each reaction. The reforming process is usually performed at a high temperature with low pressure. The hydrogen partial pressure is used to convert the aromatics into required yields by adjusting the hydrogen to hydrocarbon mole ratio.

Industrially, the product of main interest is aromatic components and the sub-division of 8-carbon aromatics needs to be taken into account. Other important reactions namely paraffin to aromatic dehydrocyclization, trans alkylation, and isomerization of aromatics have not been taken into account. New to this improved model, is the further sub-division of 8-carbon aromatics into four components (ethylbenzene, and ortho, meta, and para isomers of xylene) along with their respective variation is taken into account [32]. The dehydrogenation reaction scheme is presented in Table 2.3. along with reported rates of reaction.

In addition to the modeling of the reaction kinetics, the reactor design has been the focus of the research. A fluidized bed reactor (FBR) was proposed by Rahimpour to replace the conventional reactor. The idea behind the use of FBR is to use catalyst particles in the 100-micron range to eliminate inner mass transfer resistance combined with negligible pressure drop due to fluidization. In recent studies, the transformation of FBR into a membrane-based fluidized bed reactor has been proposed [16, 17].

2.8 Fluidized-Bed Process

The fluidization process is a method for intimate contact of a finely ground solid such as catalyst particles with a fluid such as a gas. Figure 2.6 (a) shows what happens when a fluid such as gas is passed upward from the bottom at a low flow rate through a fixed vessel filled with fine particles termed as (FBR) fixed bed reactor. This results in gas production through the interstates between stationary particles. As the flow rate is increased, particles tend to vibrate in a restricted manner and start moving apart. The bed is now just starting to expand. By increasing the gas velocity to a certain point all the particles become stationary due to the upward movement of gas. The equilibrium is established in between the frictional force of the particles and the flowing gas, adjacent particles no longer have a vertical component of compressive force, and the pressure drop through in these sections of the bed almost equals to the weight of gas and particles in that section. The bed is known as a fluidized bed or a bed at minimum fluidization.

To fluidize a fixed-bed the catalyst particles are crushed to a small size of about 100 microns. During the reforming process heat and mass transfer occurs within the reactor a hydrogen partial pressure gradient is set up which results in a net transfer of hydrogen to the shell side. This transfer of excess hydrogen results in displacing the reaction to the formation of more products.

The fluidization of catalyst particles is carried out by feeding the catalyst filled reactor with gas from the bottom through a porous plate distributor. Hydrogen is used as the sweep gas in the shell compartment where its flow is co-current with the reacting gas. The pressure drop in a fluidized bed is very low even though a very small catalyst size is used that would not be feasible in a fixed bed. The phenomena inside an FBMR is shown in Figure 2.7. The membrane material of choice is a palladium-silver alloy combining the excellent perm selectivity of palladium with silver providing mechanical stability. Hydrogen gas in the product permeates through the membrane surface, which results in the displacement of equilibrium in the forward direction and thus both reformate and hydrogen yield is increased. Hydrogen gas permeation through a dense membrane is explained via the solution diffusion model. The hydrogen gas molecules are split into atoms and diffuse through the palladium metal alloy. On the other side, the atoms are again recombined into atoms and pass into the sweep gas. The hydrogen permeation process is shown in Figure 2.8. Inside the shell, it can be a vacuum or hydrogen as sweep gas the pressure of which is a controlled variable to control the driving force for hydrogen permeation. In this simulation, the thickness of the membrane is taken to be 10 mm. Stainless steel support carries the Pd–Ag (23% Ag) membrane. Membrane length is equal to 6.29 m and its area is 30.02 m^2.

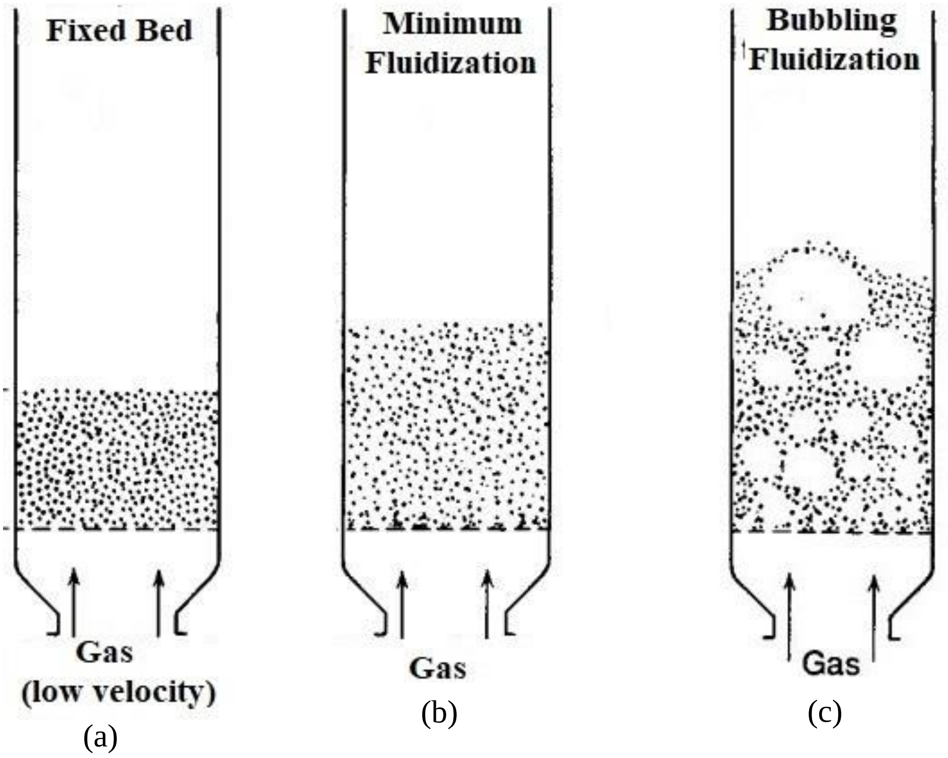

(a) (b) (c)

Figure 2.2: Different gas-solid contacting patterns in a fluidized bed

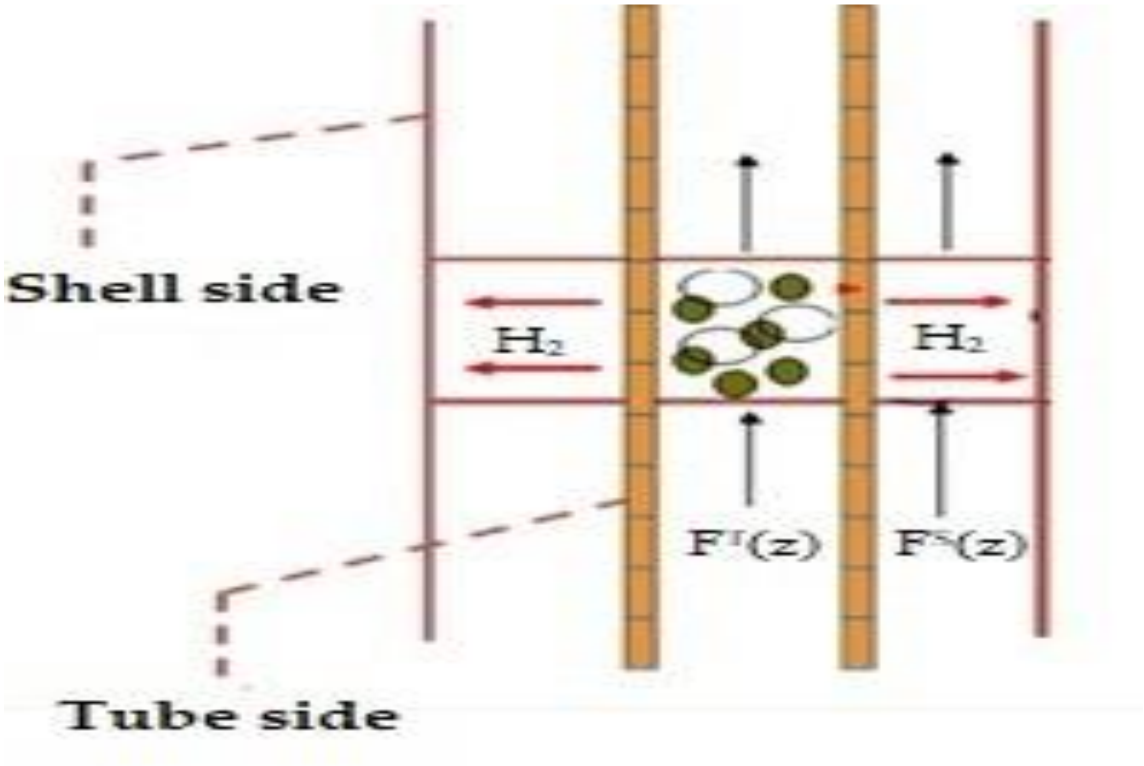

Figure 2.3: FBMR proposed model

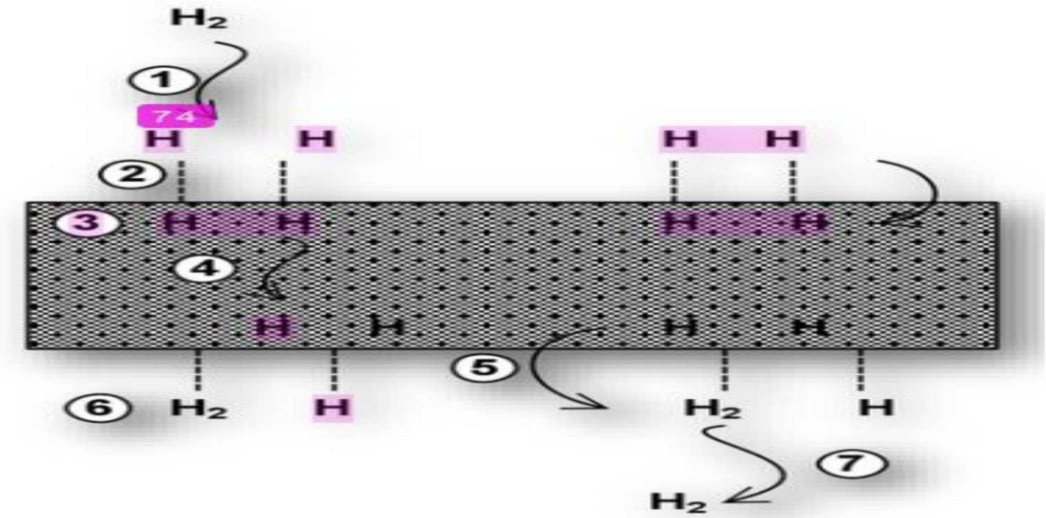

Figure 2.4:: Hydrogen permeation from walls [33]

Chapter-3

Literature Review

The catalytic reforming of naphtha is a process utilized for conversion of low-octane, straight-run naphtha into high-octane reformates which are then blended in gasoline to boost its octane rating. It is also a source of BTX (benzene, toluene, xylene isomers) which are important precursors for further chemical synthesis. A considerable amount of hydrogen gas is also produced in the process which is utilized in the refinery or other applications [1, 2]. Gasoline is still the fossil fuel of choice in terms of transportation although its combustion products are recognized as a source of global warming. In order to mitigate environmental concerns, various legislations are passed one of which is requirement of high RON [3].

RON or research octane number is the quality parameter of gasoline that shows how much compression it can withstand without knocking in a gasoline engine. The octane number of gasoline is conveniently boosted by use of catalytic reforming and it is carried out in three or four radial or axial flow fixed bed reactors. Mode of operation is semi-regenerative, cyclic or the newer continuous regenerative types classified according to their severity, and mode of catalyst regeneration. A PBR is used conventionally for naphtha reforming. It is a fixed bed type of reactor in which the catalyst is placed in a dumped arrangement. Catalyst particle size is kept at a value which is a compromise between pressure drop and increased surface area. Larger particles provide less resistance to gas flow but have low particle effectiveness factor [4]. Reducing the particle size increases area for mass transfer but the resulting low voidage causes excessive pressure to drop.

Chemical reactants are converted to products according to Le Chatelier’s principle by selective removal of the products from product gases [5,6]. One idea worth exploring is using a fluidized catalyst bed reactor with Pd membrane-based walls for naphtha reforming which is the focus of this work. This mode of reactor configuration enables simultaneous, in situ removal of hydrogen from product gases, which increases the production of aromatics as the reactants pass through the reactor. A membrane reactor is a reactor wherein the reactor walls are replaced with a perm-selective membrane material.

Various researchers have used membrane reactors for enhancement of product as a result of the shifting of thermodynamic equilibrium. Developing membrane reactor technology carries significance as a promising method for increasing hydrogen production by improving separation and recovery which will economize overall hydrogen production. In different studies palladium and its alloys such as palladium-copper [7], palladium-silver [8–9] and palladium [10] were utilized inside different reactors. For synthesis of methanol, Rahimpour and Ghader proposed membrane reactors with Pd–Ag membrane and pure Pd membrane [11,12]. Pasha [33] developed Excel interfacing with Aspen Plus to simulate FBMR for steam reforming. Tosti et al. have experimented with different configurations of palladium-based membrane reactors used for extraction of ultra-pure hydrogen [13]. One paper by Roy [14] focuses on the simulation of membrane based fluidized bed reformers and its economic aspects. Khosravanipour [15] and Rahimpour [16] presented the concept of membrane assisted naphtha reformer and studied the effects of in-situ hydrogen separation in a packed-bed reactor and fluidized bed reactor for naphtha reforming. Results presented showed an enhancement of aromatics along the reactor. Hydrogen gas is generated as the naphtha reforming reaction proceeds in the reactor. Hydrogen separation from the product side could lead to the formation of dehydrogenation products which are associated with an increase in reformate RON. In another study, Rahimpour et al [17] studied the effects of combining the endothermic naphtha reforming reaction and hydrogenation of aniline to nitrobenzene in a thermally coupled fluidized-bed reactor. All of the studies presented use MATLAB, FORTRAN or other software-based modeling approaches that are not readily accessible to design engineers in the process industry. Other than these theoretical studies not much have been explored and thus very few are available in the literature of fluidized-bed naphtha reformers within situ hydrogen separation via membrane. Modeling of a membrane reactor is a challenging task because of simultaneous occurrence of diffusion coupled with mass transfer and chemical reaction inside the reactor [18].

Aspen Plus is a widely employed process simulator for industrial process simulations in addition to various other simulation programs. In this study, an FBMR for naphtha reforming is developed on the Aspen Plus platform with Excel interfacing. In an

FBMR, both physical and chemical phenomena coexist and need to be taken into consideration. An adequate model for an FBMR thus be able to represent the physical and chemical phenomena simultaneously. The physical phenomena are implemented by utilizing the hydrodynamics theory as an integrated sub-model and chemical reactions are conveniently implemented by built-in power law input panel of Aspen Plus. Ideal reactor models are available as modules in Aspen Plus and are combined together in a sequential manner in a certain way to mimic the behavior inside the fluidized bed membrane reactors [19]. Excel is used for supplying of hydrodynamic parameters to Aspen for calculation of volumes and voidage in CSTR and PFR blocks of Aspen Plus. Membrane permeation model is based on Sievert's law given in Equation (4.1).

The reforming process is described in section 2. An industrial setup for a semi-regenerative reformer system was taken as an example from literature where three packed bed reformers are used. Section3 Provides the detail of Literature review. The details of the model building and flow sheeting process in the Aspen Plus environment with Excel interfacing is explained in Chapter 4. Results from the simulation are discussed and compared with FBR in section 5 followed by conclusions in section 6.

3.1 Objectives of the Study

Aspen Plus is an industry-leading software in terms of process design and is frequently is a program of choice for carrying out simulation and optimization studies. As of this writing, a fluidized bed membrane reactor is not available in the Aspen Plus environment so a customized approach is followed.

The first task as evident from the objectives of this study is to develop an Aspen Plus based model of a catalytic naphtha reformer. The fluidized bed reactor is represented by combining the ideal CSTR and PFR modules available inside Aspen Plus. The membrane separation process is incorporated through Excel interfacing.

The following steps were systematically followed to achieve the objective:

- Modeling of the catalytic naphtha reforming process occurring in a fluidized bed reactor in the Aspen Plus environment.
- Implement the hydrodynamic process occurring inside the fluidized bed using CSTR and PFR modules available in the Aspen Plus environment.

- Convert the model of FBR into FBMR via the addition of membrane permeation using an external Excel file through which Sievert’s equation implemented.
- Compare results from both of the reactors to study the benefits derived from the addition of membrane.

Chapter-4

Model Development

A fluidized bed being a non-ideal reactor such that its hydrodynamics cannot be simply assumed to be that of a plug flow type or a perfectly mixed one. Two distinct phases are identified in a fluidized bed: emulsion phase and bubble phase. An Excel file is developed for the calculation of the hydrodynamic parameters using the two-phase theory of fluidization. This Excel block calculates the flow distribution and the volumes of CSTR and PFR. Another Excel file implements the Sievert’s equation to simulate the phenomena of membrane permeation

Preliminary Assumptions:

Two distinct phases are identified in a fluidized bed: a dense phase and a lean phase composed of gas bubbles. The following is assumed for development of the model:

- Steady-state and pseudo-steady-state operation.
- Much of the reactions occur within the emulsion phase;
- Permeation of hydrogen occurs from emulsion phase only;
- Hydrogen diffuses through the membrane radially;
- Assumption of spherical bubbles hold;
- Movement of gas in bubbles is assumed to follow plug flow and due to very low quantity of catalyst the reaction rates are very low compared to emulsion phase gas;
- Contents of the bed are well mixed and both emulsion and bubble phase are at a uniform temperature;
- Adiabatic conditions;
- The membrane is 100% perm-selective for hydrogen;
- Sieverts’ law is applicable for hydrogen permeation through the membrane.

The following two sub-sections describe the membrane integration within Aspen Plus and the combination of CSTR and PFR reactor with the membrane module to simulate the overall FBMR process.

4.1 Simulating the Phenomena of Fluidization in Aspen Plus

A fluidized bed exhibits complex hydrodynamics to its model its behavior. The dense portion is comprised of the bubble phase and emulsion phases. Membrane permeation occurs simultaneously with the reaction. An Excel file is developed which calculates the hydrodynamic parameters of the fluidized bed. The equations used from the literature are presented in Table 4.1. The output from this file is transferred to the CSTR and PFR units through an internal Excel interface and transfer modules.

Gas flowing in the form of bubbles is modeled as flowing through a plug flow reactor and the gas flowing through the emulsion phase is modeled as flowing through a mixed flow reactor or a CSTR. In this way, the fluidized bed reactor is represented by PFR and CSTR which are available as standard modules in the Aspen Plus environment. A separate 'SPLT' Excel file is used to implement equations described in Table 4.1.

After evaluating the hydrodynamic parameters, the data is transferred to Aspen Plus which uses its internal database to calculate thermodynamic properties based on material and energy balance equations. The effluent streams from each section are then transferred to the 'TRF' Excel block where both effluent streams are mixed and besides, the Sievert's equation in the case of the FBMR is implemented. Afterward, the exit streams are transferred to respective PFR and CSTR for the next section (i+1). Calculations then proceed in this manner until they reach the topmost section of the bed.

Table 4.1: Hydrodynamic parameters [33-35]

Parameter	Equation
Superficial velocity at minimum fluidization	$\frac{1.75}{\epsilon_{mf}^3\varphi_s}\left[\frac{d_p\rho_g u_{mf}}{\mu}\right]^2+\frac{150(1-\epsilon_{mf})}{\epsilon_{mf}^3\varphi_s}\left[\frac{d_p\rho_g u_{mf}}{\mu}\right]$
Archimedes' number	$Ar=\frac{d_p^3\rho_g(\rho_p-\rho_g)g}{\mu^2}$
Bubble diameter	$d_b=d_{bm}(d_{bm}-d_{b0})exp(-0.3z/D)$ $d_{b0}=0.376(u_0-u_{mf})^2$

The coefficient for mass transfer from bubble to emulsion phase The velocity of bubble rise The volume fraction of the bubble phase to the overall bed Specific surface area for bubble Density for emulsion phase	$d_{bm} = 0.65\left[\frac{\pi}{4}D^2\left(u_0 - u_{mf}\right)\right]^{0.4}$ $K_{be} = \frac{u_{mf}}{3}\left[\left(4D_{jm}\epsilon_{mf}u_b/(\pi d_b)\right)\right]^{1/2}$ $u_b = u - u_{mf} + 0.711\sqrt{gd_b}$ $\delta = \left(u - u_{mf}\right)/u_b$ $a_b = 6\delta/d_b$ $\rho_e = \rho_p\left(1 - \epsilon_{mf}\right)$

4.2 Membrane Permeation.

The membrane performance is affected by non-uniformity in membrane fabrication, blockage of the membrane surface by catalyst dust, etc. The membrane permeation effectiveness factor (η) accounts for all these negative influences on the permeation rate and determined experimentally [15]. To simulate the hydrogen permeation process through the membrane tube, User a Model 2-unit operation block with an Excel spreadsheet was used to perform the calculations. Aspen Plus supplies properties of the feed stream of the user model and some additional parameters ($\eta, k, C_{mp}, E, R, T, P_{RH_2}, \text{and } P_{MH_2}$) to the Excel spreadsheet. Excel organizes this information and calculates product stream properties with hydrogen production rate (Q_{H_2}) based on Sieverts' law, Equation 4.1. This information is then returned to the Aspen Plus interface and results are displayed.

$$Q_{H_2} = \eta k C_{mp}\left[P_{RH_2}^{0.5} - P_{MH_2}^{0.5}\right]e^{\left(-\frac{E_a}{RT}\right)}\text{-----------------}\ (4.1)$$

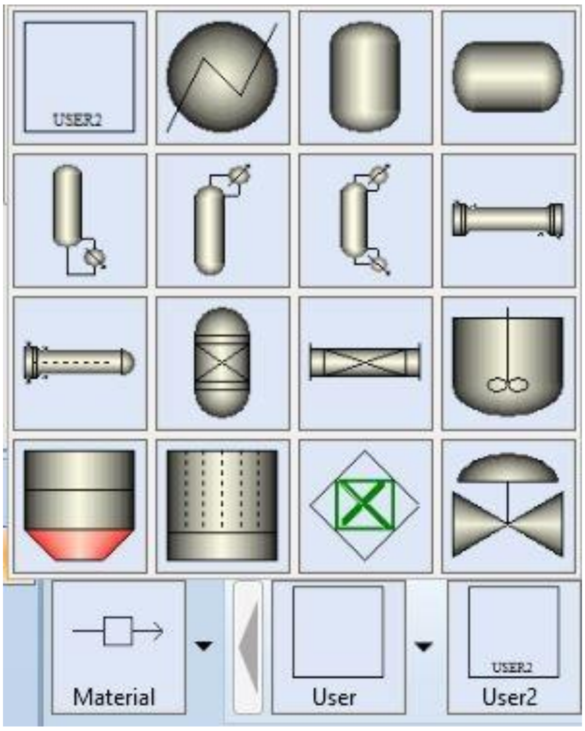

Figure 4.1: User 2 Custom Model Selection Pane in Aspen Plus.

Table 4.2: Defining Simulation Parameters.

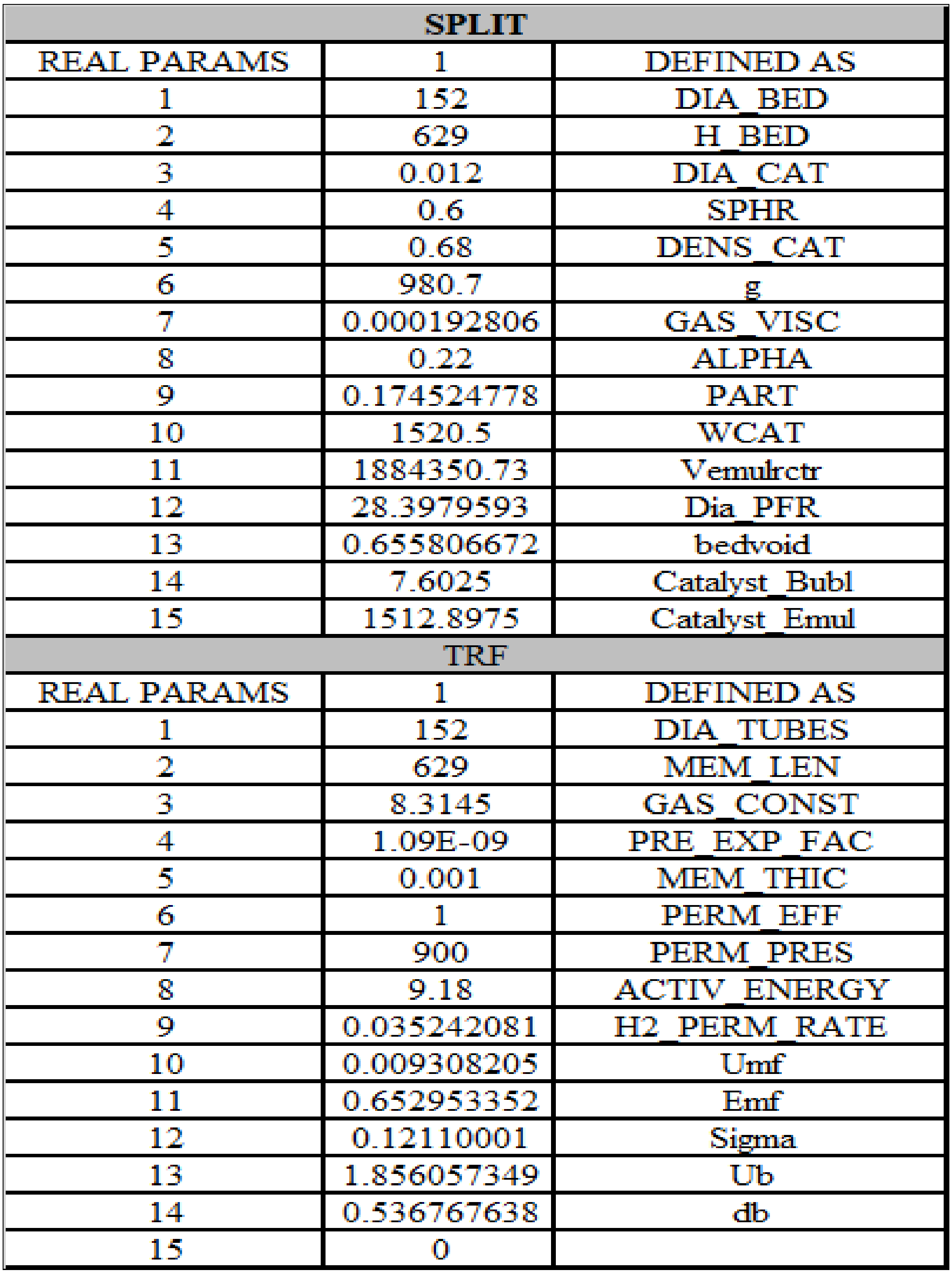

SPLIT		
REAL PARAMS	1	DEFINED AS
1	152	DIA_BED
2	629	H_BED
3	0.012	DIA_CAT
4	0.6	SPHR
5	0.68	DENS_CAT
6	980.7	g
7	0.000192806	GAS_VISC
8	0.22	ALPHA
9	0.174524778	PART
10	1520.5	WCAT
11	1884350.73	Vemulrctr
12	28.3979593	Dia_PFR
13	0.655806672	bedvoid
14	7.6025	Catalyst_Bubl
15	1512.8975	Catalyst_Emul
TRF		
REAL PARAMS	1	DEFINED AS
1	152	DIA_TUBES
2	629	MEM_LEN
3	8.3145	GAS_CONST
4	1.09E-09	PRE_EXP_FAC
5	0.001	MEM_THIC
6	1	PERM_EFF
7	900	PERM_PRES
8	9.18	ACTIV_ENERGY
9	0.035242081	H2_PERM_RATE
10	0.009308205	Umf
11	0.652953352	Emf
12	0.12110001	Sigma
13	1.856057349	Ub
14	0.536767638	db
15	0	

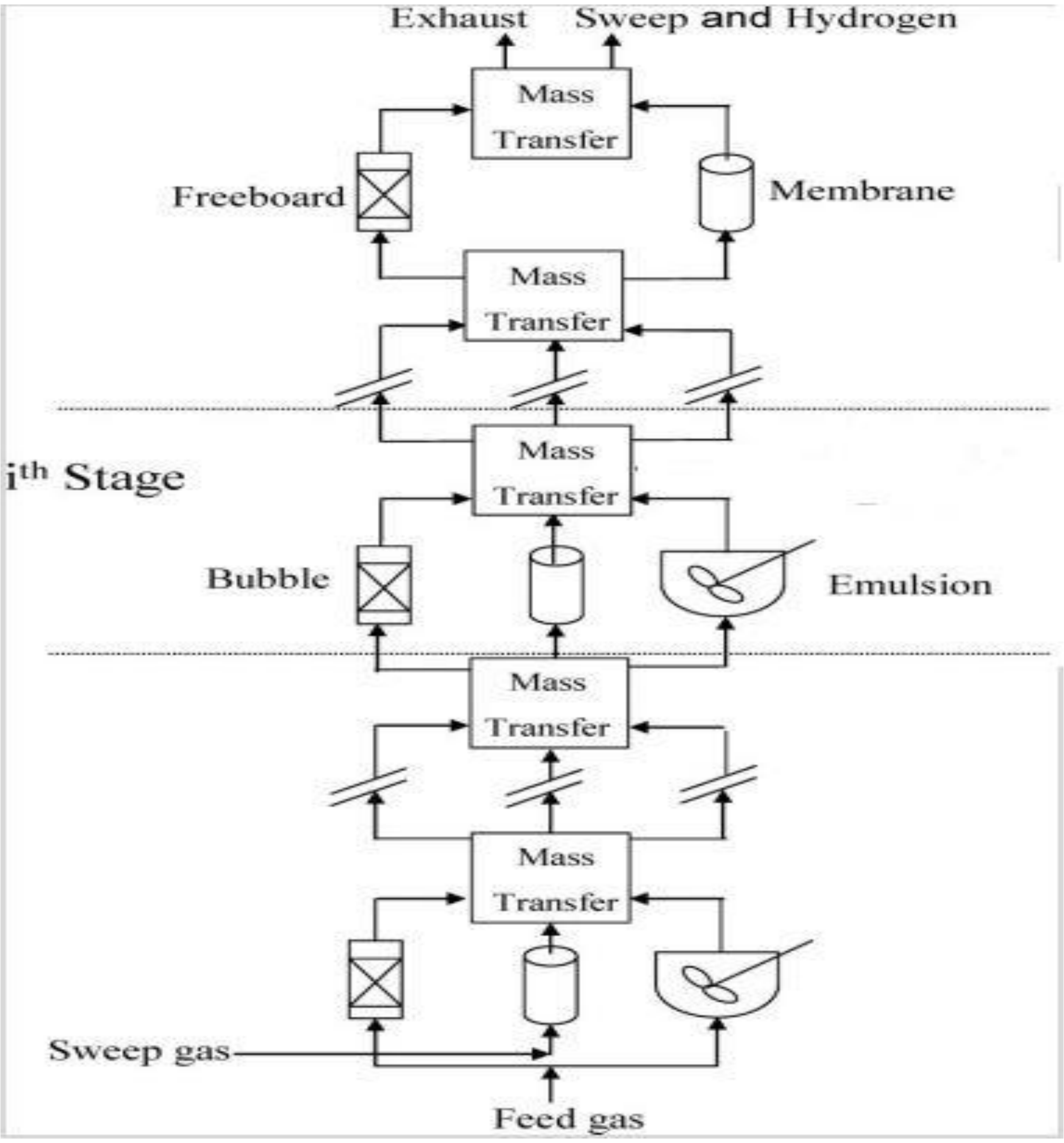

Figure 4.2: Sequential modular scheme for simulation of FBMR

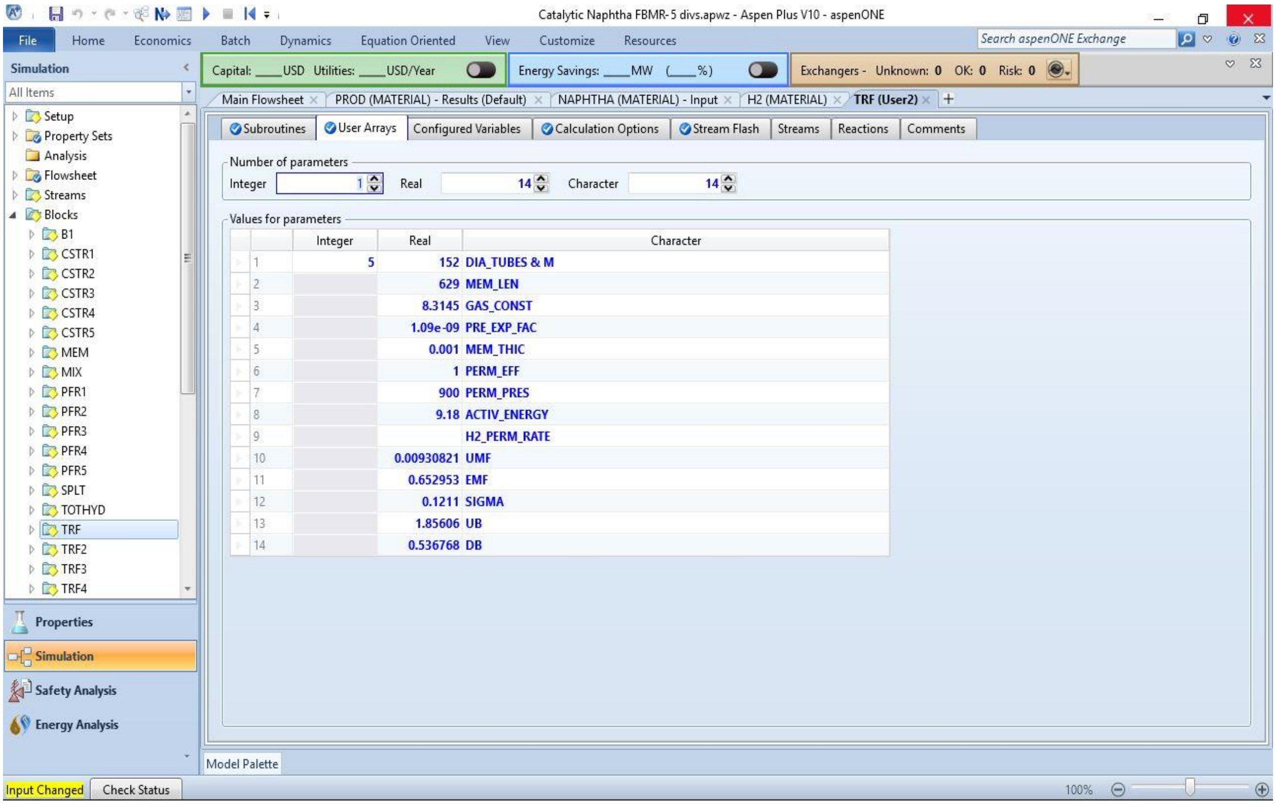

Number of parameters

Integer: 1 Real: 14 Character: 14

Values for parameters

	Integer	Real	Character
1	5	152	DIA_TUBES & M
2		629	MEM_LEN
3		8.3145	GAS_CONST
4		1.09e-09	PRE_EXP_FAC
5		0.001	MEM_THIC
6		1	PERM_EFF
7		900	PERM_PRES
8		9.18	ACTIV_ENERGY
9			H2_PERM_RATE
10		0.00930821	UMF
11		0.652953	EMF
12		0.1211	SIGMA
13		1.85606	UB
14		0.536768	DB

Figure 4.3: Mass Transfer input pane for User 2 model

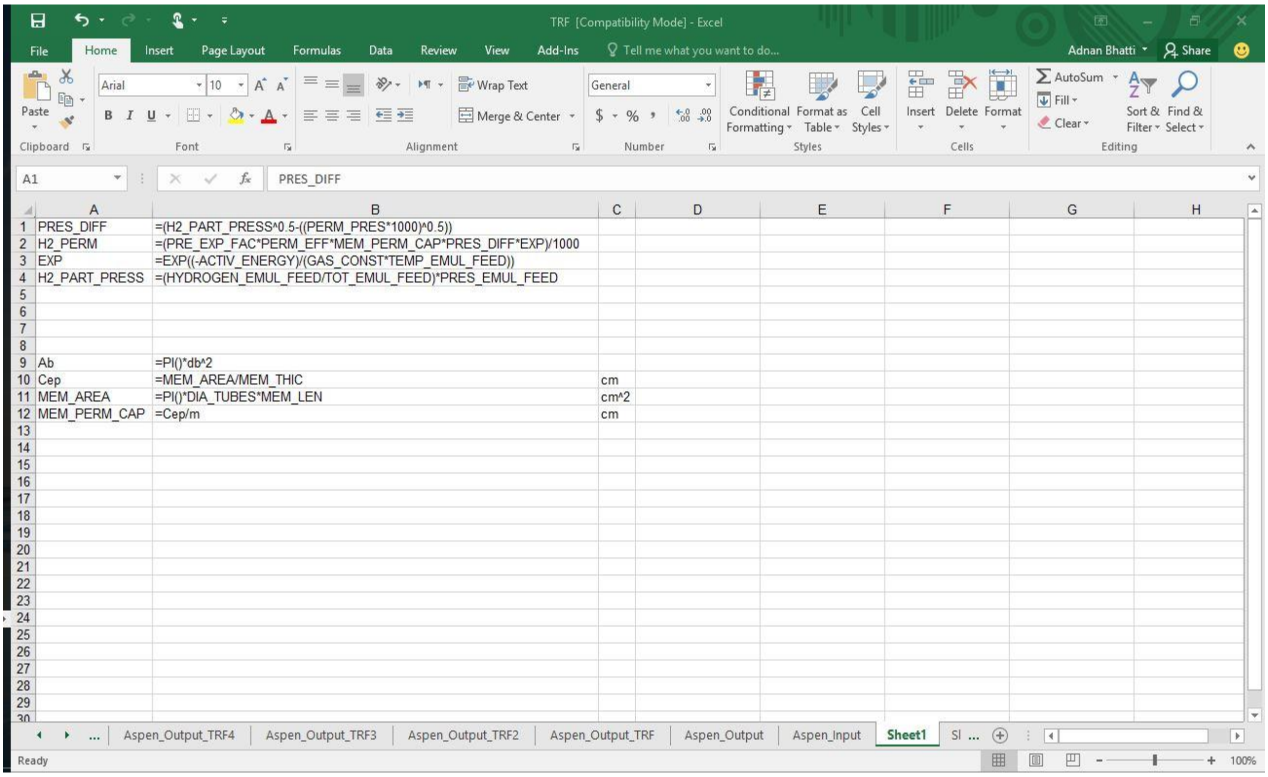

A1: PRES_DIFF

	A	B	C
1	PRES_DIFF	=(H2_PART_PRESS^0.5-((PERM_PRES*1000)^0.5))	
2	H2_PERM	=(PRE_EXP_FAC*PERM_EFF*MEM_PERM_CAP*PRES_DIFF*EXP)/1000	
3	EXP	=EXP((-ACTIV_ENERGY)/(GAS_CONST*TEMP_EMUL_FEED))	
4	H2_PART_PRESS	=(HYDROGEN_EMUL_FEED/TOT_EMUL_FEED)*PRES_EMUL_FEED	
9	Ab	=PI()*db^2	
10	Cep	=MEM_AREA/MEM_THIC	cm
11	MEM_AREA	=PI()*DIA_TUBES*MEM_LEN	cm^2
12	MEM_PERM_CAP	=Cep/m	cm

Figure 4.4: Excel Sheet for TRF Block

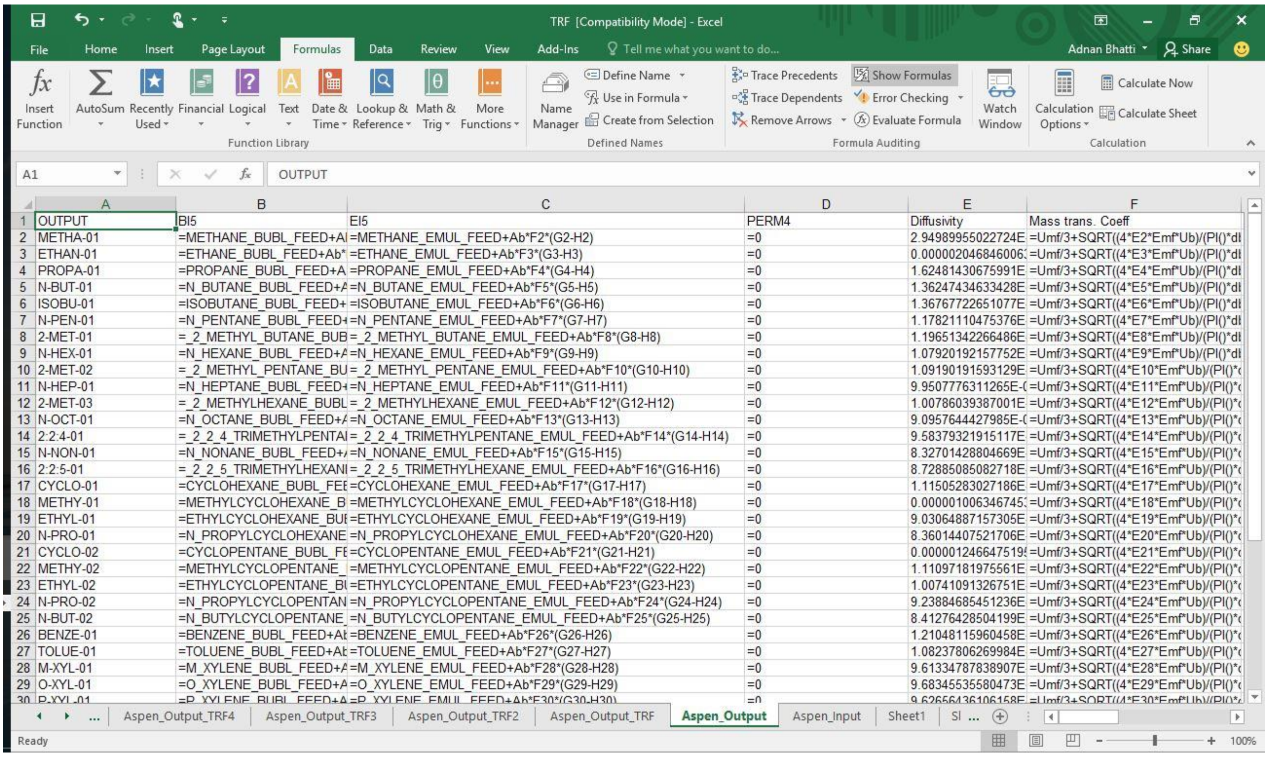

A1 OUTPUT

	A	B	C	D	E	F
1	OUTPUT	BI5	EI5	PERM4	Diffusivity	Mass trans. Coeff
2	METHA-01	=METHANE_BUBL_FEED+A	=METHANE_EMUL_FEED+Ab*F2*(G2-H2)	=0	2.94989955022724E	=Umf/3+SQRT((4*E2*Emf*Ub)/(PI()*d
3	ETHAN-01	=ETHANE_BUBL_FEED+Ab*	=ETHANE_EMUL_FEED+Ab*F3*(G3-H3)	=0	0.0000020468460063	=Umf/3+SQRT((4*E3*Emf*Ub)/(PI()*d
4	PROPA-01	=PROPANE_BUBL_FEED+A	=PROPANE_EMUL_FEED+Ab*F4*(G4-H4)	=0	1.62481430675991E	=Umf/3+SQRT((4*E4*Emf*Ub)/(PI()*d
5	N-BUT-01	=N_BUTANE_BUBL_FEED+	=N_BUTANE_EMUL_FEED+Ab*F5*(G5-H5)	=0	1.36247434633428E	=Umf/3+SQRT((4*E5*Emf*Ub)/(PI()*d
6	ISOBU-01	=ISOBUTANE_BUBL_FEED+	=ISOBUTANE_EMUL_FEED+Ab*F6*(G6-H6)	=0	1.36767722651077E	=Umf/3+SQRT((4*E6*Emf*Ub)/(PI()*d
7	N-PEN-01	=N_PENTANE_BUBL_FEED	=N_PENTANE_EMUL_FEED+Ab*F7*(G7-H7)	=0	1.17821110475376E	=Umf/3+SQRT((4*E7*Emf*Ub)/(PI()*d
8	2-MET-01	=_2_METHYL_BUTANE_BUB	=_2_METHYL_BUTANE_EMUL_FEED+Ab*F8*(G8-H8)	=0	1.19651342266486E	=Umf/3+SQRT((4*E8*Emf*Ub)/(PI()*d
9	N-HEX-01	=N_HEXANE_BUBL_FEED+	=N_HEXANE_EMUL_FEED+Ab*F9*(G9-H9)	=0	1.07920192157752E	=Umf/3+SQRT((4*E9*Emf*Ub)/(PI()*d
10	2-MET-02	=_2_METHYL_PENTANE_BU	=_2_METHYL_PENTANE_EMUL_FEED+Ab*F10*(G10-H10)	=0	1.09190191593129E	=Umf/3+SQRT((4*E10*Emf*Ub)/(PI()*
11	N-HEP-01	=N_HEPTANE_BUBL_FEED	=N_HEPTANE_EMUL_FEED+Ab*F11*(G11-H11)	=0	9.9507776311265E-	=Umf/3+SQRT((4*E11*Emf*Ub)/(PI()*
12	2-MET-03	=_2_METHYLHEXANE_BUBL	=_2_METHYLHEXANE_EMUL_FEED+Ab*F12*(G12-H12)	=0	1.00786039387001E	=Umf/3+SQRT((4*E12*Emf*Ub)/(PI()*
13	N-OCT-01	=N_OCTANE_BUBL_FEED+	=N_OCTANE_EMUL_FEED+Ab*F13*(G13-H13)	=0	9.0957644427985E-	=Umf/3+SQRT((4*E13*Emf*Ub)/(PI()*
14	2:2:4-01	=_2_2_4_TRIMETHYLPENTA	=_2_2_4_TRIMETHYLPENTANE_EMUL_FEED+Ab*F14*(G14-H14)	=0	9.58379321915117E	=Umf/3+SQRT((4*E14*Emf*Ub)/(PI()*
15	N-NON-01	=N_NONANE_BUBL_FEED+	=N_NONANE_EMUL_FEED+Ab*F15*(G15-H15)	=0	8.32701428804669E	=Umf/3+SQRT((4*E15*Emf*Ub)/(PI()*
16	2:2:5-01	=_2_2_5_TRIMETHYLHEXAN	=_2_2_5_TRIMETHYLHEXANE_EMUL_FEED+Ab*F16*(G16-H16)	=0	8.72885085082718E	=Umf/3+SQRT((4*E16*Emf*Ub)/(PI()*
17	CYCLO-01	=CYCLOHEXANE_BUBL_FE	=CYCLOHEXANE_EMUL_FEED+Ab*F17*(G17-H17)	=0	1.11505283027186E	=Umf/3+SQRT((4*E17*Emf*Ub)/(PI()*
18	METHY-01	=METHYLCYCLOHEXANE_B	=METHYLCYCLOHEXANE_EMUL_FEED+Ab*F18*(G18-H18)	=0	0.0000010063467451	=Umf/3+SQRT((4*E18*Emf*Ub)/(PI()*
19	ETHYL-01	=ETHYLCYCLOHEXANE_BU	=ETHYLCYCLOHEXANE_EMUL_FEED+Ab*F19*(G19-H19)	=0	9.03064887157305E	=Umf/3+SQRT((4*E19*Emf*Ub)/(PI()*
20	N-PRO-01	=N_PROPYLCYCLOHEXANE	=N_PROPYLCYCLOHEXANE_EMUL_FEED+Ab*F20*(G20-H20)	=0	8.36014407521706E	=Umf/3+SQRT((4*E20*Emf*Ub)/(PI()*
21	CYCLO-02	=CYCLOPENTANE_BUBL_F	=CYCLOPENTANE_EMUL_FEED+Ab*F21*(G21-H21)	=0	0.0000012466475195	=Umf/3+SQRT((4*E21*Emf*Ub)/(PI()*
22	METHY-02	=METHYLCYCLOPENTANE_	=METHYLCYCLOPENTANE_EMUL_FEED+Ab*F22*(G22-H22)	=0	1.11097181975561E	=Umf/3+SQRT((4*E22*Emf*Ub)/(PI()*
23	ETHYL-02	=ETHYLCYCLOPENTANE_B	=ETHYLCYCLOPENTANE_EMUL_FEED+Ab*F23*(G23-H23)	=0	1.00741091326751E	=Umf/3+SQRT((4*E23*Emf*Ub)/(PI()*
24	N-PRO-02	=N_PROPYLCYCLOPENTAN	=N_PROPYLCYCLOPENTANE_EMUL_FEED+Ab*F24*(G24-H24)	=0	9.23884685451236E	=Umf/3+SQRT((4*E24*Emf*Ub)/(PI()*
25	N-BUT-02	=N_BUTYLCYCLOPENTANE_	=N_BUTYLCYCLOPENTANE_EMUL_FEED+Ab*F25*(G25-H25)	=0	8.41276428504199E	=Umf/3+SQRT((4*E25*Emf*Ub)/(PI()*
26	BENZE-01	=BENZENE_BUBL_FEED+A	=BENZENE_EMUL_FEED+Ab*F26*(G26-H26)	=0	1.21048115960458E	=Umf/3+SQRT((4*E26*Emf*Ub)/(PI()*
27	TOLUE-01	=TOLUENE_BUBL_FEED+A	=TOLUENE_EMUL_FEED+Ab*F27*(G27-H27)	=0	1.08237806269984E	=Umf/3+SQRT((4*E27*Emf*Ub)/(PI()*
28	M-XYL-01	=M_XYLENE_BUBL_FEED+	=M_XYLENE_EMUL_FEED+Ab*F28*(G28-H28)	=0	9.61334787838907E	=Umf/3+SQRT((4*E28*Emf*Ub)/(PI()*
29	O-XYL-01	=O_XYLENE_BUBL_FEED+A	=O_XYLENE_EMUL_FEED+Ab*F29*(G29-H29)	=0	9.68345535580473E	=Umf/3+SQRT((4*E29*Emf*Ub)/(PI()*
30	P-XYL-01	=P_XYLENE_BUBL_FEED+A	=P_XYLENE_EMUL_FEED+Ab*F30*(G30-H30)	=0	9.62656436106158E	=Umf/3+SQRT((4*E30*Emf*Ub)/(PI()*

Figure 4.5: Aspen Output sheet in Excel for TRF block

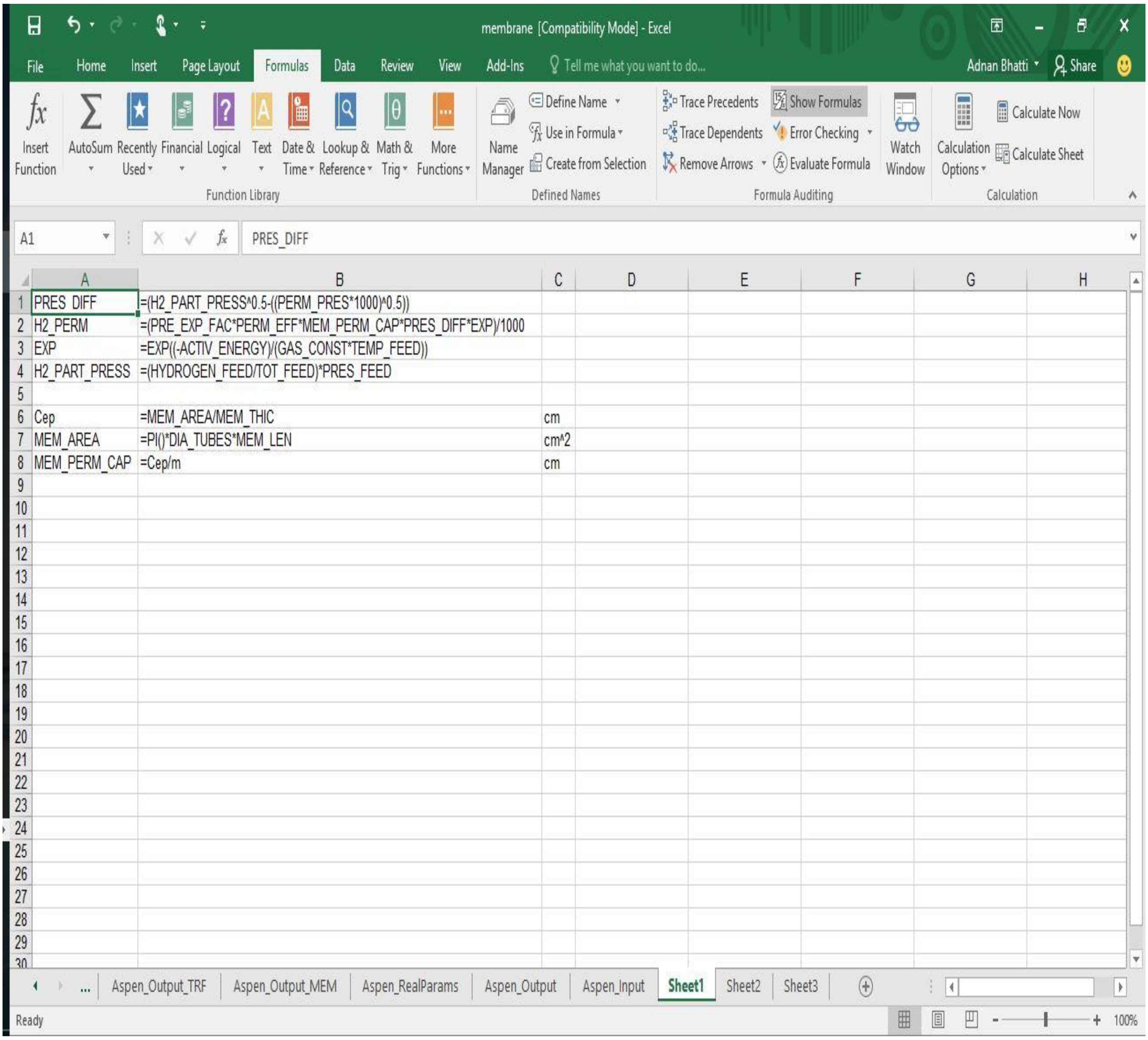

	A	B	C
1	PRES_DIFF	=(H2_PART_PRESS^0.5-((PERM_PRES*1000)^0.5))	
2	H2_PERM	=(PRE_EXP_FAC*PERM_EFF*MEM_PERM_CAP*PRES_DIFF*EXP)/1000	
3	EXP	=EXP((-ACTIV_ENERGY)/(GAS_CONST*TEMP_FEED))	
4	H2_PART_PRESS	=(HYDROGEN_FEED/TOT_FEED)*PRES_FEED	
5			
6	Cep	=MEM_AREA/MEM_THIC	cm
7	MEM_AREA	=PI()*DIA_TUBES*MEM_LEN	cm^2
8	MEM_PERM_CAP	=Cep/m	cm

Figure 4.6: Equations sheet in Excel for Simple Membrane Permeation Block

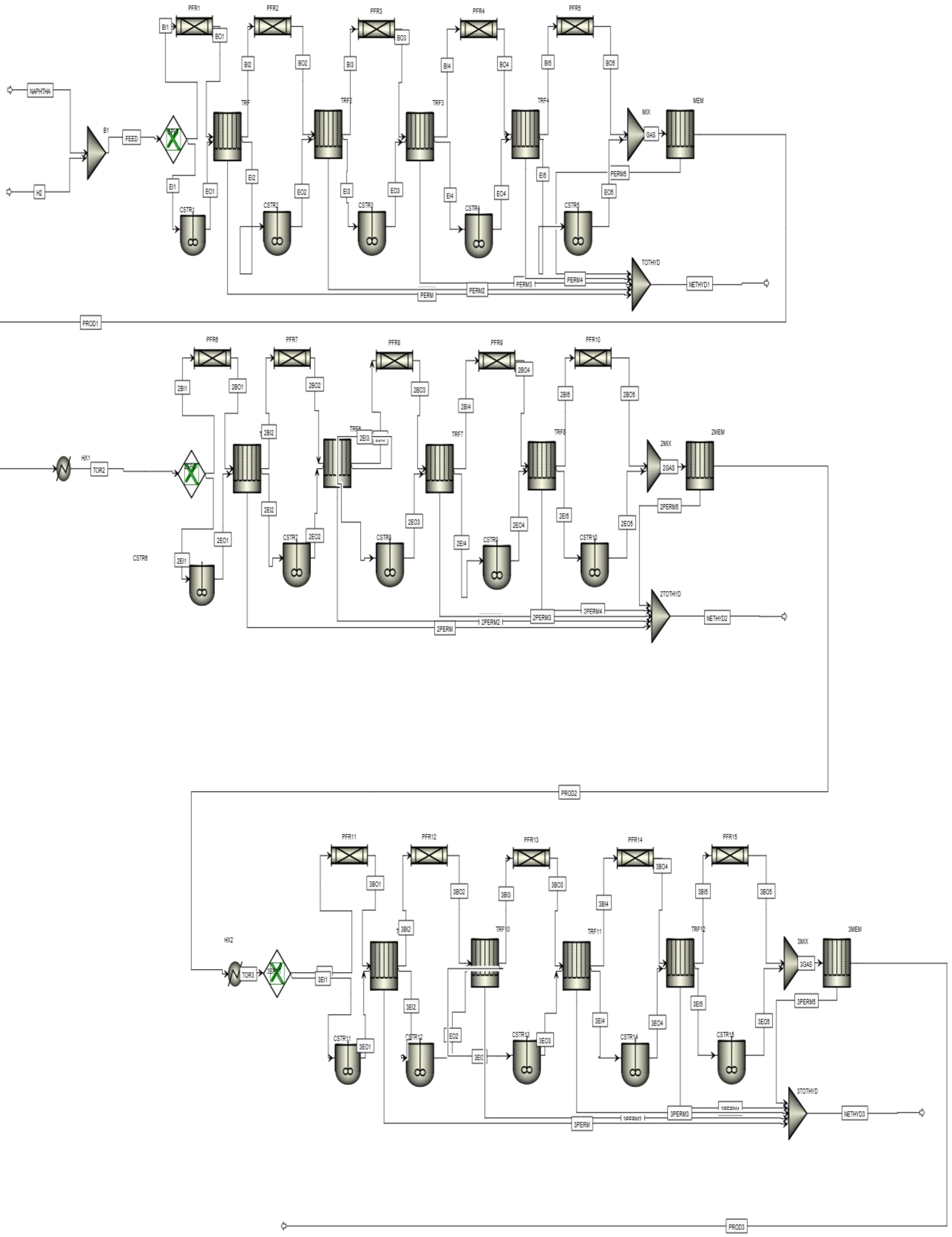

Figure 4.7: FBMR Three Reactor Configuration

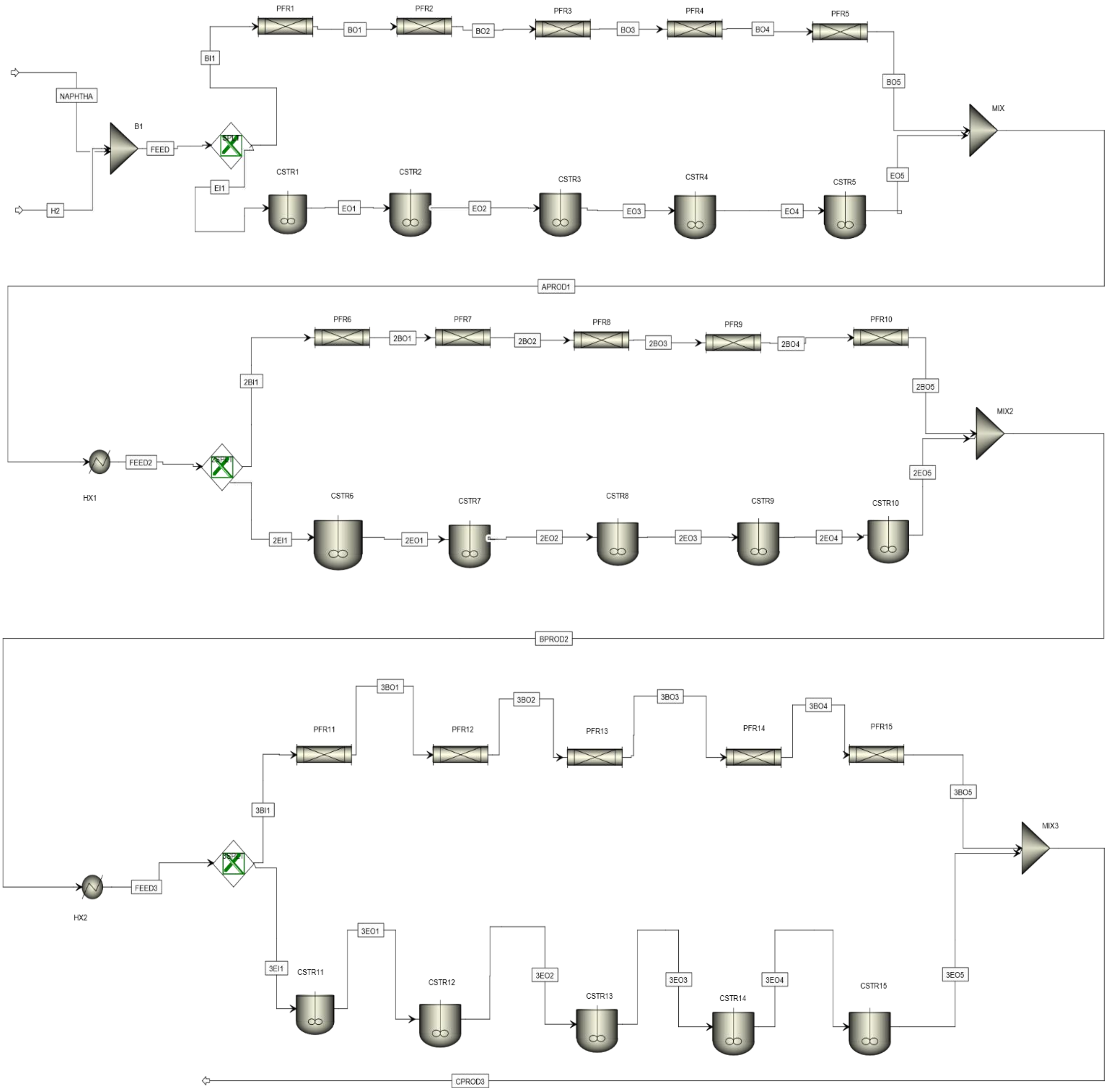

Figure 4.8: FBR Three reactors Configuration

4.3 Determination of Stages for Reactors

It explains the effect of increasing the number of stages, it will affect the transfer of partially reacted bubble gas to emulsion gas where it will have higher chances for the reaction. The right number of stages to model this system is dependent on its kinetics and hydrodynamics.

The reformer is divided into 5 sections to simulate the environment inside a real-world reforming unit. Figure 4.9 indicates that by increasing the stages no the rate of production of aromatics and hydrogen increases while the rate of naphthene decrease with the increased stages. A further increase in subsections alters the hydrodynamics from that of a CSTR to that inside a PFR. For the FBMR the number of stages was determined to be 5. For comparison, FBR with no membrane permeation was simulated and similarly, the number of optimal stages was found to be 4.

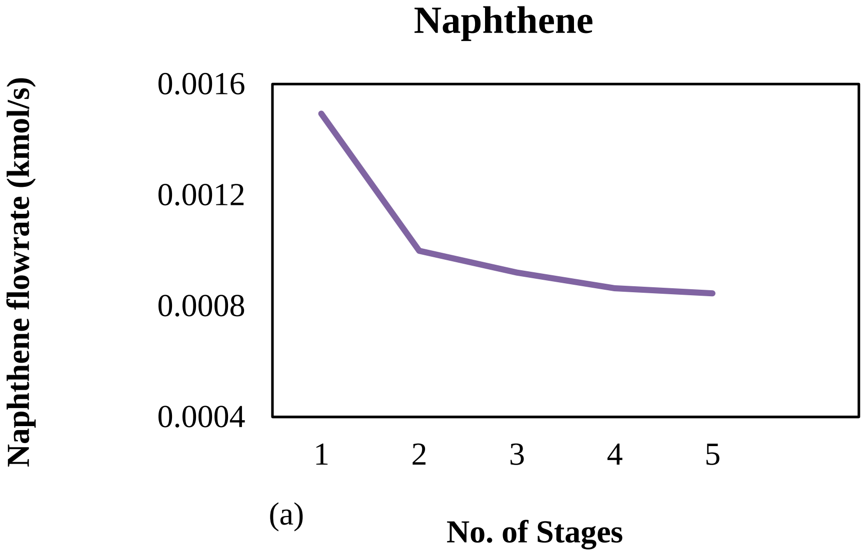

Figure 4.9: (a)**: S**tage effect on the Naphthene flow rate in FBMR System.

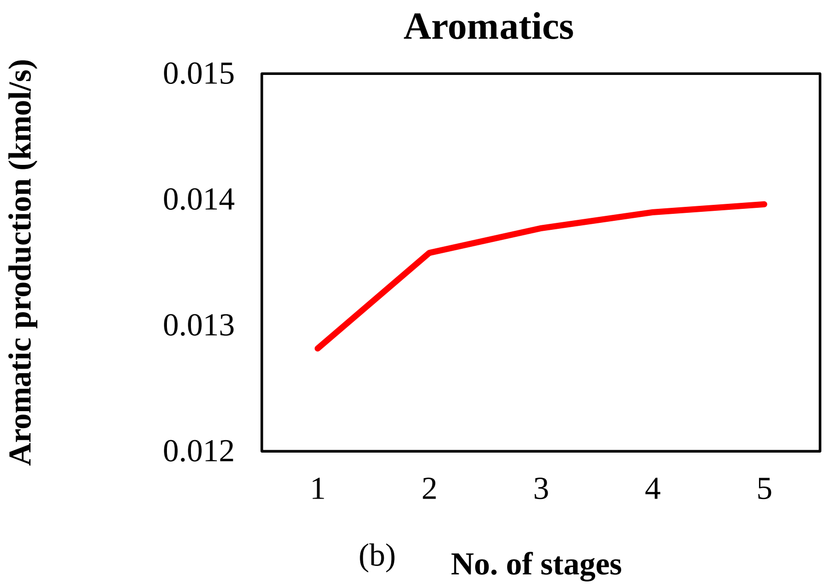

(b)

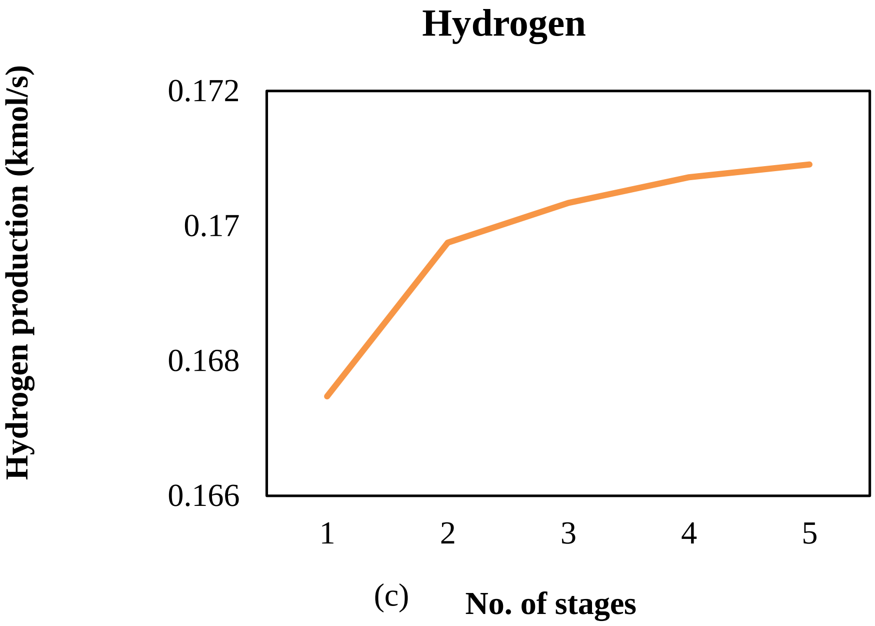

(c)

Figure 4.10: *(cont.)*: **Stages effect on production flow rates (b) aromatic production and (c) hydrogen production of FBMR System**

Chapter -5

Results and Discussion

5.0 Effect of the operating variables on the productions rates

Several variables affect catalyst performance. The results of the thesis were estimated and present their behavior on various parameters of the reactor performance. The more important parameters are the temperature at which reaction is carried out, the pressure of the shell side, properties of the naphtha feed and hydrogen to hydrocarbon molar ratio.

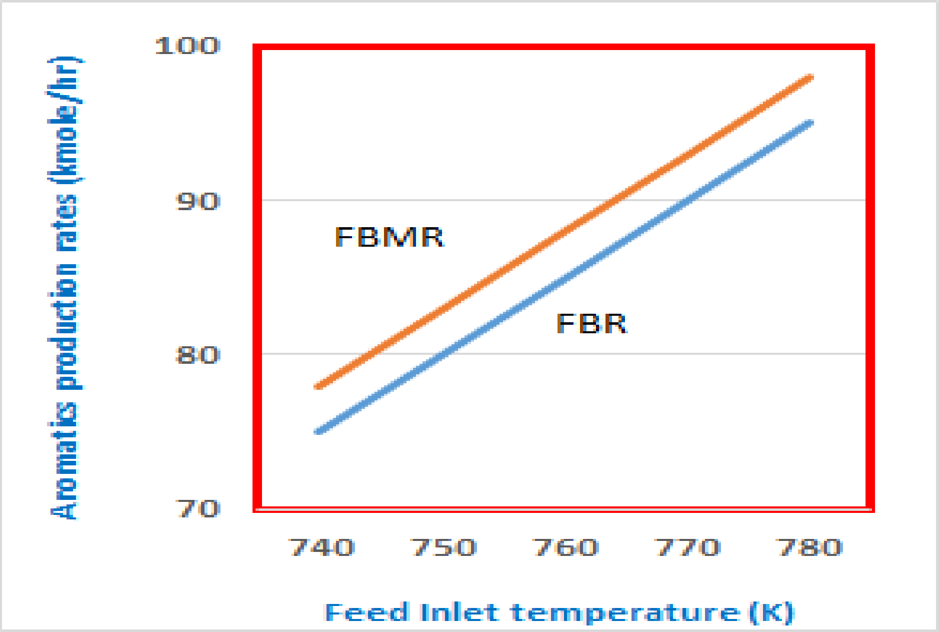

(a)

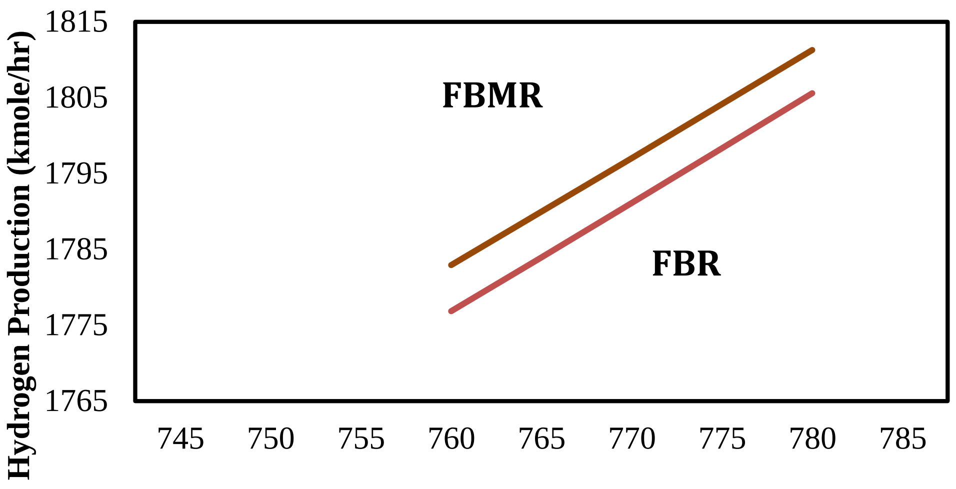

(b)

Figure 5.1: Inlet Feed temperature effects on (a) aromatic production, (b) hydrogen production

5.1 Influence of Reactor Temperature

Endothermic reactions improve in yield as the temperature is raised. The dehydrogenation reaction is highly endothermic and thus high temperature favors it. In Figure 5.1 (a) it is shown that a rise in temperature has a favorable impact on aromatic mole fraction. The temperature of the reactor drops along the reactor length being endothermic it absorbs heat and the overall temperature of the reactor drops. Further contact with a catalyst will not produce any further increase in products due to the slowing of reaction with this decrease in temperature.

As shown in figure 5.1(a) and (b) temperature drops and hydrogen production sequence in the reactors of both. The rising trend shows that with the rise in temperature the hydrogen amount produced increases in both reactors but the total amount produced is more in case of the FBMR. This can be explained due to the selective removal of hydrogen, which is a product of the reaction and driving of the reaction to the product side

5.2 Influence of shell-side pressure

The second parameter to be evaluated is the shell side pressure. The difference between the reaction side and permeate side pressure creates a driving force for hydrogen permeation. As the dehydrogenation reaction is hydrogen producer, with the reaction proceeding more hydrogen will be produced. In the case of FBR, this hydrogen accumulates inside the reactor and increases its partial pressure and increases the affinity for products to move towards the right side i.e. increasing the moles of reactants. The results are plotted in Figure 5.2 (a) and (b).

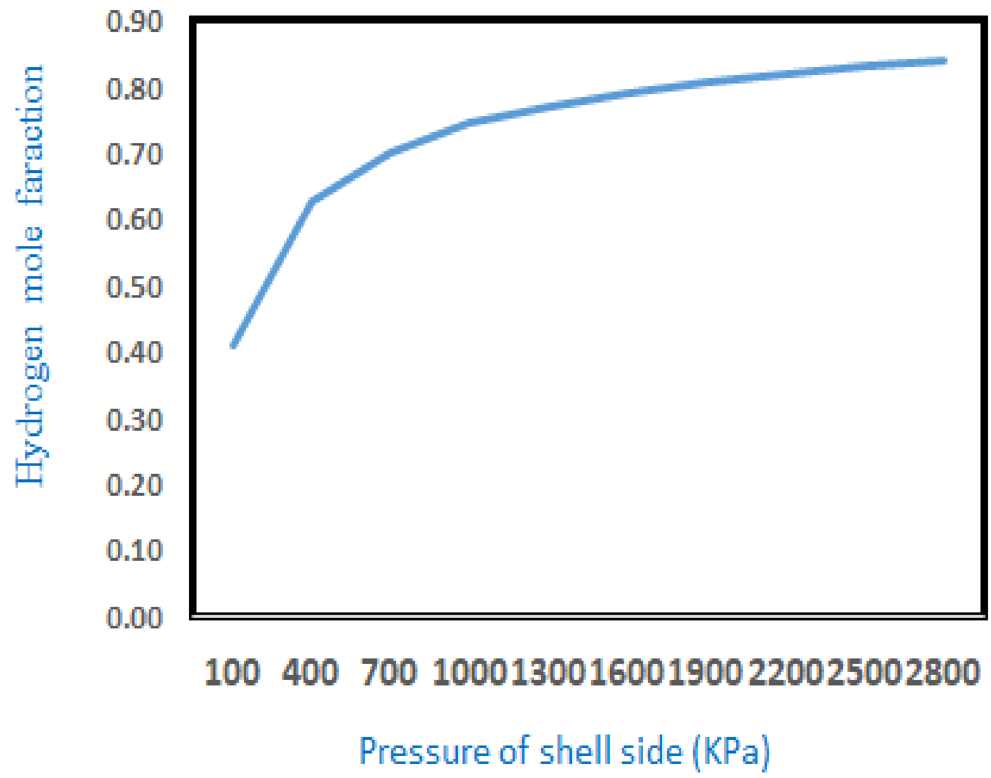

(a)

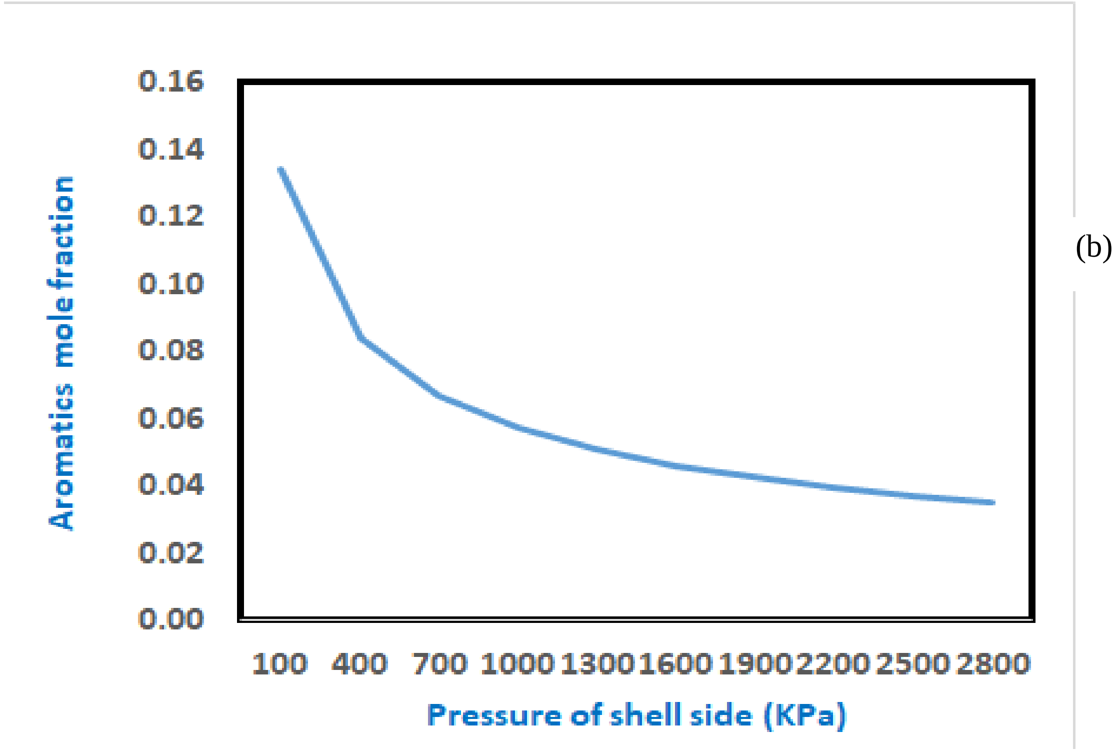

Figure 5.2: (a) Mole fraction of aromatic and (b) mole fraction of outlet hydrogen in the reaction side as a function of shell side pressure.

But in the case of the membrane reactor, the excess hydrogen is removed alongside the wall and thus keeps its partial pressure constant or even decreasing it if the shell side pressure is further reduced. This is the main reason that the FBMR produces more aromatics as compared to an FBR due to an increased rate of forwarding reaction. Also, a good quantity of ultrapure hydrogen is available for fuel cell applications from the FBMR. While the pressure inside the reactor is controlled within narrow limits the pressure inside the shell can be varied and hydrogen and thus aromatic production can be controlled in an FBMR.

5.3 Influence of membrane thickness

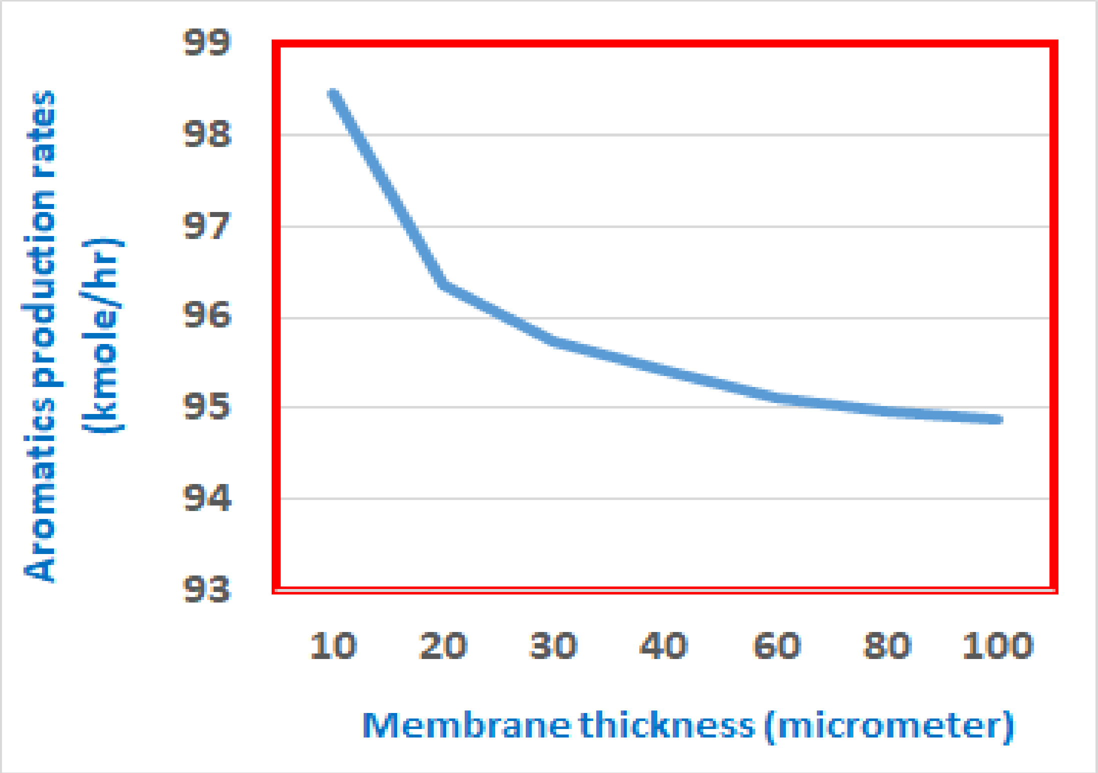

Figure 5.3: Membrane thickness effects on the production of aromatics

The third parameter to be evaluated is the membrane thickness. It was investigated the effect of membrane thickness molar aromatic production. The result is shown in Figure 5.3. It is evident that when the membrane is very thin around 10 microns, aromatic production shows a sharp increase with further reduction in thickness. Furthermore, it is also observed that when the thickness is about 20 microns, a further increase in thickness does not bring any significant reduction in aromatic molar production. The thin membrane requires a support material. Stainless steel and alumina are the more frequently used materials for this purpose. Alloying with silver is also a technique to provide mechanical strength.

5.4 Influence of H_2/HC

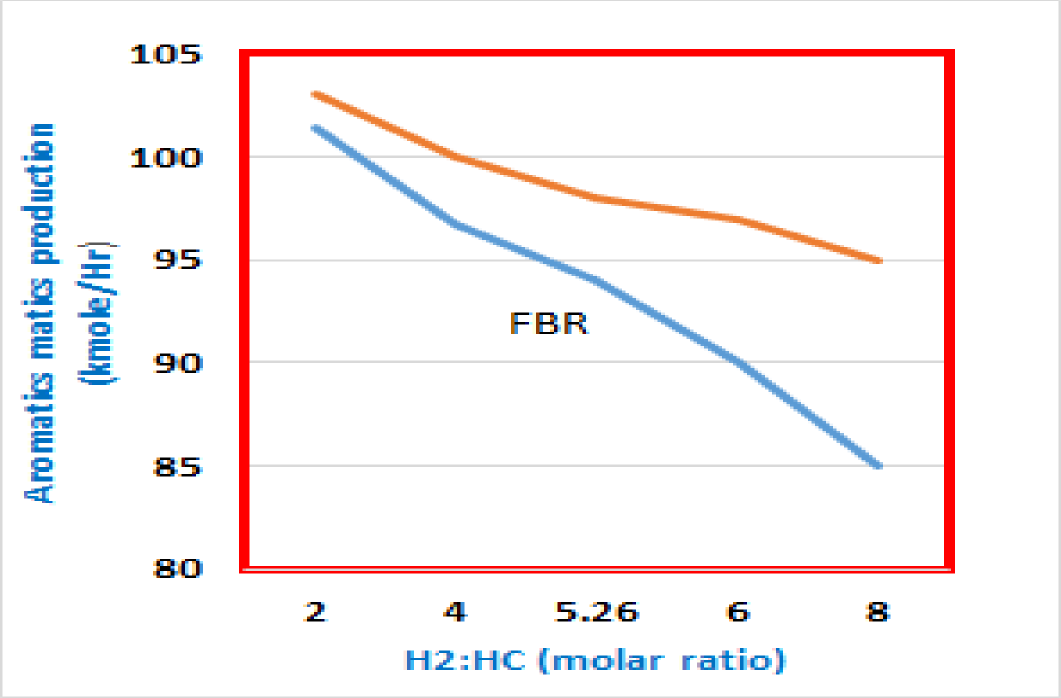

Figure 5.4: H_2/HC molar ratio effect on aromatic production,

The naphtha reforming reactions proceed under a hydrogen atmosphere to suppress the cracking reactions. The hydrogen to hydrocarbon molar ratio is an important parameter from an industrial standpoint and its variation on aromatic production is included in this study. Higher H_2/HC ratios result in a milder reaction condition inside the reformer as hydrogen removes the coke precursor from the catalyst surface. On the other hand, higher ratios mean lower aromatic molar production which can be seen in Figure 5.4. Here the advantage of the membrane becomes clear. The effect of a high H2/HC ratio is more in the case of FBR as compared with an FBMR due to in situ hydrogen removal. The reason behind this is the accumulation of product hydrogen in the FBR. In the case of the FBMR, a part of the hydrogen is continuously removed resulting in higher product concentration.

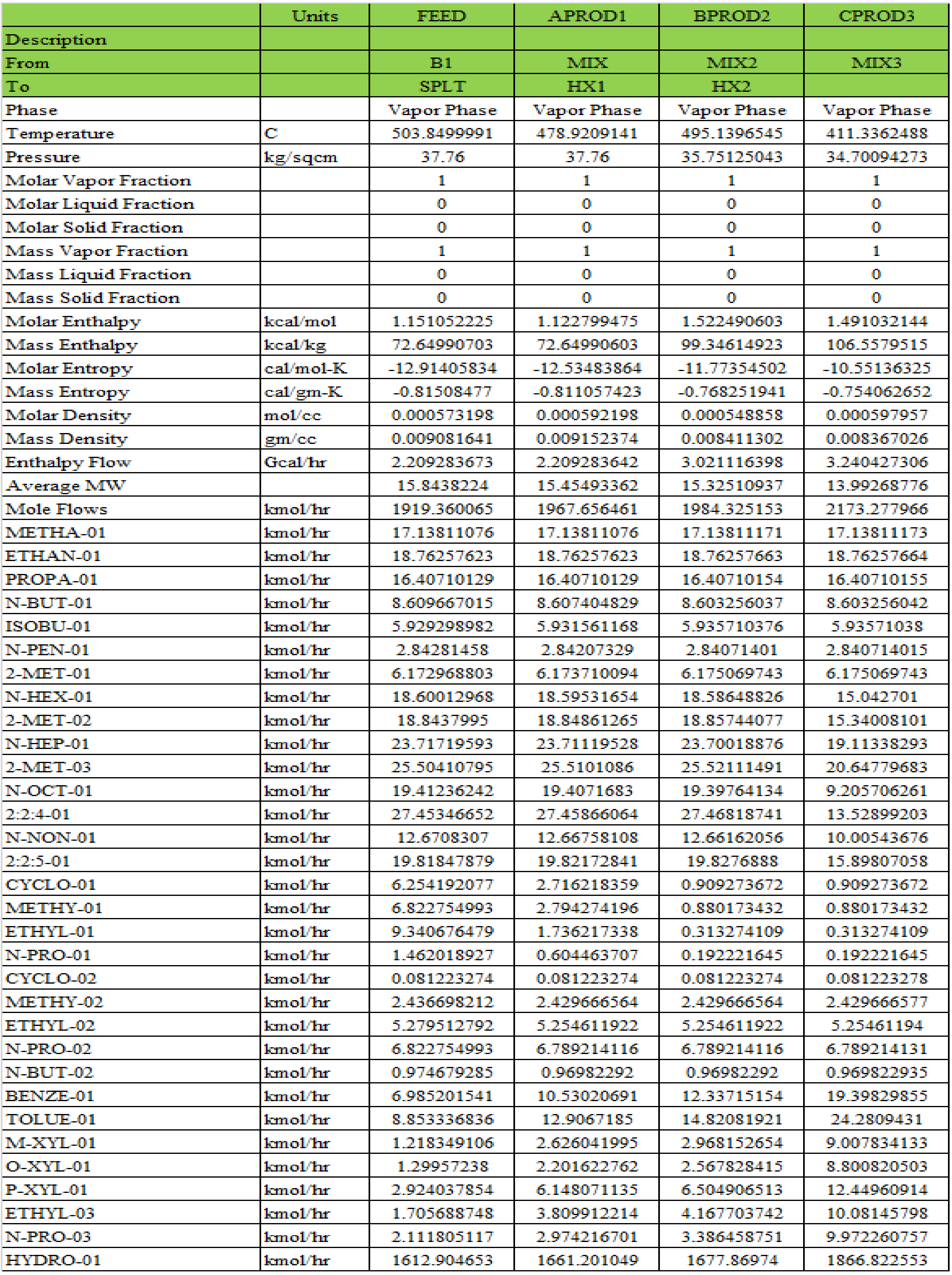

	Units	FEED	APROD1	BPROD2	CPROD3
Description					
From		B1	MIX	MIX2	MIX3
To		SPLT	HX1	HX2	
Phase		Vapor Phase	Vapor Phase	Vapor Phase	Vapor Phase
Temperature	C	503.8499991	478.9209141	495.1396545	411.3362488
Pressure	kg/sqcm	37.76	37.76	35.75125043	34.70094273
Molar Vapor Fraction		1	1	1	1
Molar Liquid Fraction		0	0	0	0
Molar Solid Fraction		0	0	0	0
Mass Vapor Fraction		1	1	1	1
Mass Liquid Fraction		0	0	0	0
Mass Solid Fraction		0	0	0	0
Molar Enthalpy	kcal/mol	1.151052225	1.122799475	1.522490603	1.491032144
Mass Enthalpy	kcal/kg	72.64990703	72.64990603	99.34614923	106.5579515
Molar Entropy	cal/mol-K	-12.91405834	-12.53483864	-11.77354502	-10.55136325
Mass Entropy	cal/gm-K	-0.81508477	-0.811057423	-0.768251941	-0.754062652
Molar Density	mol/cc	0.000573198	0.000592198	0.000548858	0.000597957
Mass Density	gm/cc	0.009081641	0.009152374	0.008411302	0.008367026
Enthalpy Flow	Gcal/hr	2.209283673	2.209283642	3.021116398	3.240427306
Average MW		15.8438224	15.45493362	15.32510937	13.99268776
Mole Flows	kmol/hr	1919.360065	1967.656461	1984.325153	2173.277966
METHA-01	kmol/hr	17.13811076	17.13811076	17.13811171	17.13811173
ETHAN-01	kmol/hr	18.76257623	18.76257623	18.76257663	18.76257664
PROPA-01	kmol/hr	16.40710129	16.40710129	16.40710154	16.40710155
N-BUT-01	kmol/hr	8.609667015	8.607404829	8.603256037	8.603256042
ISOBU-01	kmol/hr	5.929298982	5.931561168	5.935710376	5.93571038
N-PEN-01	kmol/hr	2.84281458	2.84207329	2.84071401	2.840714015
2-MET-01	kmol/hr	6.172968803	6.173710094	6.175069743	6.175069743
N-HEX-01	kmol/hr	18.60012968	18.59531654	18.58648826	15.042701
2-MET-02	kmol/hr	18.8437995	18.84861265	18.85744077	15.34008101
N-HEP-01	kmol/hr	23.71719593	23.71119528	23.70018876	19.11338293
2-MET-03	kmol/hr	25.50410795	25.5101086	25.52111491	20.64779683
N-OCT-01	kmol/hr	19.41236242	19.4071683	19.39764134	9.205706261
2:2:4-01	kmol/hr	27.45346652	27.45866064	27.46818741	13.52899203
N-NON-01	kmol/hr	12.6708307	12.66758108	12.66162056	10.00543676
2:2:5-01	kmol/hr	19.81847879	19.82172841	19.8276888	15.89807058
CYCLO-01	kmol/hr	6.254192077	2.716218359	0.909273672	0.909273672
METHY-01	kmol/hr	6.822754993	2.794274196	0.880173432	0.880173432
ETHYL-01	kmol/hr	9.340676479	1.736217338	0.313274109	0.313274109
N-PRO-01	kmol/hr	1.462018927	0.604463707	0.192221645	0.192221645
CYCLO-02	kmol/hr	0.081223274	0.081223274	0.081223274	0.081223278
METHY-02	kmol/hr	2.436698212	2.429666564	2.429666564	2.429666577
ETHYL-02	kmol/hr	5.279512792	5.254611922	5.254611922	5.25461194
N-PRO-02	kmol/hr	6.822754993	6.789214116	6.789214116	6.789214131
N-BUT-02	kmol/hr	0.974679285	0.96982292	0.96982292	0.969822935
BENZE-01	kmol/hr	6.985201541	10.53020691	12.33715154	19.39829855
TOLUE-01	kmol/hr	8.853336836	12.9067185	14.82081921	24.2809431
M-XYL-01	kmol/hr	1.218349106	2.626041995	2.968152654	9.007834133
O-XYL-01	kmol/hr	1.29957238	2.201622762	2.567828415	8.800820503
P-XYL-01	kmol/hr	2.924037854	6.148071135	6.504906513	12.44960914
ETHYL-03	kmol/hr	1.705688748	3.809912214	4.167703742	10.08145798
N-PRO-03	kmol/hr	2.111805117	2.974216701	3.386458751	9.972260757
HYDRO-01	kmol/hr	1612.904653	1661.201049	1677.86974	1866.822553

Tables 5.1 The production profile of FBR (kmole/hr) three Reactor System.

The first column shows the components chosen from the Aspen Plus database to represent the hydrocarbon. The second column is for the units of the parameters. The next four columns show the feed and products flow rates FBR for three reactors.

Table 5.2 shows the output from the FBMR as reported by the Aspen Plus simulator. The reactants are partially converted into products and the output from the second phase is combined. In the FBMR hydrogen is removed and then products become the input to the next phase.

Table 5.2: Production Profile FBMR Three Reactors System.

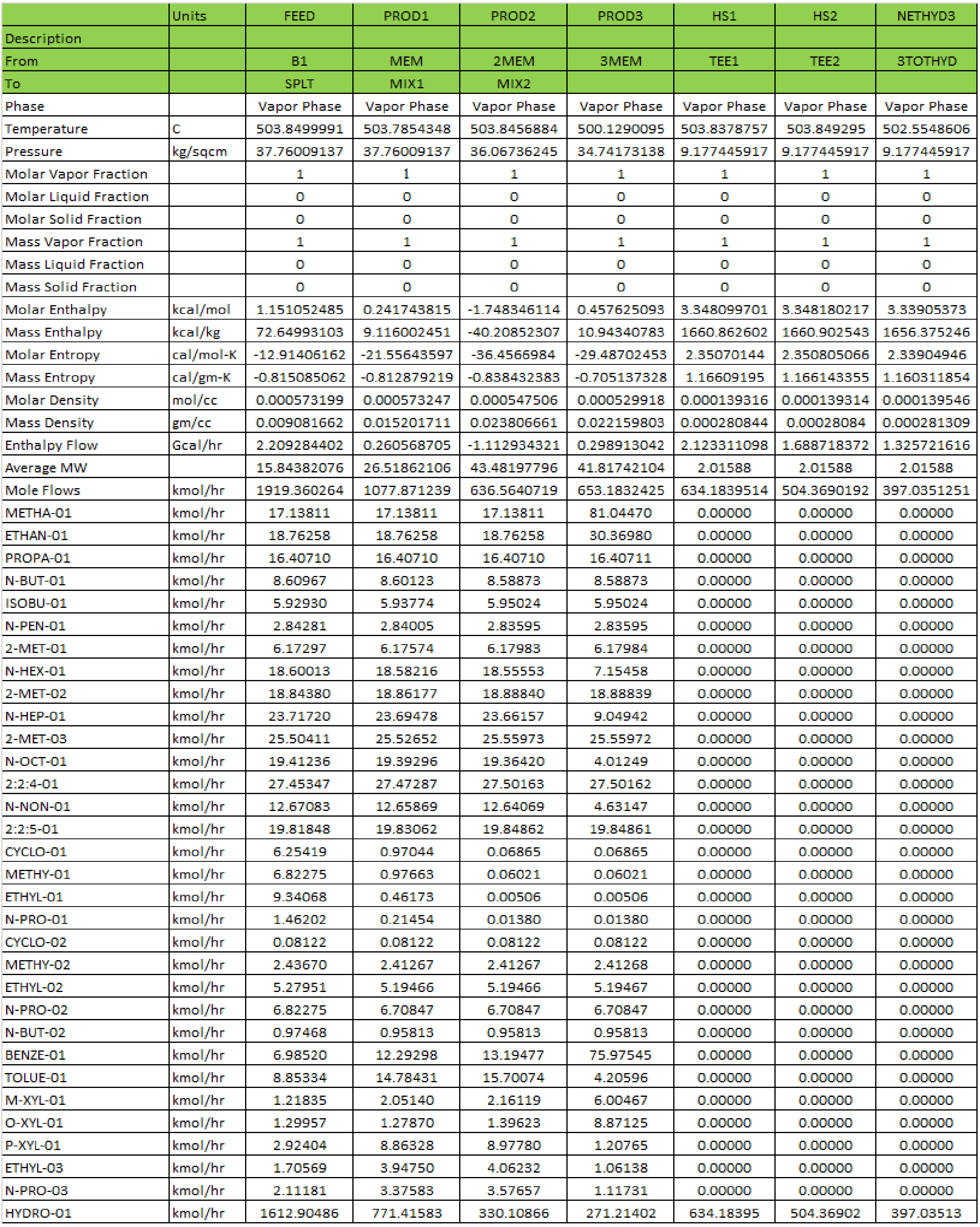

	Units	FEED	PROD1	PROD2	PROD3	HS1	HS2	NETHYD3
Description								
From		B1	MEM	2MEM	3MEM	TEE1	TEE2	3TOTHYD
To		SPLT	MIX1	MIX2				
Phase		Vapor Phase	Vapor Phase	Vapor Phase	Vapor Phase	Vapor Phase	Vapor Phase	Vapor Phase
Temperature	C	503.8499991	503.7854348	503.8456884	500.1290095	503.8378757	503.849295	502.5548606
Pressure	kg/sqcm	37.76009137	37.76009137	36.06736245	34.74173138	9.177445917	9.177445917	9.177445917
Molar Vapor Fraction		1	1	1	1	1	1	1
Molar Liquid Fraction		0	0	0	0	0	0	0
Molar Solid Fraction		0	0	0	0	0	0	0
Mass Vapor Fraction		1	1	1	1	1	1	1
Mass Liquid Fraction		0	0	0	0	0	0	0
Mass Solid Fraction		0	0	0	0	0	0	0
Molar Enthalpy	kcal/mol	1.151052485	0.241743815	-1.748346114	0.457625093	3.348099701	3.348180217	3.33905373
Mass Enthalpy	kcal/kg	72.64993103	9.116002451	-40.20852307	10.94340783	1660.862602	1660.902543	1656.375246
Molar Entropy	cal/mol-K	-12.91406162	-21.55643597	-36.4566984	-29.48702453	2.35070144	2.350805066	2.33904946
Mass Entropy	cal/gm-K	-0.815085062	-0.812879219	-0.838432383	-0.705137328	1.16609195	1.166143355	1.160311854
Molar Density	mol/cc	0.000573199	0.000573247	0.000547506	0.000529918	0.000139316	0.000139314	0.000139546
Mass Density	gm/cc	0.009081662	0.015201711	0.023806661	0.022159803	0.000280844	0.00028084	0.000281309
Enthalpy Flow	Gcal/hr	2.209284402	0.260568705	-1.112934321	0.298913042	2.123311098	1.688718372	1.325721616
Average MW		15.84382076	26.51862106	43.48197796	41.81742104	2.01588	2.01588	2.01588
Mole Flows	kmol/hr	1919.360264	1077.871239	636.5640719	653.1832425	634.1839514	504.3690192	397.0351251
METHA-01	kmol/hr	17.13811	17.13811	17.13811	81.04470	0.00000	0.00000	0.00000
ETHAN-01	kmol/hr	18.76258	18.76258	18.76258	30.36980	0.00000	0.00000	0.00000
PROPA-01	kmol/hr	16.40710	16.40710	16.40710	16.40711	0.00000	0.00000	0.00000
N-BUT-01	kmol/hr	8.60967	8.60123	8.58873	8.58873	0.00000	0.00000	0.00000
ISOBU-01	kmol/hr	5.92930	5.93774	5.95024	5.95024	0.00000	0.00000	0.00000
N-PEN-01	kmol/hr	2.84281	2.84005	2.83595	2.83595	0.00000	0.00000	0.00000
2-MET-01	kmol/hr	6.17297	6.17574	6.17983	6.17984	0.00000	0.00000	0.00000
N-HEX-01	kmol/hr	18.60013	18.58216	18.55553	7.15458	0.00000	0.00000	0.00000
2-MET-02	kmol/hr	18.84380	18.86177	18.88840	18.88839	0.00000	0.00000	0.00000
N-HEP-01	kmol/hr	23.71720	23.69478	23.66157	9.04942	0.00000	0.00000	0.00000
2-MET-03	kmol/hr	25.50411	25.52652	25.55973	25.55972	0.00000	0.00000	0.00000
N-OCT-01	kmol/hr	19.41236	19.39296	19.36420	4.01249	0.00000	0.00000	0.00000
2:2:4-01	kmol/hr	27.45347	27.47287	27.50163	27.50162	0.00000	0.00000	0.00000
N-NON-01	kmol/hr	12.67083	12.65869	12.64069	4.63147	0.00000	0.00000	0.00000
2:2:5-01	kmol/hr	19.81848	19.83062	19.84862	19.84861	0.00000	0.00000	0.00000
CYCLO-01	kmol/hr	6.25419	0.97044	0.06865	0.06865	0.00000	0.00000	0.00000
METHY-01	kmol/hr	6.82275	0.97663	0.06021	0.06021	0.00000	0.00000	0.00000
ETHYL-01	kmol/hr	9.34068	0.46173	0.00506	0.00506	0.00000	0.00000	0.00000
N-PRO-01	kmol/hr	1.46202	0.21454	0.01380	0.01380	0.00000	0.00000	0.00000
CYCLO-02	kmol/hr	0.08122	0.08122	0.08122	0.08122	0.00000	0.00000	0.00000
METHY-02	kmol/hr	2.43670	2.41267	2.41267	2.41268	0.00000	0.00000	0.00000
ETHYL-02	kmol/hr	5.27951	5.19466	5.19466	5.19467	0.00000	0.00000	0.00000
N-PRO-02	kmol/hr	6.82275	6.70847	6.70847	6.70847	0.00000	0.00000	0.00000
N-BUT-02	kmol/hr	0.97468	0.95813	0.95813	0.95813	0.00000	0.00000	0.00000
BENZE-01	kmol/hr	6.98520	12.29298	13.19477	75.97545	0.00000	0.00000	0.00000
TOLUE-01	kmol/hr	8.85334	14.78431	15.70074	4.20596	0.00000	0.00000	0.00000
M-XYL-01	kmol/hr	1.21835	2.05140	2.16119	6.00467	0.00000	0.00000	0.00000
O-XYL-01	kmol/hr	1.29957	1.27870	1.39623	8.87125	0.00000	0.00000	0.00000
P-XYL-01	kmol/hr	2.92404	8.86328	8.97780	1.20765	0.00000	0.00000	0.00000
ETHYL-03	kmol/hr	1.70569	3.94750	4.06232	1.06138	0.00000	0.00000	0.00000
N-PRO-03	kmol/hr	2.11181	3.37583	3.57657	1.11731	0.00000	0.00000	0.00000
HYDRO-01	kmol/hr	1612.90486	771.41583	330.10866	271.21402	634.18395	504.36902	397.03513

Table 5.3: Mole fraction Profile of FBMR

Table 5.3 shows the mole fraction of the FBMR. The naphtha feed has further reacted to convert naphthenes present in the feed to aromatics which are the desirable products. The reactions occur in both PFR and CSTR which represent the bubble and emulsion phases respectively. Most of the catalyst is in the CSTR. The PFR has a very less quantity of catalyst and so the reaction rate is very low. As the bubble phase is dispersed within the emulsion phase, products from the PFR have a chance to move into the CSTR. This mass transfer allows the unreacted material to react in the CSTR thus improving the reactor effectiveness.

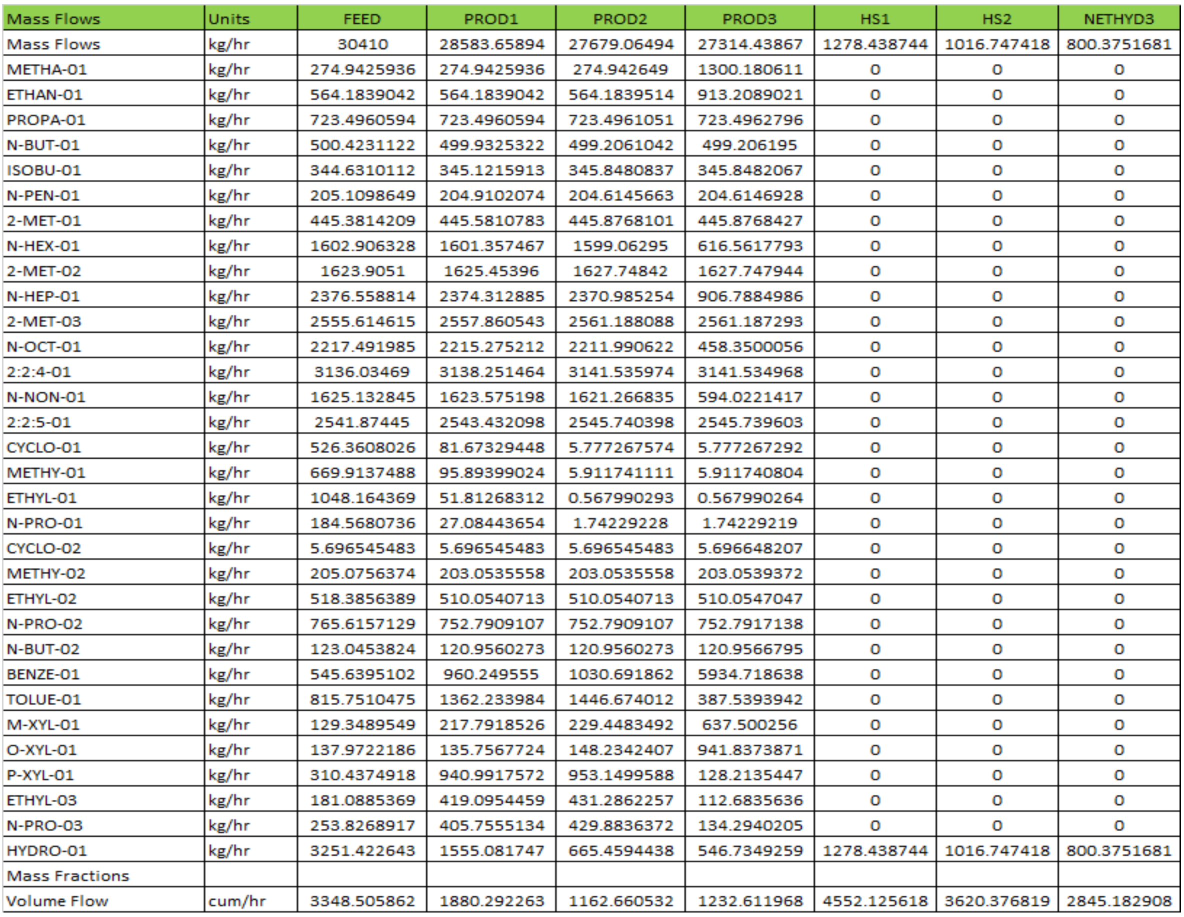

Mass Flows	Units	FEED	PROD1	PROD2	PROD3	HS1	HS2	NETHYD3
Mass Flows	kg/hr	30410	28583.65894	27679.06494	27314.43867	1278.438744	1016.747418	800.3751681
METHA-01	kg/hr	274.9425936	274.9425936	274.942649	1300.180611	0	0	0
ETHAN-01	kg/hr	564.1839042	564.1839042	564.1839514	913.2089021	0	0	0
PROPA-01	kg/hr	723.4960594	723.4960594	723.4961051	723.4962796	0	0	0
N-BUT-01	kg/hr	500.4231122	499.9325322	499.2061042	499.206195	0	0	0
ISOBU-01	kg/hr	344.6310112	345.1215913	345.8480837	345.8482067	0	0	0
N-PEN-01	kg/hr	205.1098649	204.9102074	204.6145663	204.6146928	0	0	0
2-MET-01	kg/hr	445.3814209	445.5810783	445.8768101	445.8768427	0	0	0
N-HEX-01	kg/hr	1602.906328	1601.357467	1599.06295	616.5617793	0	0	0
2-MET-02	kg/hr	1623.9051	1625.45396	1627.74842	1627.747944	0	0	0
N-HEP-01	kg/hr	2376.558814	2374.312885	2370.985254	906.7884986	0	0	0
2-MET-03	kg/hr	2555.614615	2557.860543	2561.188088	2561.187293	0	0	0
N-OCT-01	kg/hr	2217.491985	2215.275212	2211.990622	458.3500056	0	0	0
2:2:4-01	kg/hr	3136.03469	3138.251464	3141.535974	3141.534968	0	0	0
N-NON-01	kg/hr	1625.132845	1623.575198	1621.266835	594.0221417	0	0	0
2:2:5-01	kg/hr	2541.87445	2543.432098	2545.740398	2545.739603	0	0	0
CYCLO-01	kg/hr	526.3608026	81.67329448	5.777267574	5.777267292	0	0	0
METHY-01	kg/hr	669.9137488	95.89399024	5.911741111	5.911740804	0	0	0
ETHYL-01	kg/hr	1048.164369	51.81268312	0.567990293	0.567990264	0	0	0
N-PRO-01	kg/hr	184.5680736	27.08443654	1.74229228	1.74229219	0	0	0
CYCLO-02	kg/hr	5.696545483	5.696545483	5.696545483	5.696648207	0	0	0
METHY-02	kg/hr	205.0756374	203.0535558	203.0535558	203.0539372	0	0	0
ETHYL-02	kg/hr	518.3856389	510.0540713	510.0540713	510.0547047	0	0	0
N-PRO-02	kg/hr	765.6157129	752.7909107	752.7909107	752.7917138	0	0	0
N-BUT-02	kg/hr	123.0453824	120.9560273	120.9560273	120.9566795	0	0	0
BENZE-01	kg/hr	545.6395102	960.249555	1030.691862	5934.718638	0	0	0
TOLUE-01	kg/hr	815.7510475	1362.233984	1446.674012	387.5393942	0	0	0
M-XYL-01	kg/hr	129.3489549	217.7918526	229.4483492	637.500256	0	0	0
O-XYL-01	kg/hr	137.9722186	135.7567724	148.2342407	941.8373871	0	0	0
P-XYL-01	kg/hr	310.4374918	940.9917572	953.1499588	128.2135447	0	0	0
ETHYL-03	kg/hr	181.0885369	419.0954459	431.2862257	112.6835636	0	0	0
N-PRO-03	kg/hr	253.8268917	405.7555134	429.8836372	134.2940205	0	0	0
HYDRO-01	kg/hr	3251.422643	1555.081747	665.4594438	546.7349259	1278.438744	1016.747418	800.3751681
Mass Fractions								
Volume Flow	cum/hr	3348.505862	1880.292263	1162.660532	1232.611968	4552.125618	3620.376819	2845.182908

Table 5.4: Mass Flow Rates of Three Reactors System FBMR.

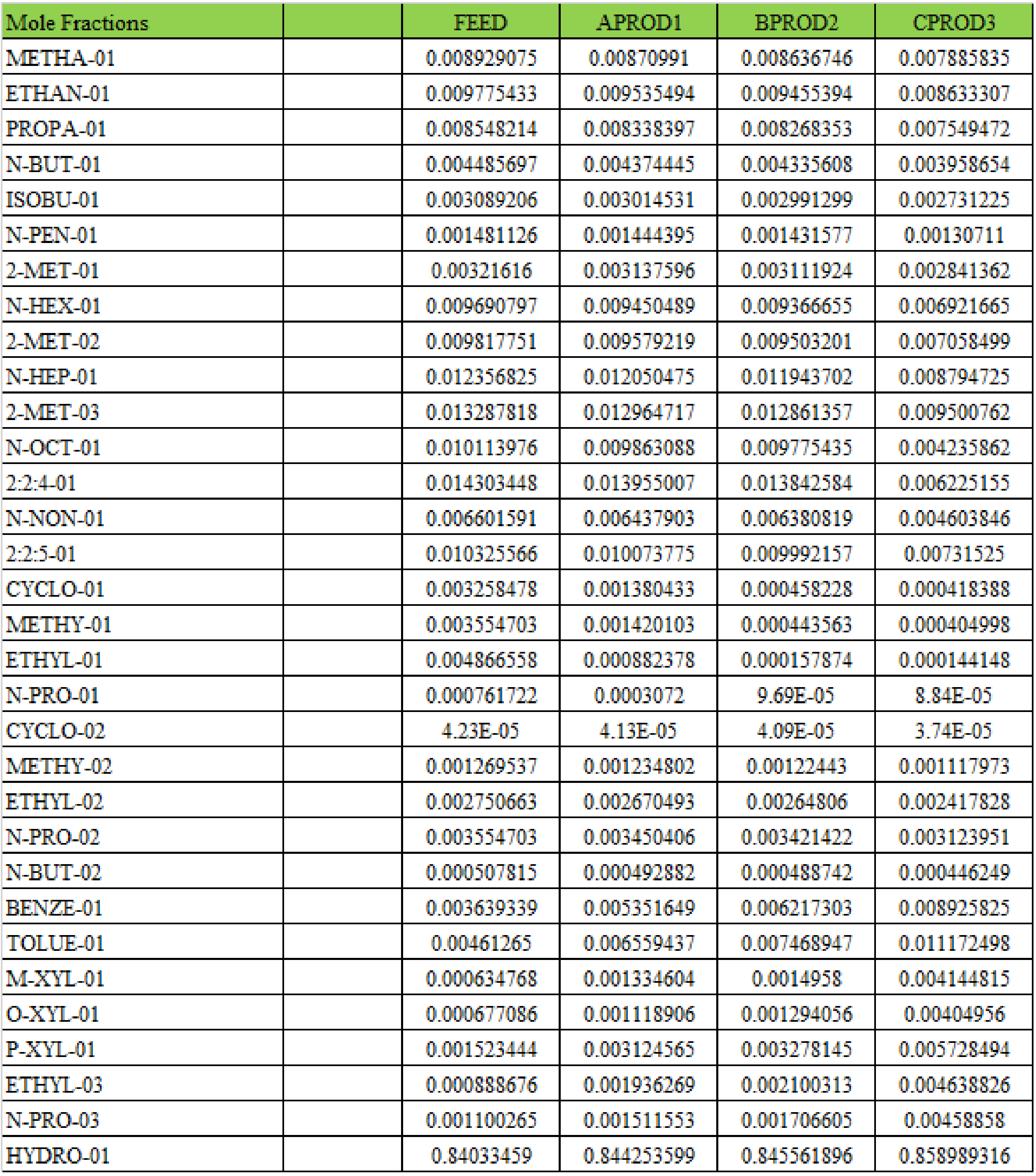

Mole Fractions		FEED	APROD1	BPROD2	CPROD3
METHA-01		0.008929075	0.00870991	0.008636746	0.007885835
ETHAN-01		0.009775433	0.009535494	0.009455394	0.008633307
PROPA-01		0.008548214	0.008338397	0.008268353	0.007549472
N-BUT-01		0.004485697	0.004374445	0.004335608	0.003958654
ISOBU-01		0.003089206	0.003014531	0.002991299	0.002731225
N-PEN-01		0.001481126	0.001444395	0.001431577	0.00130711
2-MET-01		0.00321616	0.003137596	0.003111924	0.002841362
N-HEX-01		0.009690797	0.009450489	0.009366655	0.006921665
2-MET-02		0.009817751	0.009579219	0.009503201	0.007058499
N-HEP-01		0.012356825	0.012050475	0.011943702	0.008794725
2-MET-03		0.013287818	0.012964717	0.012861357	0.009500762
N-OCT-01		0.010113976	0.009863088	0.009775435	0.004235862
2:2:4-01		0.014303448	0.013955007	0.013842584	0.006225155
N-NON-01		0.006601591	0.006437903	0.006380819	0.004603846
2:2:5-01		0.010325566	0.010073775	0.009992157	0.00731525
CYCLO-01		0.003258478	0.001380433	0.000458228	0.000418388
METHY-01		0.003554703	0.001420103	0.000443563	0.000404998
ETHYL-01		0.004866558	0.000882378	0.000157874	0.000144148
N-PRO-01		0.000761722	0.0003072	9.69E-05	8.84E-05
CYCLO-02		4.23E-05	4.13E-05	4.09E-05	3.74E-05
METHY-02		0.001269537	0.001234802	0.00122443	0.001117973
ETHYL-02		0.002750663	0.002670493	0.00264806	0.002417828
N-PRO-02		0.003554703	0.003450406	0.003421422	0.003123951
N-BUT-02		0.000507815	0.000492882	0.000488742	0.000446249
BENZE-01		0.003639339	0.005351649	0.006217303	0.008925825
TOLUE-01		0.00461265	0.006559437	0.007468947	0.011172498
M-XYL-01		0.000634768	0.001334604	0.0014958	0.004144815
O-XYL-01		0.000677086	0.001118906	0.001294056	0.00404956
P-XYL-01		0.001523444	0.003124565	0.003278145	0.005728494
ETHYL-03		0.000888676	0.001936269	0.002100313	0.004638826
N-PRO-03		0.001100265	0.001511553	0.001706605	0.00458858
HYDRO-01		0.84033459	0.844253599	0.845561896	0.858989316

Table 5.5: Mass Fraction of FBR Rectors.

Table 5.6: Comparison between FBMR and FBR Production Rate Using Three Reactors

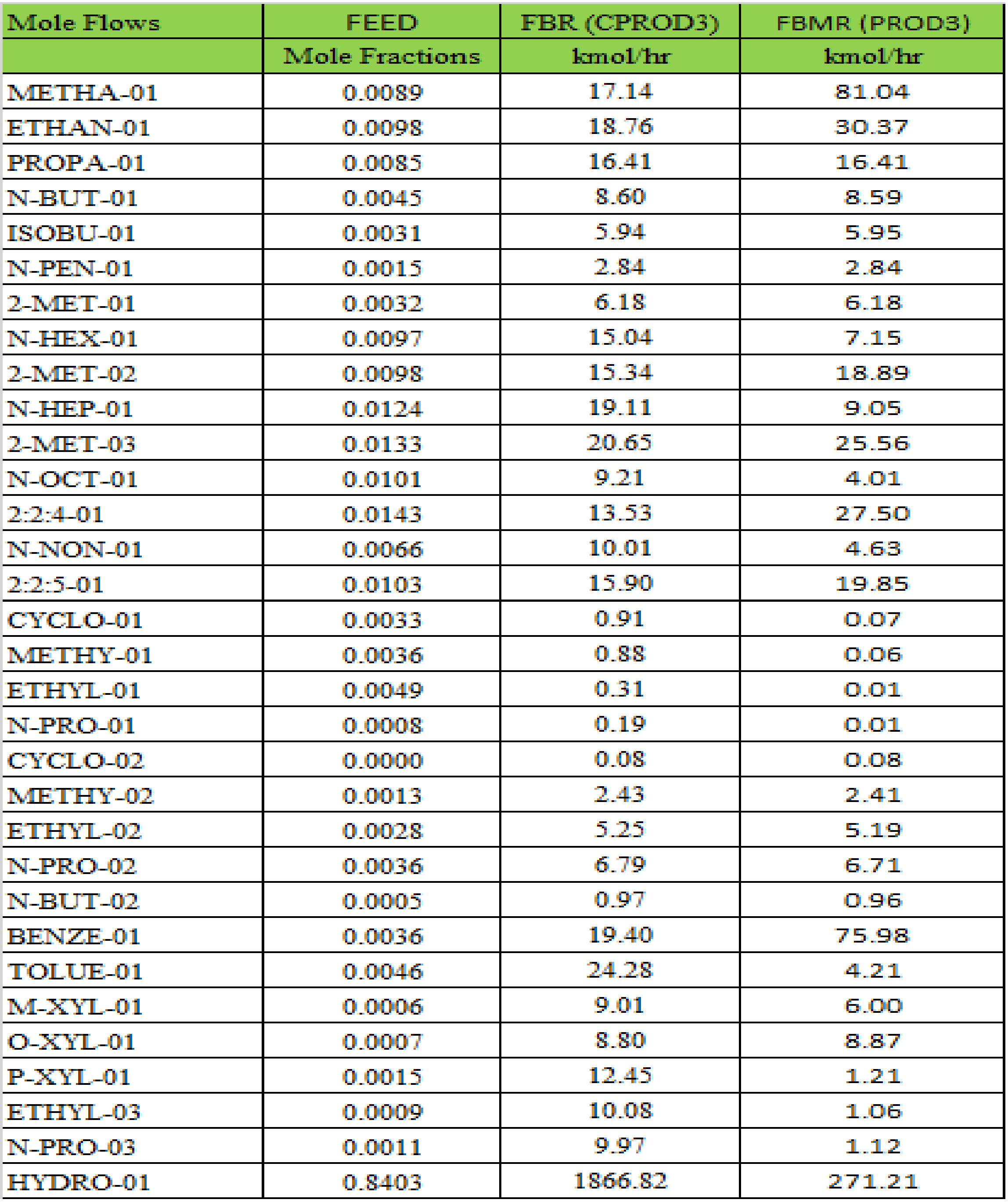

Mole Flows	FEED	FBR (CPROD3)	FBMR (PROD3)
	Mole Fractions	kmol/hr	kmol/hr
METHA-01	0.0089	17.14	81.04
ETHAN-01	0.0098	18.76	30.37
PROPA-01	0.0085	16.41	16.41
N-BUT-01	0.0045	8.60	8.59
ISOBU-01	0.0031	5.94	5.95
N-PEN-01	0.0015	2.84	2.84
2-MET-01	0.0032	6.18	6.18
N-HEX-01	0.0097	15.04	7.15
2-MET-02	0.0098	15.34	18.89
N-HEP-01	0.0124	19.11	9.05
2-MET-03	0.0133	20.65	25.56
N-OCT-01	0.0101	9.21	4.01
2:2:4-01	0.0143	13.53	27.50
N-NON-01	0.0066	10.01	4.63
2:2:5-01	0.0103	15.90	19.85
CYCLO-01	0.0033	0.91	0.07
METHY-01	0.0036	0.88	0.06
ETHYL-01	0.0049	0.31	0.01
N-PRO-01	0.0008	0.19	0.01
CYCLO-02	0.0000	0.08	0.08
METHY-02	0.0013	2.43	2.41
ETHYL-02	0.0028	5.25	5.19
N-PRO-02	0.0036	6.79	6.71
N-BUT-02	0.0005	0.97	0.96
BENZE-01	0.0036	19.40	75.98
TOLUE-01	0.0046	24.28	4.21
M-XYL-01	0.0006	9.01	6.00
O-XYL-01	0.0007	8.80	8.87
P-XYL-01	0.0015	12.45	1.21
ETHYL-03	0.0009	10.08	1.06
N-PRO-03	0.0011	9.97	1.12
HYDRO-01	0.8403	1866.82	271.21

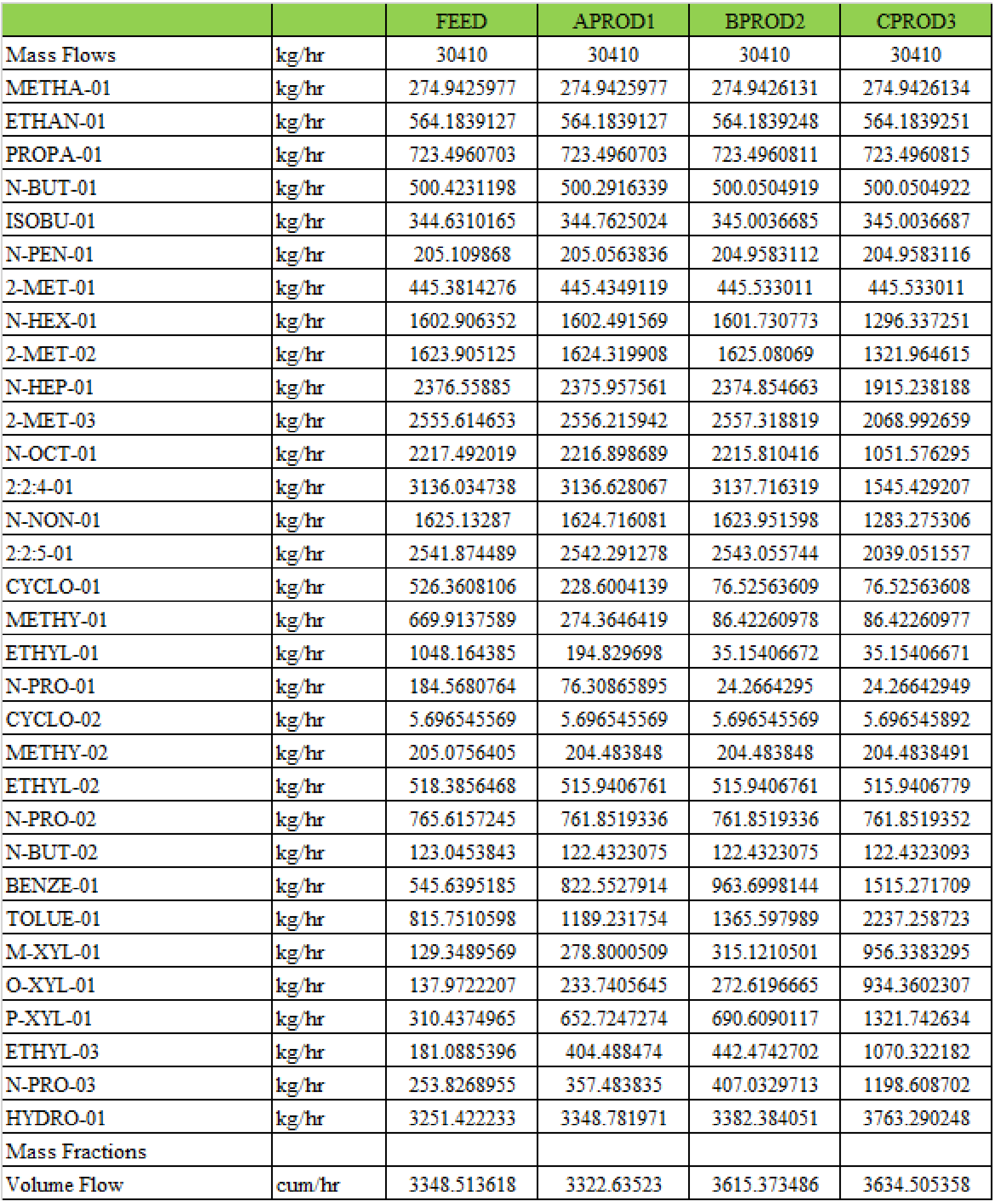

		FEED	APROD1	BPROD2	CPROD3
Mass Flows	kg/hr	30410	30410	30410	30410
METHA-01	kg/hr	274.9425977	274.9425977	274.9426131	274.9426134
ETHAN-01	kg/hr	564.1839127	564.1839127	564.1839248	564.1839251
PROPA-01	kg/hr	723.4960703	723.4960703	723.4960811	723.4960815
N-BUT-01	kg/hr	500.4231198	500.2916339	500.0504919	500.0504922
ISOBU-01	kg/hr	344.6310165	344.7625024	345.0036685	345.0036687
N-PEN-01	kg/hr	205.109868	205.0563836	204.9583112	204.9583116
2-MET-01	kg/hr	445.3814276	445.4349119	445.533011	445.533011
N-HEX-01	kg/hr	1602.906352	1602.491569	1601.730773	1296.337251
2-MET-02	kg/hr	1623.905125	1624.319908	1625.08069	1321.964615
N-HEP-01	kg/hr	2376.55885	2375.957561	2374.854663	1915.238188
2-MET-03	kg/hr	2555.614653	2556.215942	2557.318819	2068.992659
N-OCT-01	kg/hr	2217.492019	2216.898689	2215.810416	1051.576295
2:2:4-01	kg/hr	3136.034738	3136.628067	3137.716319	1545.429207
N-NON-01	kg/hr	1625.13287	1624.716081	1623.951598	1283.275306
2:2:5-01	kg/hr	2541.874489	2542.291278	2543.055744	2039.051557
CYCLO-01	kg/hr	526.3608106	228.6004139	76.52563609	76.52563608
METHY-01	kg/hr	669.9137589	274.3646419	86.42260978	86.42260977
ETHYL-01	kg/hr	1048.164385	194.829698	35.15406672	35.15406671
N-PRO-01	kg/hr	184.5680764	76.30865895	24.2664295	24.26642949
CYCLO-02	kg/hr	5.696545569	5.696545569	5.696545569	5.696545892
METHY-02	kg/hr	205.0756405	204.483848	204.483848	204.4838491
ETHYL-02	kg/hr	518.3856468	515.9406761	515.9406761	515.9406779
N-PRO-02	kg/hr	765.6157245	761.8519336	761.8519336	761.8519352
N-BUT-02	kg/hr	123.0453843	122.4323075	122.4323075	122.4323093
BENZE-01	kg/hr	545.6395185	822.5527914	963.6998144	1515.271709
TOLUE-01	kg/hr	815.7510598	1189.231754	1365.597989	2237.258723
M-XYL-01	kg/hr	129.3489569	278.8000509	315.1210501	956.3383295
O-XYL-01	kg/hr	137.9722207	233.7405645	272.6196665	934.3602307
P-XYL-01	kg/hr	310.4374965	652.7247274	690.6090117	1321.742634
ETHYL-03	kg/hr	181.0885396	404.488474	442.4742702	1070.322182
N-PRO-03	kg/hr	253.8268955	357.483835	407.0329713	1198.608702
HYDRO-01	kg/hr	3251.422233	3348.781971	3382.384051	3763.290248
Mass Fractions					
Volume Flow	cum/hr	3348.513618	3322.63523	3615.373486	3634.505358

Table 5.7: Mass Flow Rates (Kg /hr) of FBR

As the reactions inside the bed proceed more naphthenes in the feed are converted to aromatics thus further increasing the reformate quality. Table 5.6 shows the comparison of both system FBR&FBMR. The reaction is now almost complete and the rate of reaction has decreased.

Table 5.8: FBR mole fraction production rate

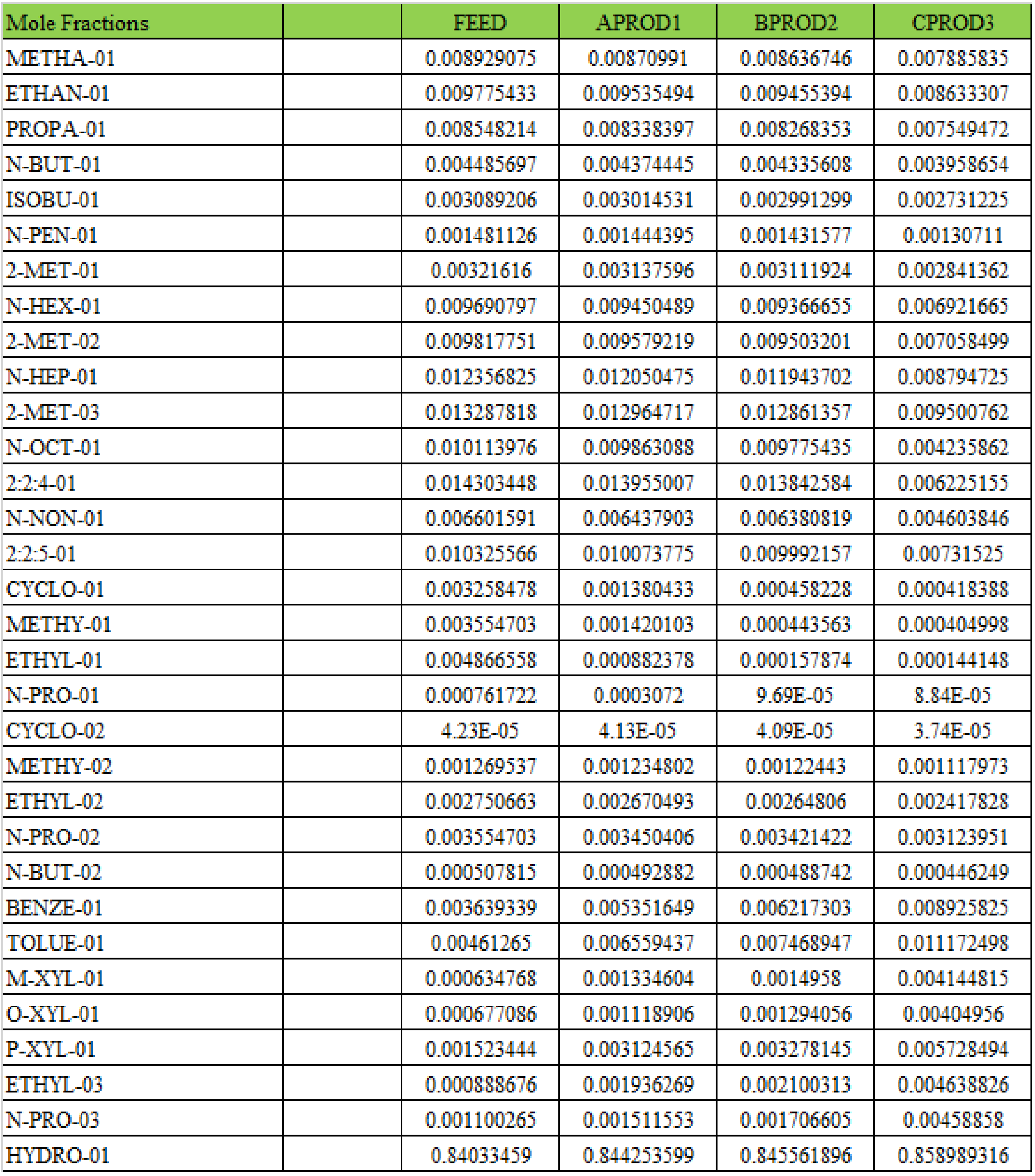

Mole Fractions		FEED	APROD1	BPROD2	CPROD3
METHA-01		0.008929075	0.00870991	0.008636746	0.007885835
ETHAN-01		0.009775433	0.009535494	0.009455394	0.008633307
PROPA-01		0.008548214	0.008338397	0.008268353	0.007549472
N-BUT-01		0.004485697	0.004374445	0.004335608	0.003958654
ISOBU-01		0.003089206	0.003014531	0.002991299	0.002731225
N-PEN-01		0.001481126	0.001444395	0.001431577	0.00130711
2-MET-01		0.00321616	0.003137596	0.003111924	0.002841362
N-HEX-01		0.009690797	0.009450489	0.009366655	0.006921665
2-MET-02		0.009817751	0.009579219	0.009503201	0.007058499
N-HEP-01		0.012356825	0.012050475	0.011943702	0.008794725
2-MET-03		0.013287818	0.012964717	0.012861357	0.009500762
N-OCT-01		0.010113976	0.009863088	0.009775435	0.004235862
2:2:4-01		0.014303448	0.013955007	0.013842584	0.006225155
N-NON-01		0.006601591	0.006437903	0.006380819	0.004603846
2:2:5-01		0.010325566	0.010073775	0.009992157	0.00731525
CYCLO-01		0.003258478	0.001380433	0.000458228	0.000418388
METHY-01		0.003554703	0.001420103	0.000443563	0.000404998
ETHYL-01		0.004866558	0.000882378	0.000157874	0.000144148
N-PRO-01		0.000761722	0.0003072	9.69E-05	8.84E-05
CYCLO-02		4.23E-05	4.13E-05	4.09E-05	3.74E-05
METHY-02		0.001269537	0.001234802	0.00122443	0.001117973
ETHYL-02		0.002750663	0.002670493	0.00264806	0.002417828
N-PRO-02		0.003554703	0.003450406	0.003421422	0.003123951
N-BUT-02		0.000507815	0.000492882	0.000488742	0.000446249
BENZE-01		0.003639339	0.005351649	0.006217303	0.008925825
TOLUE-01		0.00461265	0.006559437	0.007468947	0.011172498
M-XYL-01		0.000634768	0.001334604	0.0014958	0.004144815
O-XYL-01		0.000677086	0.001118906	0.001294056	0.00404956
P-XYL-01		0.001523444	0.003124565	0.003278145	0.005728494
ETHYL-03		0.000888676	0.001936269	0.002100313	0.004638826
N-PRO-03		0.001100265	0.001511553	0.001706605	0.00458858
HYDRO-01		0.84033459	0.844253599	0.845561896	0.858989316

In this phase, the quantity of naphthenes has reduced significantly due to their conversion into aromatics that have increased significantly. Dehydrogenation reactions are the major reforming reactions and produce a lot of hydrogen as a useful byproduct. More quantity of hydrogen and aromatics is produced from the FBMR when compared with the FBR as evident from Table. 5.6

Table 5.9: Parameters for FBMR and FBR

	FBMR			FBR	
	In	Out	Out H_2	In	Out
Temperature, C	503.78	656	680	777	667
Pressure, Kg/cm^2	3.703	3.703	0.9	3.703	3.703
Flowrate, Kg/hr	30410	15045	4195	30410	30410
Molar Enthalpy, KJ/mol	4.83	-3.09	11.18	4.83	3.25
Molar Entropy, J/mol-K	-54033.8	-84841.9	5936.7	-54033.8	-49834.3

Table 5.9 details the important parameters of the FBMR and FBR. Temperature, pressure, and feed flow rate are the more important variables that affect the reactor performance. The pressure of the reactor is fixed after and cannot be varied except within a slight margin. This leaves the temperature and feed flowrate the primary manipulated variables. Higher temperature results in higher aromatic production with the upper limit set by the metallurgy of the system. There is no separate stream of hydrogen from the FBR and it is combined with the reformate.

Table 5.10: Comparison of FBMR and FBR in terms of hydrogen and aromatics production

COMPONENTS	Increase in Aromatics and Hydrogen				
	FBR	FMBR	DIFF	INCREMENT	
	kg/hr	kg/hr	kg/hr	kg/Day	kg/Year
Aromatics	14816	15045	229	5496	2006040
Hydrogen	4179	4195	16	384	140160

In Table, 5.6 the output from both the FBMR and FBR is compared. The first column shows the quantity of aromatic and hydrogen in the feed. The second and third column shows the production rate of the respective component. The calculated daily and yearly increase in aromatic and hydrogen is tabulated in the last two columns for comparison.

In this study, a semi-regenerative type of reformer was modeled and simulated. A Pt/Re-type catalyst on chloride alumina support is used in the industrial semi-regenerative reformers. Other types of reformers such as the continuous catalyst recirculation type reformer use a platinum doped with a tin catalyst due to its harsher environment. A catalyst promotes both forward and reverses reactions but it cannot change the position of equilibrium. The thermodynamics of the reaction solely governs the equilibrium concentration of products. To promote the reaction further heating of the reaction mixture is required thus the reaction is carried out in three separate adiabatic reactor vessels with varying catalyst amount and inter-stage heaters are provided to reheat the product stream to the reaction temperature [2].

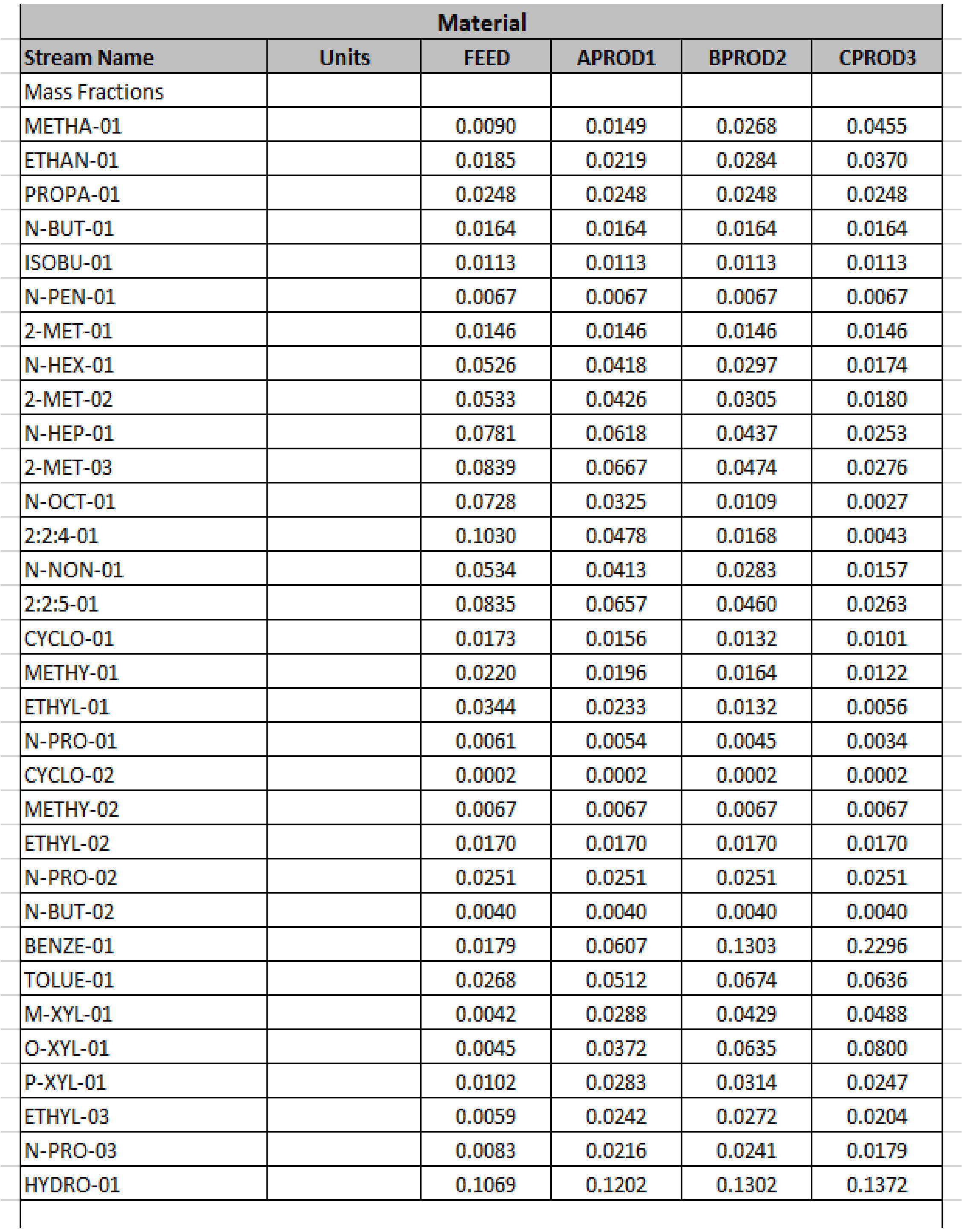

Material					
Stream Name	**Units**	**FEED**	**APROD1**	**BPROD2**	**CPROD3**
Mass Fractions					
METHA-01		0.0090	0.0149	0.0268	0.0455
ETHAN-01		0.0185	0.0219	0.0284	0.0370
PROPA-01		0.0248	0.0248	0.0248	0.0248
N-BUT-01		0.0164	0.0164	0.0164	0.0164
ISOBU-01		0.0113	0.0113	0.0113	0.0113
N-PEN-01		0.0067	0.0067	0.0067	0.0067
2-MET-01		0.0146	0.0146	0.0146	0.0146
N-HEX-01		0.0526	0.0418	0.0297	0.0174
2-MET-02		0.0533	0.0426	0.0305	0.0180
N-HEP-01		0.0781	0.0618	0.0437	0.0253
2-MET-03		0.0839	0.0667	0.0474	0.0276
N-OCT-01		0.0728	0.0325	0.0109	0.0027
2:2:4-01		0.1030	0.0478	0.0168	0.0043
N-NON-01		0.0534	0.0413	0.0283	0.0157
2:2:5-01		0.0835	0.0657	0.0460	0.0263
CYCLO-01		0.0173	0.0156	0.0132	0.0101
METHY-01		0.0220	0.0196	0.0164	0.0122
ETHYL-01		0.0344	0.0233	0.0132	0.0056
N-PRO-01		0.0061	0.0054	0.0045	0.0034
CYCLO-02		0.0002	0.0002	0.0002	0.0002
METHY-02		0.0067	0.0067	0.0067	0.0067
ETHYL-02		0.0170	0.0170	0.0170	0.0170
N-PRO-02		0.0251	0.0251	0.0251	0.0251
N-BUT-02		0.0040	0.0040	0.0040	0.0040
BENZE-01		0.0179	0.0607	0.1303	0.2296
TOLUE-01		0.0268	0.0512	0.0674	0.0636
M-XYL-01		0.0042	0.0288	0.0429	0.0488
O-XYL-01		0.0045	0.0372	0.0635	0.0800
P-XYL-01		0.0102	0.0283	0.0314	0.0247
ETHYL-03		0.0059	0.0242	0.0272	0.0204
N-PRO-03		0.0083	0.0216	0.0241	0.0179
HYDRO-01		0.1069	0.1202	0.1302	0.1372

Figure 5.11: Mass fraction of FBR System

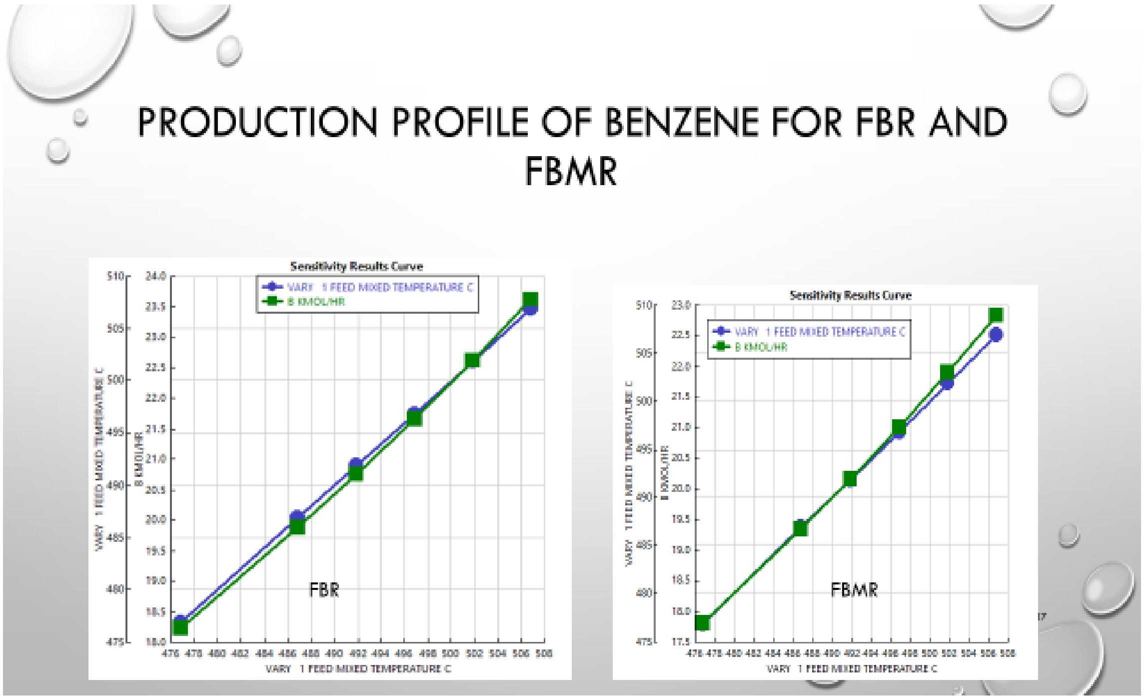

PRODUCTION PROFILE OF BENZENE FOR FBR AND FBMR

Figure 5.5.FBR and FBMR Benzene Production Profile

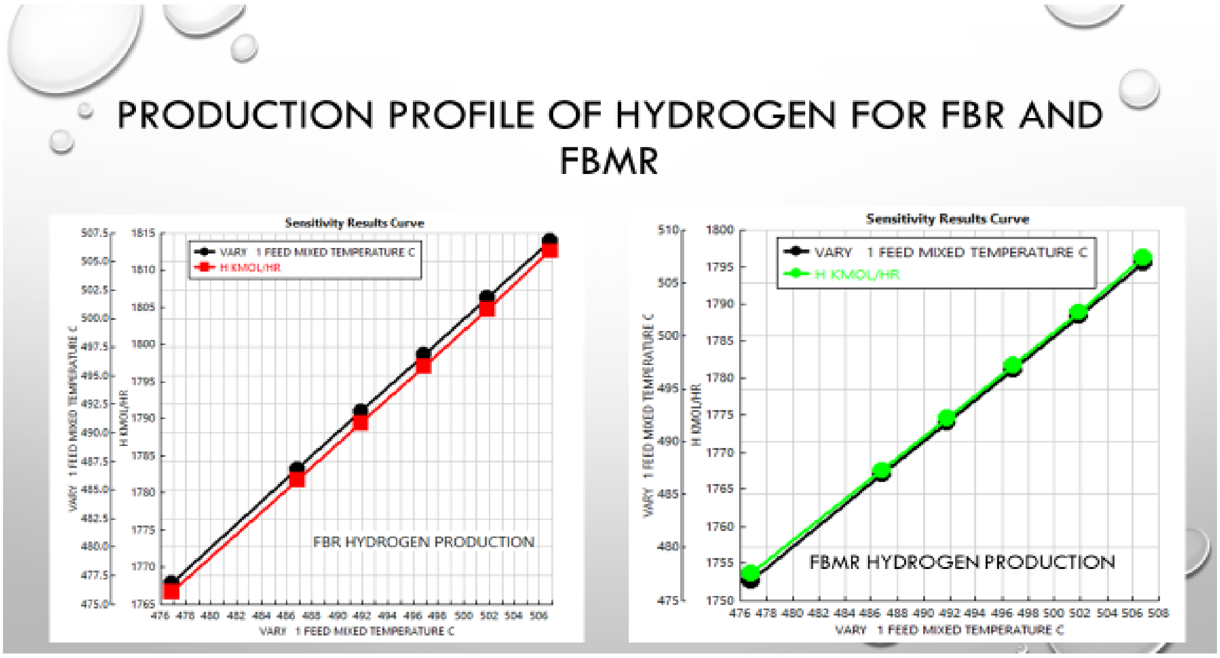

PRODUCTION PROFILE OF HYDROGEN FOR FBR AND FBMR

Figure 5.6. FBR and FBMR Hydrogen Production Profile

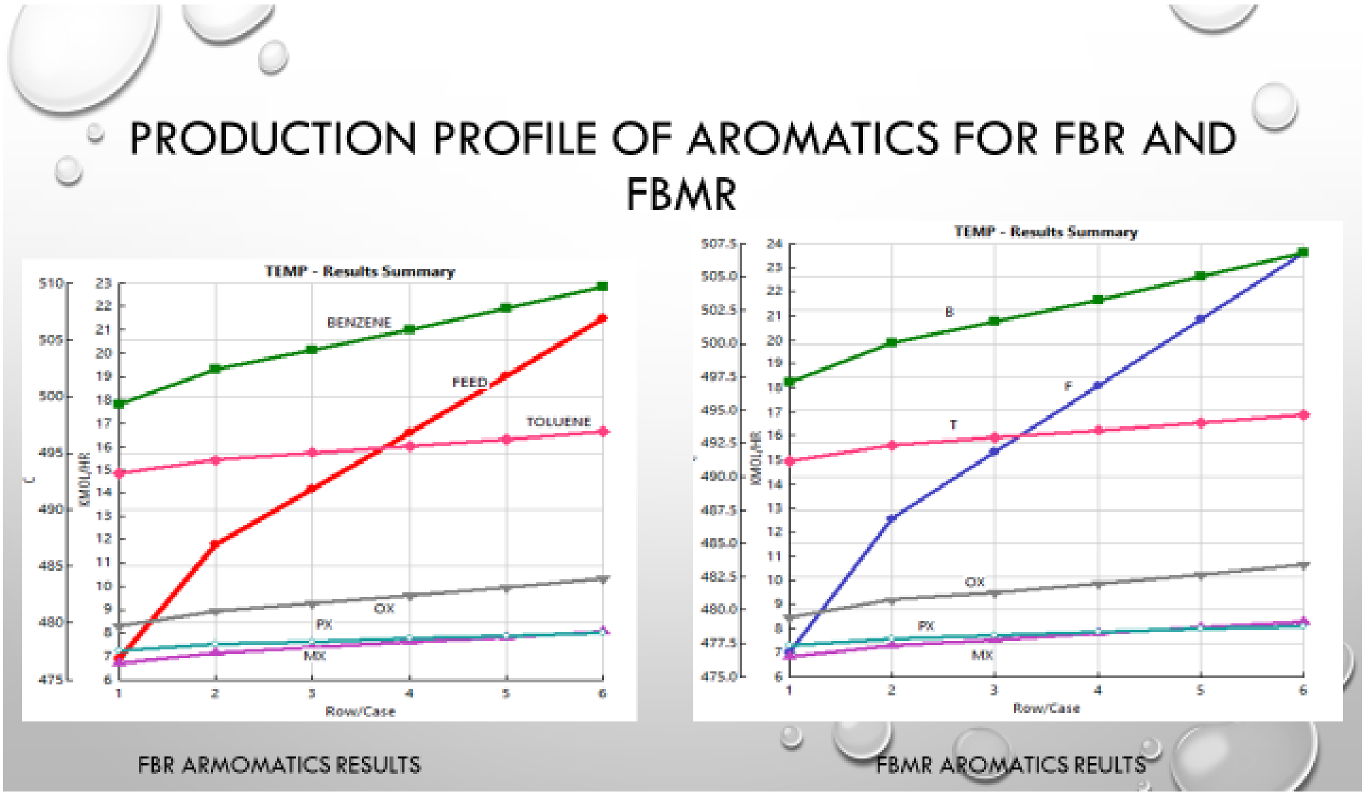

PRODUCTION PROFILE OF AROMATICS FOR FBR AND FBMR

FBR ARMOMATICS RESULTS

FBMR AROMATICS REULTS

Figure 5.7. FBR and FBMR Aromatics Production Profile

5.5 Economic Analysis

Economics is the main instrument that deals and dictates a project's fate. The economic evaluation used in this working for naphtha reforming process was carried by considering the capital investment expenditure on naphtha reforming unit, operating cost that includes utility, taxes, insurance and feeds cost, etc. Although there are no, of economics parameters that are being used in the industries to show their financial inputs and outputs like NPV, IRR, PBP, Cash Flows, Balance Sheets, and annual general reports (AGR). All of these financial terms and statements provide the company’s financial indicators.

Two process models were simulated in Aspen Plus Software and their results were studied and compared to show the production rates of aromatics and hydrogen. In this study, a very simple approach is adopted to show the profitability and production margin of both configurations that can be used in the industries and for academic purposes to show the viability of the system. The PBP is the period (years) required to recover the cost of an investment. It is the capital investment cost divided by the annual profit only. An economic evaluation of aromatics production configurations based on 0.3 million tons per year of straight-run naphtha feedstock (PBP) for both simulation configuration was used. In this study, the cost estimation was calculated by evaluating the capital cost of the reforming unit through Aspen plus Economizer tool and using the cost index of Nelson Farrar Index a well-known reference used for the cost calculation of industrial equipment. The following references are used in calculating the capital cost of the processing plant is a very simple and quick manner.

1. Rule-of – thumb estimates
2. Cost-Curve estimates
3. Major Equipment factor estimates.
4. Definitive estimates

5.5.1 Rule-of-Thumb Estimates

These are used in most cases only to book an estimated project capital cost, which is derived on best industrial practices for evaluating the costs used for major and minor process industries over the years. The capital cost based on these estimates reflect the cost per unit of product or feed flow rates, but in most cases feed flow rates are taken as basis by considering impurities, shrinkage factor. The estimated provided under for four major industrial units are based on 1999, estimates which and can be extrapolated by incorporating escalation of (03.0 %) per five years, owing to the steel cost and other overheads changes during this period.

I. Coal-fired electric power plant Capital Cost: \$2,500/kW
II. Synthetic ammonia plant Capital Cost: \$200,000/TPD
III. Gas Plant Capital Cost: \$1000000/MMSFC
IV. Petroleum Refinery Capital Cost: \$25,000/BPD

There may be a deviation of more than 50 % of cost estimation. However, they can be used as a quick reference for ballpark cost estimation.

5.5.2 Cost Curve Estimates

This method has addressed the flaws in the rule of thumb estimates by incorporating plants' equipment's size and capacity on the costs. These curves compare the cost of a similar project as follows:

$$\frac{\text{Plant A Cost}}{\text{Plant B Cost}} = \frac{(\text{Plant A Capacity}}{Plant\ B\ Capacity})^\wedge x \qquad (5.1)$$

The Lang [2] has used this relationship and has suggested an average value of 0.6 of the exponent (x). These cost curves have been used for the cost estimation of refineries cost in the past however these cost curves didn't provide the estimates of off-sites and location costs differential Therefore, separate data is required to estimates this cost. There is almost a 25 % adjustment required in this method to predict the accuracy to this level.

5.5.3. Major Equipment Factor Estimates

The estimates are made based on plants' major equipment's cost break up. There are almost different factors that are considered for each major equipment like main columns, pressure vessels heat exchangers, pumps, compressors, turbines. Defiantly the equipment sizes have a very sound effect on a systematic strategy that was adopted to calculate the cost of major equipment along with heat and material balances with basic specifications. This method can provide/predict the cost estimation in the range of 10 to 20 % accuracy if the equipment size specification is implemented carefully. A shortcut single multiple factors can be used for all equipment a factor of 4.5 is used for petroleum refining. The accuracy of this shortcut factor is less as compared to the individual cost factors.

5.5.4. Definitive Estimates

This method is the most accurate one among the other quick cost estimation methods although it consumes more time and is very difficult to prepare the estimations. These estimates require plot plans, construction drawings, and complete (BOQs) of the plant equipment and material. The complete project estimates for example man-hours' timesheets for each activity, indirect and direct field costs including boarding and logging mom-demob of heavy machinery used for the erection of plant pressure vessels, etc. Plant commissioning cost was also included in the estimation along with other heads of calculations. Hence it gives an accuracy of around'± 5%.

5.6 Summary form for Cost Estimates:

The items to be considered when estimating investment from cost-curves are:

1) Process equipment
2) Storage vessels
3) Steam unit
4) Cooling water section.
5) Offsite/Utilities
6) Different costs
7) Site factor
8) Contingency
9) Escalation
10) Plant Location

5.7 Offsite/Utilities

Offsite is the facilities required in a refinery which are not included in the costs of major facilities. A typical list of off-sites is shown below:

5.7.1 Electric power distribution

5.7.3 Fuel oil and fuel gas facilities
5.7.4 Water supply, treatment, and disposal
5.7.4 Plant air systems
5.7.5 Fire protection systems
5.7.6 Flare, drain and waste containment systems
5.7.7 Plant communication systems
5.7.8 Roads and walks
5.7.9 Railroads
5.7.10 Fence
5.7.11 Buildings
5.7.12 Vehicles
5.7.13 Product and additives blending facilities
5.7.14 Product loading facilities

5.8 Material Cost Estimation (Raw and Product)

A realistic approach must be adopted to predict very realistic and possible cost estimates of raw and product materials. As it is evident that the currently available process cannot be a true representative of the future conditions particularly the present geo-political scenario of around the globe. Any of the realistic methods can be used to provide an average published data that justified the lower and upper limits of the estimates as reference.

5.9 RETURN ON ORIGINAL INVESTMENT

This is an engineering method that does the time value of money bur simply offers a realistic conclusion of the last year's returns on the investment not considered. The rate of return on investment can be calculated as under:

$$ROI = \left(\frac{\text{Annual Profit x100}}{\text{(Originalfixed investment+working capital}}\right) \quad (5.2)$$

5.10 PAYBACK PERIOD

The payback period is defined as the investment recovery time every year and can be calculated with a very simple formula.

Payback period =Original depreciable fixed investment/Annual cash flow (5.3)

Table 5.12: Total capital Investment cost estimation basis.

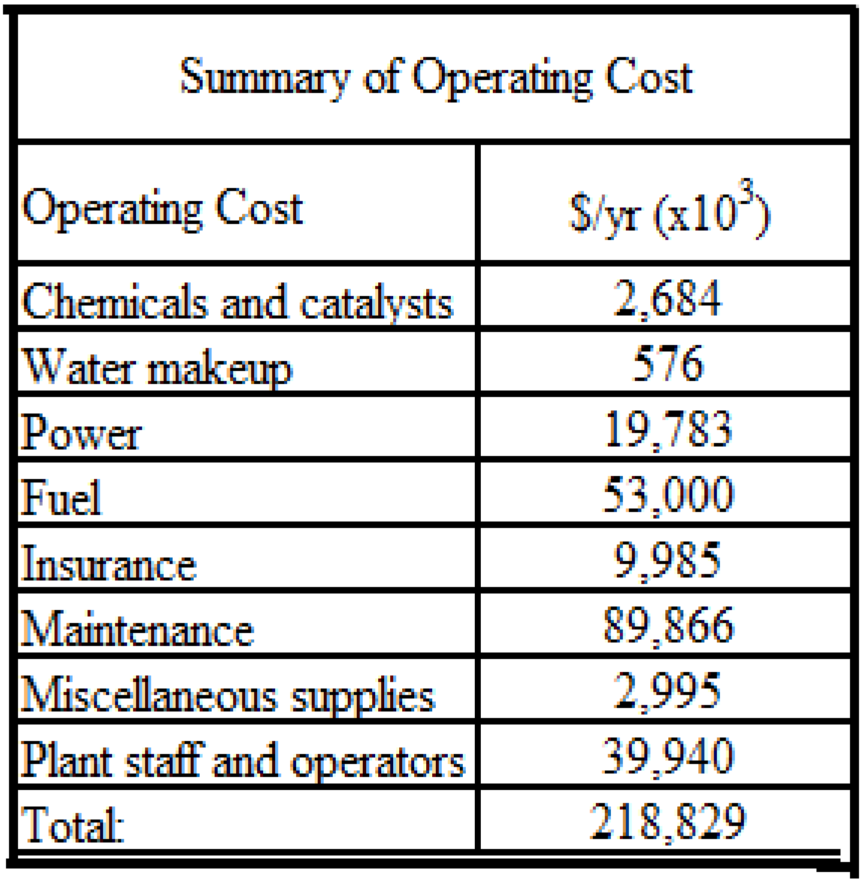

Summary of Operating Cost	
Operating Cost	\$/yr ($x10^3$)
Chemicals and catalysts	2,684
Water makeup	576
Power	19,783
Fuel	53,000
Insurance	9,985
Maintenance	89,866
Miscellaneous supplies	2,995
Plant staff and operators	39,940
Total:	218,829

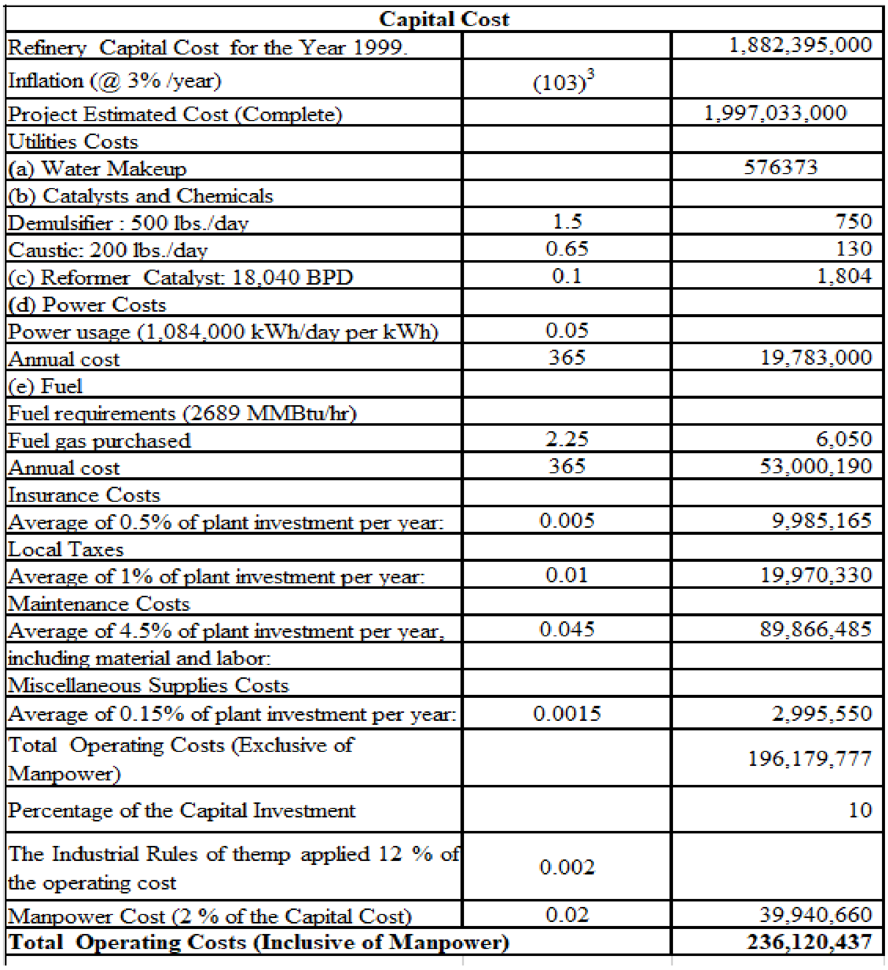

Capital Cost		
Refinery Capital Cost for the Year 1999.		1,882,395,000
Inflation (@ 3% /year)	$(103)^3$	
Project Estimated Cost (Complete)		1,997,033,000
Utilities Costs		
(a) Water Makeup		576373
(b) Catalysts and Chemicals		
Demulsifier : 500 lbs./day	1.5	750
Caustic: 200 lbs./day	0.65	130
(c) Reformer Catalyst: 18,040 BPD	0.1	1,804
(d) Power Costs		
Power usage (1,084,000 kWh/day per kWh)	0.05	
Annual cost	365	19,783,000
(e) Fuel		
Fuel requirements (2689 MMBtu/hr)		
Fuel gas purchased	2.25	6,050
Annual cost	365	53,000,190
Insurance Costs		
Average of 0.5% of plant investment per year:	0.005	9,985,165
Local Taxes		
Average of 1% of plant investment per year:	0.01	19,970,330
Maintenance Costs		
Average of 4.5% of plant investment per year,	0.045	89,866,485
including material and labor:		
Miscellaneous Supplies Costs		
Average of 0.15% of plant investment per year:	0.0015	2,995,550
Total Operating Costs (Exclusive of Manpower)		196,179,777
Percentage of the Capital Investment		10
The Industrial Rules of themp applied 12 % of the operating cost	0.002	
Manpower Cost (2 % of the Capital Cost)	0.02	39,940,660
Total Operating Costs (Inclusive of Manpower)		**236,120,437**

Table 5.13: Capital Cost and Operating Cost breakup

Table 5.14: Summary of Refinery Raw and Products Materials

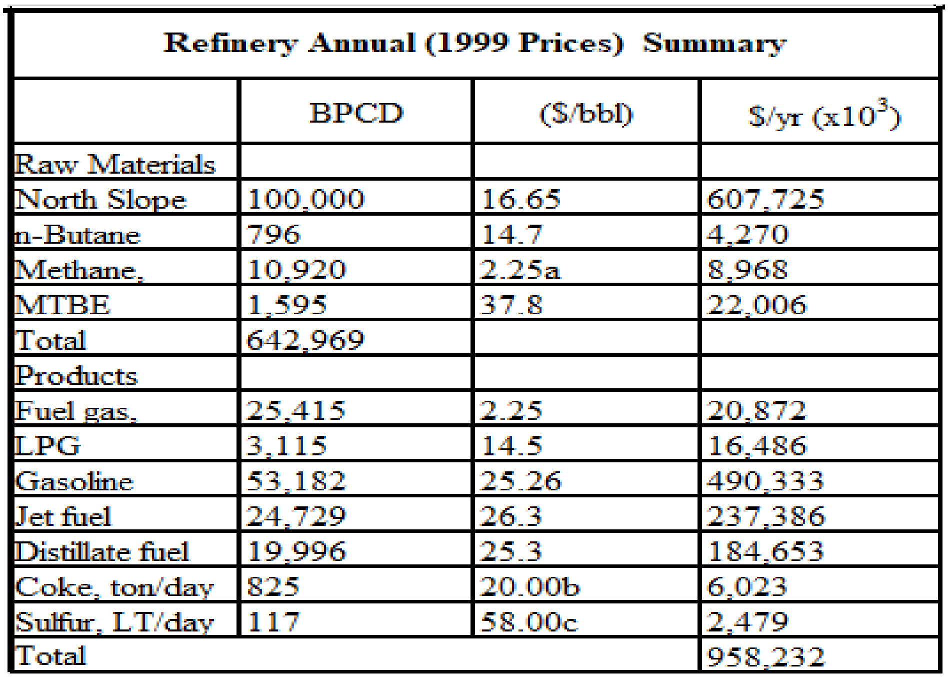

Refinery Annual (1999 Prices) Summary			
	BPCD	(\$/bbl)	\$/yr ($x10^3$)
Raw Materials			
North Slope	100,000	16.65	607,725
n-Butane	796	14.7	4,270
Methane,	10,920	2.25a	8,968
MTBE	1,595	37.8	22,006
Total	642,969		
Products			
Fuel gas,	25,415	2.25	20,872
LPG	3,115	14.5	16,486
Gasoline	53,182	25.26	490,333
Jet fuel	24,729	26.3	237,386
Distillate fuel	19,996	25.3	184,653
Coke, ton/day	825	20.00b	6,023
Sulfur, LT/day	117	58.00c	2,479
Total			958,232

Economics analysis assumption

- Capital investment.
- Aspen Economies Analyzer.
- Nelson and Farrar Cost Index used for equipment cost estimation.
- Membrane cost (MoE) department of USA.
- Catalyst cost and estimation refinery Cost (1999).
- Operating cost @ 12 % of the capital investment.
- Straight line method for deprecation @ 10 % / years
- Payback period (capital investment /net profit).

Table 5.15: Summary of Proposed Models (FBMR &FBR) payback periods

	FBMR	**FBR**
Item	$ MM	$ MM
Capital Cost of plant	230	235
Associated Cost (Membrane)	20	0
Total Investment	250	235
Gross Income	204	188
Revenue		
Naphtha Cost	82	82
Operating Cost	30	28
Depreciation	25	23.5
Net Income before Tax	67	54
Tax @ 42.5 %	28	23
Net Income after Tax	38	31
Payback Periods	**6**	**8**

Gross Income Product Slate (FBMR)			
Products	**Production rate (tons/ yr.)**	**Rate ($/Ton)**	**$ MM**
*NG (1872450 MMBtu)	25052	2.54	4.8
Gasoline	82881	212	18
Aromatics	145382	900	131
H_2	40536	1260	51
Total Revenue			204
(Feed Cost)	293851	273	80

Gross Income Product Slate (FBR)			
Products	**Prodcution rate (tons/ yr)**	**Rate ($/Ton)**	**$ MM**
*NG (1203393 MMBtu)	15357	2.54	3.1
Gasoline	116103	212	25
Aromatics	123432	900	111
H_2	38959	1260	49
Total Revenue			188
(Feed Cost)	293851	273	80

*Gas Rate is 2.54 $/Mmbtu

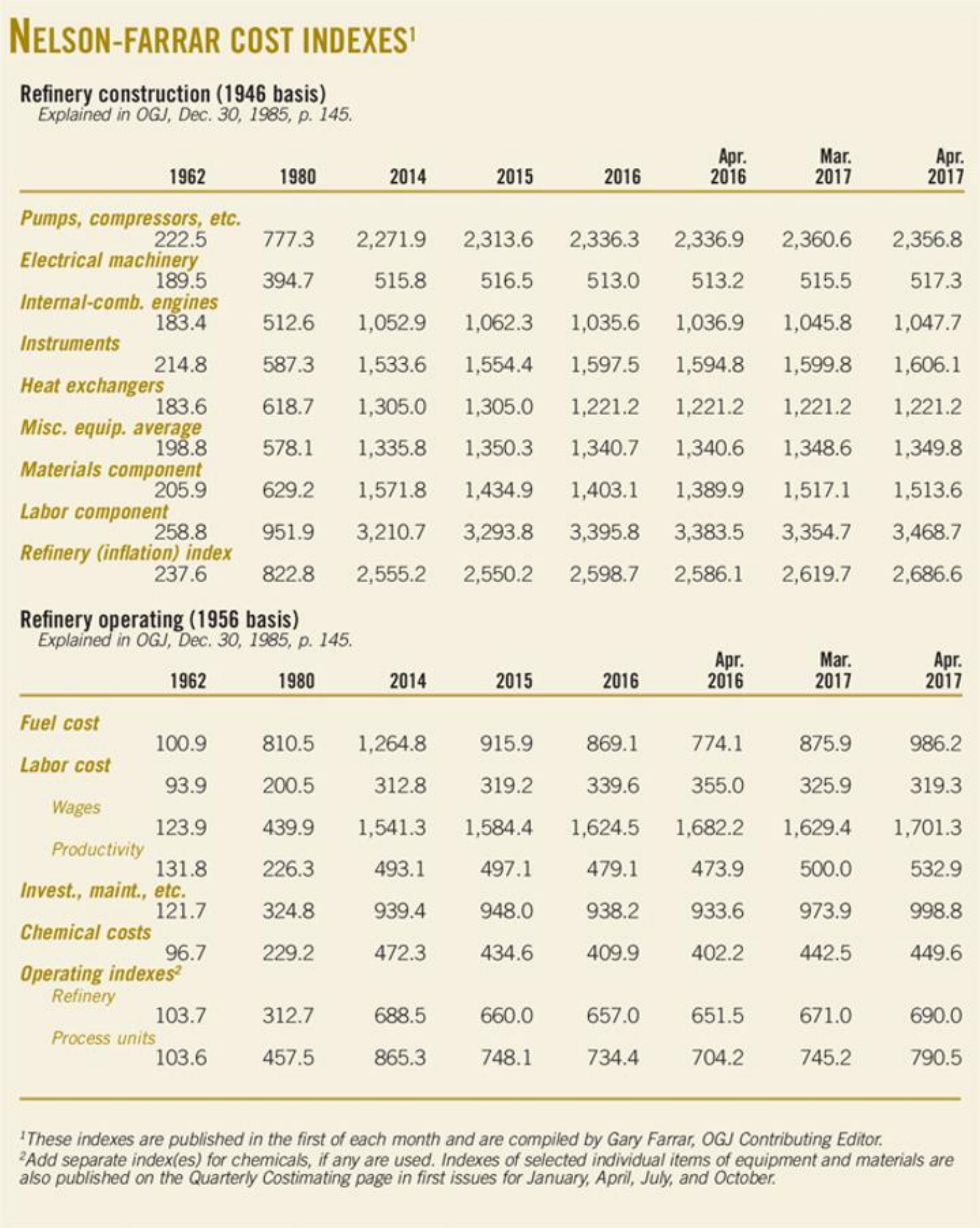

NELSON-FARRAR COST INDEXES[1]

Refinery construction (1946 basis)
Explained in OGJ, Dec. 30, 1985, p. 145.

	1962	1980	2014	2015	2016	Apr. 2016	Mar. 2017	Apr. 2017
Pumps, compressors, etc.	222.5	777.3	2,271.9	2,313.6	2,336.3	2,336.9	2,360.6	2,356.8
Electrical machinery	189.5	394.7	515.8	516.5	513.0	513.2	515.5	517.3
Internal-comb. engines	183.4	512.6	1,052.9	1,062.3	1,035.6	1,036.9	1,045.8	1,047.7
Instruments	214.8	587.3	1,533.6	1,554.4	1,597.5	1,594.8	1,599.8	1,606.1
Heat exchangers	183.6	618.7	1,305.0	1,305.0	1,221.2	1,221.2	1,221.2	1,221.2
Misc. equip. average	198.8	578.1	1,335.8	1,350.3	1,340.7	1,340.6	1,348.6	1,349.8
Materials component	205.9	629.2	1,571.8	1,434.9	1,403.1	1,389.9	1,517.1	1,513.6
Labor component	258.8	951.9	3,210.7	3,293.8	3,395.8	3,383.5	3,354.7	3,468.7
Refinery (inflation) index	237.6	822.8	2,555.2	2,550.2	2,598.7	2,586.1	2,619.7	2,686.6

Refinery operating (1956 basis)
Explained in OGJ, Dec. 30, 1985, p. 145.

	1962	1980	2014	2015	2016	Apr. 2016	Mar. 2017	Apr. 2017
Fuel cost	100.9	810.5	1,264.8	915.9	869.1	774.1	875.9	986.2
Labor cost	93.9	200.5	312.8	319.2	339.6	355.0	325.9	319.3
Wages	123.9	439.9	1,541.3	1,584.4	1,624.5	1,682.2	1,629.4	1,701.3
Productivity	131.8	226.3	493.1	497.1	479.1	473.9	500.0	532.9
Invest., maint., etc.	121.7	324.8	939.4	948.0	938.2	933.6	973.9	998.8
Chemical costs	96.7	229.2	472.3	434.6	409.9	402.2	442.5	449.6
Operating indexes[2]								
Refinery	103.7	312.7	688.5	660.0	657.0	651.5	671.0	690.0
Process units	103.6	457.5	865.3	748.1	734.4	704.2	745.2	790.5

---

[1] *These indexes are published in the first of each month and are compiled by Gary Farrar, OGJ Contributing Editor.*

[2] *Add separate index(es) for chemicals, if any are used. Indexes of selected individual items of equipment and materials are also published on the Quarterly Costimating page in first issues for January, April, July, and October.*

Table 5.16: Nelson- Farrar Cost Index

5.11 Exergy Analysis

The term Exergy can be defined as maximum obtained work through an energy carrier by bringing it to its thermodynamic state and it established a chemical equilibrium with the environment mathematically it can be express as follows.

$$E = E^{\mathrm{ph}} + E^{\mathrm{ch}} + E^{\mathrm{mix}} \tag{1}$$

where E total molar exergy of a stream, E^{ph} molar physical exergy, E^{ch} molar chemical exergy, and E^{mix} molar mixture exergy.

Physical exergy represents the thermomechanical portion of the total exergy stream. It is the maximum obtainable amount of work when this stream is brought from actual conditions (T, P) to thermomechanical equilibrium at ambient temperature (T_o, P_o) by reversible processes.

On a molar basis, physical exergy is given by the following:

$$E^{\mathrm{ph}} = \mathrm{R}T_o \sum\nolimits_{\mathrm{i}\,=\,1}^{\mathrm{n}} ln\frac{p_i}{p_o} + \sum\nolimits_{\mathrm{i}\,=\,1}^{\mathrm{n}} C_{p_i}^{\mathrm{mean}}\left(T_i - T_o - T_o \ln\left(\frac{T_i}{T_o}\right)\right) \tag{2}$$

$$C_{p_i^{\mathrm{mean}}} = \int_{T_1}^{T_2} C_{p_i} dT \tag{3}$$

$$C_{p_i}\left(\frac{j}{mol.K}\right) = \mathrm{a_i} + \mathrm{b_i}T + \mathrm{c_i}T^2 + \mathrm{d_i}T^3 \tag{4}$$

where $\mathrm{a_i}$, $\mathrm{b_i}$, $\mathrm{c_i}$, and $\mathrm{d_i}$ are heat capacity coefficients and R is the ideal gas constant. P_i and T_i represent the partial pressure and temperature of individual components, respectively, at each point in the reactor. Chemical exergy is the maximum obtainable work from a material stream by taking it from a state of thermomechanical equilibrium to a state of thermomechanical and chemical equilibrium with the environment Chemical exergy of a material stream on a molar basis is given by Equation (5):

$$E^{\mathrm{ch}} = \sum_{\mathrm{i}\,=\,1}^{\mathrm{n}} \mathrm{\nu_i}\bar{G}_i(\mathrm{Reactants}) - \sum_{\mathrm{i}\,=\,1}^{\mathrm{n}} \mathrm{\nu_i}\bar{G}_i(\mathrm{Products}) \tag{5}$$

$$\bar{G}_i = G_f^0 + [\bar{G}_{i(T,P)} - \bar{G}_{i(To,Po)}] \tag{6}$$

where v_i is the respective stoichiometric coefficients, $\bar{G}_i$ is the molar Gibbs function of components i, and G_f^0 is the molar Gibbs function of formation at a reference temperature and pressure. Mixing exergy accounts for the mixing effect arising from the isothermal and isobaric mixing of pure components at process conditions. It can be calculated by the following:

$$E_{mix} = \sum_{i=1}^{n} x_i T_o R \ln x_i, \tag{7}$$

where x_i is a mass fraction of component i. Mixing exergy is always a negative value because the mixing of different components decreases the exergy continuously along the length of the reactor. It can also be written in the form of $\sum_{i=1}^{n} \frac{x_i R T_o \ln p_i}{P_o}$, where P_i is the partial pressure of each component ($P_i = \mathcal{X}_i P_{total}$) according to Dalton's law.

Table 5.17. Exergy Analysis for FBMR and FBR Configuration.

		Phy-Exergy (KW)	Che-Exergy (KW)	Mix-Exergy (KW)	Total-Exergy (KW)
Feed	H2	3152	6553	-4268	5437
	Naphtha	1827	30420	-1642	30604
FBMR	Nethyd1	28	69	-41	56
	Nethyd2	2138	5298	-3214	4222
	Nethyd3	1672	4088	-2499	3261
	Prod3	1414	28187	-928	28672
	Total	5252	37642	-6683	36212
FBR	BPROD3	5371	37515	-6650	36235
Difference (FBMR-FBR)		-119	127	-259	-24

Conclusions and Recommendations

A fluidized-bed naphtha reformer within combination with the membrane separation process model has been developed in the Aspen Plus environment. Hydrodynamic parameters and membrane permeation phenomena were implemented using Excel interfacing. The results of the FBMR were compared with a simple fluidized bed reactor (FBR). It was observed that hydrogen removal from the permeate side drove the reaction forward and resulted in an increase of the aromatic yield. Besides, hydrogen production also increased due to its simultaneous separation during the reaction. The endothermic nature of the dehydrogenation reaction causes a sharp drop in temperature inside the reactor while operating in the adiabatic mode. Another important benefit of implementing the fluidized bed reactor is its superior heat transfer characteristics. The use of external heating coils can be implemented for converting the reactor to the isothermal mode. This mode cannot be used in packed bed reactors due to the difficulty and complex nature of internal heating arrangements. This work shows that the FBMR outperformed the FBR in terms of the output of both hydrogen and aromatics. Preliminary economics analysis of both systems was carried out that shows a very marginal cost-benefit of FBMR over FBR, therefore, there is a need for proper and detail working for scale-up of an industrial production comparative cost analysis of the membrane material against the extra profit from increased production is required. The proper investigation for the use of Pd-Ag Membrane material for these sever conditions required both at the pilot level and the extent in the industry. A fluidized-bed naphtha reformer in situ membrane separation was modeled by utilizing the Aspen Plus environment. The results of the FBMR were compared with a simple fluidized bed reactor (FBR). FBMR outperformed the FBR in terms of their products yields. The net annual income was 38 and 31 MUSD and payback periods for FBMR and FBR system were 6 and 8 years respectively. The chemical exergy of FBMR system was 37642 KW as compared to 37515 KW of FBR system. An increase of 127 KW in chemical exergy was noticed.

References

[1] Petroleum Refining 3 Conversion Process By P.Leprince (Institute Francais Du Petrol Publication.

[2] Petroleum Refining Technology and Economics Fourth Edition James H. Gary Colorado School of Mines Golden, Colorado Glenn E. Handwork Consulting Chemical Engineer Golden, Colorado.

[3]. M/s UOP Fixed-Bed Platforming Technical Document.

[4] Patil, C. S., van Sint Annaland, M., & Kuipers, J. A. (2005). Design of a novel auto thermal membrane-assisted fluidized-bed reactor for the production of ultrapure hydrogen from methane. Industrial & engineering chemistry research, 44(25), 9502-9512.

[5] Barbieri, G., Marigliano, G., Perri, G., & Drioli, E. (2001). Conversion−temperature diagram for a palladium membrane reactor. Analysis of an endothermic reaction: Methane steam reforming. Industrial & engineering chemistry research, 40(9), 2017-2026.

[6] Wieland, S., Melin, T., & Lamm, A. (2002). Membrane reactors for hydrogen production. Chemical Engineering Science, 57(9), 1571-1576.

[7] Howard, B. H., Killmeyer, R. P., Rothenberger, K. S., Cugini, A. V., Morreale, B. D., Enick, R. M., & Bustamante, F. (2004). Hydrogen permeance of palladium–copper alloy membranes over a wide range of temperatures and pressures. Journal of Membrane Science, 241(2), 207- 218.

[8] Barbieri, G., & Di Maio, F. P. (1997). Simulation of the methane steam reforming process in a catalytic Pd-membrane reactor. Industrial & engineering chemistry research, 36(6), 2121-2127.

[9]. Shu, J., Grandjean, B. P., & Kaliaguine, S. (1994). Methane steam reforming in asymmetric Pd-and Pd-Ag/porous SS membrane reactors. Applied Catalysis A: General, 119(2), 305-325.

[10]. Keuler, J. N., & Lorenzen, L. (2002). Comparing and Modeling the Dehydrogenation of Ethanol in a Plug-Flow Reactor and a Pd− Ag Membrane reactor. Industrial & engineering chemistry research, 41(8), 1960-1966.

[11]. Gobina, E. N., Oklany, J. S., & Hughes, R. (1995). Elimination of ammonia from coal gasification streams by using a catalytic membrane reactor. Industrial & engineering chemistry research, 34(11), 3777-3783.

[12]. Rahimpour, M. R., & Ghader, S. (2003). Theoretical investigation of a membrane reactor for methanol synthesis. Chemical Engineering & Technology: Industrial Chemistry-Plant Equipment-Process Engineering Biotechnology, 26(8), 902-907.

[13]. Tosti, S., Basile, A., Bettinali, L., Borgognoni, F., Gallucci, F., & Rizzello, C. (2008). Design and process study of Pd membrane reactors. International Journal of Hydrogen Energy, 33(19), 5098-5105.

[14]. Roy, S., Cox, B. G., Adris, A. M., & Pruden, B. B. (1998). Economics and simulation of fluidized bed membrane reforming. International journal of hydrogen energy, 23(9), 745-752.

[15]. Mostafazadeh, A. K., & Rahimpour, M. R. (2009). A membrane catalytic bed concept for naphtha reforming in the presence of catalyst deactivation. Chemical Engineering and Processing: Process Intensification, 48(2), 683-694.

[16]. Rahimpour, M. R. (2009). Enhancement of hydrogen production in a novel fluidized-bed membrane reactor for naphtha forming. International Journal of Hydrogen Energy, 34(5), 2235-2251.

[17]. Rahimpour, M. R., Vakili, R., Pourazadi, E., Iranshahi, D., & Paymooni, K. (2011). A novel integrated, thermally coupled fluidized bed configuration for catalytic naphtha reforming to enhance aromatic and hydrogen productions in refineries. International journal of hydrogen energy, 36(4), 2979-2991.

[18]. Grace, J. R., Li, X., & Lim, C. J. (2001). Equilibrium modeling of catalytic steam reforming of methane in membrane reactors with oxygen addition. Catalysis Today, 64(3-4), 141-149.

[19]. Sarvar-Amini, A., Sotudeh-Gharebagh, R., Bashiri, H., Mostoufi, N., & Haghtalab, A. (2007). Sequential simulation of a fluidized bed membrane reactor for the steam methane reforming using Aspen PLUS. Energy & Fuels, 21(6), 3593-3598.

[20]. Ye, G., Xie, D., Qiao, W., Grace, J. R., & Lim, C. J. (2009). Modeling of fluidized bed membrane reactors for hydrogen production from steam methane reforming with Aspen Plus. International journal of hydrogen energy, 34(11), 4755-4762.

[21]. Benitez, V. M., & Pieck, C. L. (2010). Influence of indium content on the properties of Pt–Re/Al2O3 naphtha reforming catalysts. Catalysis Letters, 136(1-2), 45-51.

[22]. Mazzieri, V. A., Pieck, C. L., Vera, C. R., Yori, J. C., & Grau, J. M. (2009). Effect of Ge content on the metal and acid properties of Pt-Re-Ge/Al2O3-Cl catalysts for naphtha reforming. Applied Catalysis A: General, 353(1), 93-100.

[23]. Benitez, V., Boutzeloit, M., Mazzieri, V. A., Especel, C., Epron, F., Vera, C. R., & Pieck, C. L. (2007). Preparation of trimetallic Pt–Re–Ge/Al2O3 and Pt–Ir–Ge/Al2O3 naphtha reforming catalysts by a surface redox reaction. Applied Catalysis A: General, 319, 210-217.

[24]. Smith R. Kinetic analysis of naphtha reforming with a platinum catalyst. Chem Eng Prog 1959; 55:76–80.

[25]. Marin, G. B., Froment, G. F., Lerou, J. J., & De Backer, W. 1983). Simulation of a catalytic naphtha reforming unit.

[26]. Froment G. The kinetics of complex catalytic reactions. Chem Eng Sci 1987; 42:1073.

[27]. Ramage MP, Graziani KR, Krubeck FJ. Development of Mobil's kinetic reforming model. Chem Eng Sci 1980; 35:41–8.

[28]. Ancheyta-Juarez J, Villafuerte-Macias E. Kinetic modeling of naphtha catalytic reforming reactions. Energy Fuels 2000; 14:1032–7.

[29]. Hu Y, Xu W, Su H, Chu J. A dynamic model for naphtha catalytic reformers. In: International conference on control applications, Taipei, Taiwan; 2004

[30]. Weifeng H, Hongye S, Yongyou U, Jian C. Modeling, simulation and optimization of a whole industrial catalytic naphtha reforming process on the Aspen Plus platform. Chin J Chem Eng 2006; 14:584–91.

[31]. Vathi GP, Chaughuri KK. Modeling and simulation of commercial catalytic naphtha reformers. Can J Chem Eng 1997; 75:930–7.

[32]. Modeling and Simulation of a Novel Membrane Reactor in continuous Catalytic Regenerative (CCR) Naphtha Reformer Accompanied with Detailed Description of Kinetic Davood Iranshahi, Shahram Amiri, Mohsen Karimi, Razieh Rafiei, Mitra Jafari, and Mohammad Reza Rahimpour

[33]. Pasha, Mustafa & Ahmad, Iftikhar & Mustafa, Jawad & Kano, Manabu. (2018). Modeling of a Nickel-based Fluidized Bed Membrane Reactor for Steam Methane Reforming Process. Journal- Chemical Society of Pakistan.

[34]. Porrazzo, R., White, G., & Ocone, R. (2014). Aspen PLUS simulations of fluidized beds for chemical looping combustion. Fuel, 136, 46-56.

[35]. Fazeli, A., Fatemi, S., Mahdavian, M., & Ghaee, A. (2009). Mathematical modeling of an industrial naphtha reformer with three adiabatic reactors in series. Iranian Journal of Chemistry and Chemical Engineering (IJCCE), 28(3), 97-102.

[36]. Krane, H. G., Groh, A. B., Schulman, B. L., & Sinfelt, J. H. (1959, January 1). Reactions in Catalytic Reforming of Naphthas. World Petroleum Congress.

[37]. Kmak, W. S., & Stuckey, A. N. (1973). Performing process studies with a kinetic simulation model. AlChE National Meeting, New Orleans, March, Paper No. 56a.

[38]. Lee, J. W., Ko, Y. C., Jung, Y. K., Lee, K. S., & Yoon, E. S. (1997). A modeling and simulation study on a naphtha reforming unit with a catalyst circulation and regeneration system. Computers & chemical engineering, 21, S1105-S1110.

[39]. Lid, T., & Skogestad, S. (2008). Data reconciliation and optimal operation of a catalytic naphtha reformer. Journal of Process Control, 18(3-4), 320-331.

[40]. Exergy Energy and Environment sustainable development by Ibrahim Dincer and Marc A. Rosen June 2007